CAPITAL UNIVERSITY OF SCIENCE AND TECHNOLOGY, ISLAMABAD

Cattaneo-Christov Double Diffusion Model for the Entropy Analysis of a Non-Darcian MHD Williamson Nanofluid

by

Zahfran Sajid

A thesis submitted in partial fulfillment for the degree of Master of Philosophy

in the

Faculty of Computing
Department of Mathematics

2022

*I dedicate my dissertation work to my **family** and dignified **teachers**. A special feeling of gratitude to my loving parents who have supported me in my studies.*

CERTIFICATE OF APPROVAL

Cattaneo-Christov Double Diffusion Model for the Entropy Analysis of a Non-Darcian MHD Williamson Nanofluid

by

Zahfran Sajid

(MMT191021)

THESIS EXAMINING COMMITTEE

(a)	External Examiner	Dr. Taimoor Salahuddin	MUST, Mirpur
(b)	Internal Examiner	Dr. Muhammad Afzal	CUST, Islamabad
(c)	Supervisor	Dr. Muhammad Sagheer	CUST, Islamabad

Dr. Muhammad Sagheer
Thesis Supervisor
November, 2022

Dr. Muhammad Sagheer
Head
Dept. of Mathematics
November, 2022

Dr. M. Abdul Qadir
Dean
Faculty of Computing
November, 2022

Author's Declaration

I, **Zahfran Sajid**, hereby state that my MPhil thesis titled "**Cattaneo-Christov Double Diffusion Model for the Entropy Analysis of a Non-Darcian MHD Williamson Nanofluid**" is my own work and has not been submitted previously by me for taking any degree from Capital University of Science and Technology, Islamabad or anywhere else in the country/abroad.

At any time if my statement is found to be incorrect even after my graduation, the University has the right to withdraw my MPhil Degree.

(Zahfran Sajid)

Registration No: MMT191021

Plagiarism Undertaking

I solemnly declare that research work presented in this thesis titled "**Cattaneo-Christov Double Diffusion Model for the Entropy Analysis of a Non-Darcian MHD Williamson Nanofluid**" is solely my research work with no significant contribution from any other person. Small contribution/help wherever taken has been dully acknowledged and that complete thesis has been written by me.

I understand the zero tolerance policy of the HEC and Capital University of Science and Technology towards plagiarism. Therefore, I as an author of the above titled thesis declare that no portion of my thesis has been plagiarized and any material used as reference is properly referred/cited.

I undertake that if I am found guilty of any formal plagiarism in the above titled thesis even after award of MPhil Degree, the University reserves the right to withdraw/revoke my MPhil degree and that HEC and the University have the right to publish my name on the HEC/University website on which names of students are placed who submitted plagiarized work.

(Zahfran Sajid)
Registration No: MMT191021

Acknowledgement

I got no words to articulate my cordial sense of gratitude to **Almighty Allah** who is the most merciful and most beneficent to his creation.

I also express my gratitude to the last Prophet of **Almighty Allah, Prophet Muhammad (PBUH)** the supreme reformer of the world and knowledge for human being.

I would like to be thankful to all those who provided support and encouraged me during this work.

I would like to be grateful to my thesis supervisor **Dr. Muhammad Sagheer**, the Head of the Department of Mathematics, for guiding and encouraging towards writing this thesis. It would have remained incomplete without his endeavours. Due to his efforts I was able to write and complete this assertation. Also special thanks to **Dr. Dur-e-Shehwar Sagheer** for her valuable suggestions and co-operation and all other faculty members.

I would like to pay great tribute to my **parents**, for their prayers, moral support, encouragment and appreciation.

Last but not the least, I want to express my gratitude to my class fellow **Mehwish Ibrahim** who encouraged me throughout my MPhil research.

(Zahfran Sajid)

Abstract

This study is carried out to observe the fluid flow across a stratified sheet in the presence of non-linear thermal radiation. Through the process of similarity transformations, the partial differential equations (PDEs) governing the flow model are transformed into ordinary differential equations (ODEs). The shooting method is then used to numerically solve the reduced equations. In this thesis, it is investigated how various flow parameters, such as the magnetic parameter, the Prandtl number, the Brownian motion parameter, the inertial cofficient, the radiation parameter, the thermophoresis parameter and the Brinkman number affect the skin friction coefficient, the Nusselt number, the Sherwood number and the rate of entropy generation. The MATLAB software is utilized to construst the tables and graphs which illustrate the numerical results. It has been found that the Cattaneo-Christov temperature parameter, is reduced, the temperature profile falls and the concentration profile rises. Similarly, as the Cattaneo-Christov concentration parameter is reduced, the temperature distribution rises while the concentration distribution declines. Furthermore, as the Weissenburg number's values climb, the rate of entropy generation rises as well. Numerous industries including solar engineering, polymer extrusion, electronic components, and biomedicine, can benefit from this kind of research.

Contents

Author's Declaration iv

Plagiarism Undertaking v

Acknowledgement vi

Abstract vii

List of Figures x

List of Tables xii

Abbreviations xiii

Symbols xiv

1 Introduction and Literature Review 1
- 1.1 Contribution to the Thesis . . . 6
- 1.2 Thesis Outline . . . 7

2 Some Basic Terminologies and Method of Solution 8
- 2.1 Some Basic Terminologies . . . 8
- 2.2 Classification of Fluid . . . 10
- 2.3 Types of Flow . . . 11
- 2.4 Modes of Heat Transfer . . . 13
- 2.5 Dimensionless Numbers . . . 14
- 2.6 Governing Laws . . . 16
- 2.7 Shooting Method . . . 17

3 Non-Darcian MHD Williamson Nanofluid for the Entropy Analysis in the Presence of Nonlinear Thermal Radiation across a Stratified Sheet 20
- 3.1 Introduction . . . 20
- 3.2 Description of Problem . . . 21
  - 3.2.1 The Governing PDEs . . . 22

3.2.2 Similarity Transformations . . . 22
3.2.3 Physical Quantities of Interest . . . 24
3.2.4 Entropy Generation Modeling . . . 24
3.3 Conversion of Mathematical Model into Dimentionless Form . . . 25
3.3.1 The Governing ODEs . . . 25
3.3.2 Physical Quantities of Interest . . . 39
3.3.2.1 Skin Friction Coefficient . . . 39
3.3.2.2 Nusselt Number . . . 40
3.3.2.3 Sherwood Number . . . 41
3.3.3 Entropy Generation . . . 42
3.4 Solution Methodology . . . 44
3.5 Numerical Results and Discussion . . . 49
3.5.1 Numerical Data for Skin Friction Coefficient . . . 49
3.5.2 Numerical Data for Nusselt and Sherwood Numbers . . . 50
3.5.3 Velocity Profile . . . 52
3.5.4 Temperature Profile . . . 55
3.5.5 Concentration Profile . . . 56
3.5.6 Entropy Generation . . . 61

4 Cattaneo-Christov Double Diffusion Model for the Entropy Analysis of a Non-Darcian MHD Williamson Nanofluid 65
4.1 Introduction . . . 65
4.2 Mathematical Formulations . . . 66
4.2.1 The Governing PDEs . . . 66
4.2.2 Similarity Transformations . . . 67
4.2.3 Physical Quantities of Interest . . . 67
4.2.4 Entropy Optimization . . . 68
4.3 PDEs to ODEs Transformation . . . 68
4.3.1 Transformation of the Governing PDEs . . . 68
4.3.2 Entropy Optimization . . . 78
4.4 Numerical Solution . . . 81
4.5 Numercial Results and Discussion . . . 84
4.5.1 Numerical Results for Nusselt and Sherwood Numbers . . . 85
4.5.2 Temperature Profile . . . 87
4.5.3 Concentration Profile . . . 94
4.5.4 Entropy Generation . . . 99

5 Conclusion 104

Bibliography 107

List of Figures

3.1 Geometry of physical model 21
3.2 Effect of M on $f'(\eta)$ 53
3.3 Effect of We on $f'(\eta)$ 53
3.4 Effect of Fr on $f'(\eta)$ 54
3.5 Effect of λ on $f'(\eta)$ 54
3.6 Effect of M on $\theta(\eta)$ 56
3.7 Effect of Nb on $\theta(\eta)$ 57
3.8 Effect of Nt on $\theta(\eta)$ 57
3.9 Effect of Pr on $\theta(\eta)$ 58
3.10 Effect of λ on $\theta(\eta)$ 58
3.11 Effect of N_3 on $\theta(\eta)$ 59
3.12 Effect of Rd on $\theta(\eta)$ 59
3.13 Effect of N_1 on $\theta(\eta)$ 60
3.14 Effect of k on $\phi(\eta)$ 60
3.15 Effect of M on $N_G(\eta)$ 62
3.16 Effect of We on $N_G(\eta)$ 62
3.17 Effect of Br on $N_G(\eta)$ 63
3.18 Effect of β_2 on $N_G(\eta)$ 63
3.19 Effect of N_2 on $N_G(\eta)$ 64
3.20 Effect of L on $N_G(\eta)$ 64

4.1 Influence of M on $\theta(\eta)$ 89
4.2 Influence of λ on $\theta(\eta)$ 89
4.3 Impact of Fr on $\theta(\eta)$ 90
4.4 Influence of λ_t on $\theta(\eta)$ 90
4.5 Influence of Pr on $\theta(\eta)$ 91
4.6 Influence of Nt on $\theta(\eta)$ 91
4.7 Influence of Nb on $\theta(\eta)$ 92
4.8 Influence of Ec on $\theta(\eta)$ 92
4.9 Influence of N_1 on $\theta(\eta)$ 93
4.10 Influence of N_2 on $\theta(\eta)$ 93
4.11 Influence of Rd on $\theta(\eta)$ 94
4.12 Influence of N_1 on $\phi(\eta)$ 95
4.13 Influence of Le on $\phi(\eta)$ 96
4.14 Influence of Pr on $\phi(\eta)$ 96

4.15 Influence of Nt on $\phi(\eta)$ 97
4.16 Influence of Nb on $\phi(\eta)$ 97
4.17 Influence of k on $\phi(\eta)$ 98
4.18 Influence of λ_d on $\phi(\eta)$ 98
4.19 Influence of Br on $N_G(\eta)$ 100
4.20 Influence of M on $N_G(\eta)$ 100
4.21 Influence of We on $N_G(\eta)$ 101
4.22 Influence of τ_1 on $N_G(\eta)$ 101
4.23 Influence of τ_2 on $N_G(\eta)$ 102
4.24 Influence of L on $N_G(\eta)$ 102
4.25 Influence of Xr on $N_G(\eta)$ 103
4.26 Influence of Xb on $N_G(\eta)$ 103

List of Tables

3.1 Results of $C_f(Re_x)^{\frac{1}{2}}$ for various parameters 50
3.2 Results of $Nu(Re_x)^{-\frac{1}{2}}$ *and* $Sh(Re_x)^{-\frac{1}{2}}$ when $N_1 = 0.8$, $N_2 = 0.8$, $N_3 = 1.0$, $k = 0.1$, $Le = 1.0$, $We = 0.3$. 51

4.1 Results of $Nu(Re_x)^{-\frac{1}{2}}$ *and* $Sh(Re_x)^{-\frac{1}{2}}$ when $N_1 = 0.8$, $N_2 = 0.8$, $N_3 = 1.0$, $Pr = 0.7$, $Le = 1.0$, $We = 0.3$. 86

Abbreviations

BCs	Boundary Conditions
IVPs	Initial value problems
MHD	Magnetohydrodynamics
ODEs	Ordinary differential equations
PDEs	Partial differential equations
RK	Runge-Kutta

Symbols

μ	Viscosity
ρ	Density
ν	Kinematic viscosity
τ	Stress tensor
λ	Porosity constant
N_1	Solutal stratification parameter
N_2, N_3	Temperature ratios
α	Thermal diffisuitivity
σ	Electrical conductivity
u	x-component of fluid velocity
v	y-component of fluid velocity
B_0	Magnetic field constant
a	Stretching constant
T_w	Temperature of the wall
T_∞	Ambient temperature of the nanofluid
T	Temperature
ρ_f	Density of the fluid
μ_f	Viscosity of the fluid
ν_f	Kinematic viscosity of the base fluid
ρ_{nf}	Density of the nanofluid
μ_{nf}	Viscosity of the nanofluid
q_r	Radiative heat flux
q	Heat generation constant

q_w	Heat flux
q_m	Mass flux
σ^*	Stefan Boltzmann constant
k^*	Absorption coefficient
η	Similarity variable
C_f	Skin friction coefficient
Nu	Nusselt number
Nu_x	Local Nusselt number
Sh	Sherwood number
Sh_x	Local Sherwood number
Re	Reynolds number
Re_x	Local Reynolds number
ϕ	Nanoparticle volume fraction
R	Thermal radiation parameter
M	Magnetic parameter
We	Weissenburg number
k	Chemical reaction parameter
Ec	Eckert number
Pr	Prandtl number
Q	Heat generation parameter
λ_t	Cattaneo-Christov temperature parameter
λ_d	Cattaneo-Christov concentration parameter
γ_1	Relaxation time parameter
Nb	Brownain motion parameter
Nt	Thermophoresis parameter
γ_2	Chemical reaction parameter
Le	Lewis number
Fr	Inertial coefficient
ρ_f	Density of the pure fluid
ρ_s	Density of nanoparticle
μ_f	Viscosity of the base fluid

$(\rho C_p)_f$	Heat capacitance of base fluid
$(\rho C_p)_s$	Heat capacitance of nanoparticle
f	Dimensionless velocity
θ	Dimensionless temperature
C_∞	Ambient concentration
C	Concentration
C_w	Nanoparticles concentration at the stretching surface

Chapter 1

Introduction and Literature Review

A phase of matter known as a fluid deforms or flows in response to an applied external force. There are three types of fluid: liquids, gases, and plasma [1]. It is a substance with vanishing shear modulus or put another way, a substance that is incapable of withstanding any applied shear force. Since fluid is a necessity for daily life and plays a crucial role in many natural processes, experts from all over the world are working to uncover interesting information about fluid movement. The branch of fluid mechanics known as fluid dynamics in which we analyse fluid flow while simultaneously examining its causes, as well as how forces affect fluid movement. It offers strategies for comprehending the evolution of the stars, the ocean, the current, the tectonic plate, and the blood flow [2]. Wind turbines, oil pipelines, rocket engines, and air conditioning systems are only a few significant applications of fluid fluxes [3]. The Archimedes principle, which is related to the motion of objects, was first developed by Archimedes. Fluid dynamics foundational principle is the static behaviour of fluids. Fluid mechanics has been properly studied since the early fifteenth century. Depending on the relationship between two physical parameters, namely the relationship between stress and strain, fluid can be further characterised as Newtonian or non-Newtonian fluid. Non-Newtonian fluids are those that do not exhibit a linear correlation between

the shear stress and the rate of deformation. In other words, fluids that defy Newton's viscosity law are referred to as non-Newtonian fluids. Ketchup, paint, and blood, Shampoo, mud, and other liquids exhibit non-Newtonian behaviour. One of the most widely used fluids that are not Newtonian are called Williamson fluids. Williamson fluids have a wide range of applications in many areas of science, technology, and engineering, including material processing, the nuclear and chemical industries, bio-engineering, and geophysics. A wide variety of mathematical models have been created to simulate the flow behaviour of these non-Newtonian fluids in the light of these applications. A variety of industries, including oil recovery, filtration, polymer engineering, ceramic production, and petroleum production, use non-Newtonian fluid. Additionally, it plays a crucial part in the design of solid matrix, heat geothermal energy production, the removal of nuclear waste, and petroleum reservoirs, among other things [4]. Williamson [5] talked on the flow of pseudoplastic materials, developed a model equation to talk about the flow of pseudoplastic fluids, and then experimentally confirmed the findings. In their presentation of the Williamson fluid flow across a stretched surface, Nadeem et al. [6] observed that the dimensionless velocity falls as the values of the Williamson fluid parameter increases.

Choi [7] initially used the term nanofluid to describe a new form of fluid. Nanofluid is a blend of conventional low thermal conductivity fluid with nanoparticles with a size smaller than 100 nm. It can also be defined as "the tinny size particles suspended in a base fluid are known as nanofluids". The most popular nanoparticles in use today are carbon nanotubes, carbides, metals, oxides nanofluids etc. These fluids are created synthetically to have better thermal conductivity than any basic fluids. Nanofluids' thermal conductivity can be boosted by adding gold, copper, silver, and other nanoparticles to the base fluid. Buongiorno [8] studied the element that increased the thermal conductivity of nanofluids. He noticed that a change in the fluid's thermal conductivity is caused by both the thermophoresis effect and Brownian motion. In the heavy vehicle and information technology

industries, nanofluids can also be utilised as a coolant. In many industrial, biomedical, and technical domains, nanofluid is a blessing. Ibrahim and Shankar [9] used the slip boundary condition, heat radiation, and magnetic field effect to study the boundary layer flow of a non-Newtonian nanofluid. Using slip velocity and surface boundary conditions, Abolbashari et al. [10] examined the transmission of energy and heat in the steady laminar Casson nanofluid flow. The impact of thermal radiation on MHD nanofluid on a stretched surface was examined by Naramgari and Soluchana [11]. Krishnamurthy et al. [12] explored the numerical study of Williamson nanofluid flow through a permeable surface coupled with the impact of chemical parameter in the presence of nanoparticles. A porous non linear sheet was used by Ghadikolaei et al. [13] to explore the effects of several physical parameters on the MHD flow of Casson nanofluid, including chemical reaction, thermal radiation, suction, Joule heating, heat generation, and absorption. Shahzad et al. [14] used the Joule heating effect to study the nanofluid flow along a horizontal sheet in the presence of an external magnetic field.

The field of mechanics known as magnetohydrodynamics studies conduction fluid flow in the presence of an external magnetic field. The MHD fluid was first introduced by Swedish physicist Alfen [15]. The petroleum industry, MHD power generators, crystal formation, etc. are just a few engineering scenarios where MHD fluid flow through a heated surface has numerous critical applications. By assuming various physical parameters, Attia [16] investigated the heat transfer using MHD Couette flow in a special kind of fluid termed as dusty fluid and discovered that both the temperature of the fluid and the dust particles fluctuate considerably. The MHD natural convection flow of spinning fluid through a porous sheet was studied by Mbeledogu and Ogulu [17]. They also studied the effects of radiation and heat transport. Through MHD, the boundary layer structure can be altered, improving fluid flow in a particular direction. Several industrial operations, such as the production of materials and metal casting, depend heavily on the application of an external magnetic field. Chauhan and Agrawal [18] conducted

an analysis of the MHD flow and heat transfer across a channel employing a permeable sheet. They discovered that two variables, such as the magnetic number and suction parameter, can control the cooling rate. They discovered that the magnetic number and the suction parameter, respectively, can control the rate of cooling. Zhang et al. [19] conducted an analysis of the heat transfer in 2D MHD fluid flow utilising a permeable surface with rapid slip velocity and temperature gradient changes. They noticed that by changing the system's shrinking parameter, the thermal boundary layer could be increased. Yazdi et al. [20] used a vertical plate filled with nanofluid to illustrate the 2D mixed convection MHD boundary layer stagnation point flow in the presence of thermal radiation. The most frequent types of magnetic fluid are plasma, liquid metals, salt water, and electrolytes. It establishes a link between the Navier-Stoke equation for fluid dynamics and the Maxwell equations for electromagnetism. The basic idea behind MHD is that when an external magnetic field produces an electric current in a conducting fluid, force is applied to the flowing fluid, which in turn influences the magnetic field. Due to MHD's significance, it is important in many flow phenomena. It has a wide range of applications in many scientific disciplines, including metallurgical science, mental processing, aerodynamics, fluid dynamics, and several engineering disciplines, such as ceramic and biomedical engineering, among others [21].

The inability of the system to fully utilize the available energy is known as entropy. Heat transfer irreversibility, fluid friction and mass transfer irreversibility are the main causes of a rise in a system's entropy. The overall entropy of the system is defined as the sum of these three variables. The importance of irreversible elements related to heat transfer, friction, and other imperfect processes within a system is highlighted by entropy formation. The amount of entropy produced during a specific task can be used to predict the quantity of energy wasted. Entropy increases over time and this process is irreversible. According to the second law of thermodynamics, entropy generally develops in a variety of systems, especially, those involving fluid viscous force, flow-driven force, Joule heating, and thermal management since heat transfer is irreversible in these systems.

The technical and scientific communities have already begun to take entropy generation seriously. In the past, various fluid models have been used for entropy generation analysis. To reduce entropy generation, different liquid models are taken into account for specific systems. Numerous scholars have conducted numerical investigations on the entropy generation in convective heat transfer situations. Abu-Hijleh et al. investigated numerical prediction of entropy generation owing to natural convection from a horizontal cylinder in their study [22]. In a different study, Abu-Nada [23] discusses numerical prediction of entropy generation in separated flows. Abu-Nada researched the creation of entropy resulting from heat and fluid flow in a backward facing step flow with different expansion ratios [24]. The primary objectives of this study are to examine the impact of Cattaneo-Christov double diffusion, multiple slips, and Darcy-Forchheimer on entropy optimised and thermally radiative flow, thermal and mass transport of hybrid nanoliquids past a stretched cylinder subject to viscous dissipation, and Arrhenius activation energy. Chen et al. [25] claim that the primary reason entropy forms in low Reynolds number situations is because chemical reactions become irreversible.

Models of non-Newtonian fluids are more suitable for simulating the behaviour of nanofluids. Ellahi et al. [26] utilised OHAM to apply the Brinkman nanofluid model to discover the precise solution of the Power-law nanofluid with copper nanoparticles. They discovered that raising the nanoparticle volume fraction causes a decrease in the velocity profile of fluids that are shear thinning. Pakdemirli and Yilbas take into account the non-Newtonian fluid flow in a pipe system with entropy formation. They claim that as the Brinkman number rises, the entropy number does as well [27]. Using the finite volume approach and the SIMPLE algorithm, Govone et al. [28] examined the heat transfer and entropy generation of Al_2O_3-water nanofluid flow through isotropic porous media made up of staggered and in-line arrangements of square pillars. According to their findings, for both arrangements, the entropy generation is reduced as the volume fraction of solid nanoparticles increases. In their research [29], Afridi and Qasim examined how the creation of entropy affected the heat transfer and radiative flow via a thin

moving needle. Viscose dissipation and nonlinear radiative heat flux help to solve the flow problems. Utilizing viscous dissipation and nonlinear radiative heat flow, the properties of heat transmission are studied. Entropy production in the Darcy-Forchheimer transport of hybrid nanofluids with Cattaneo-Christov double diffusion is computed numerically [30]. According to [31], [32] and [33], similar investigation of entropy generation on nanofluid with stretching surface taking different geometries is conducted. In Qing et al. study [34], entropy analysis was done on a Casson nanofluid flow that was travelling through a permeable stretching surface. Using the numerical successive linearization method, they discovered that an increase in the permeability parameter, Reynolds, Brinkman, and Hartmann numbers results in an increase in the creation of entropy. Williamson nanoliquid flow that is chemically reactive was studied by Hayat et al. [35] with mixed convection. They made use of thermophoresis and Brownian motion. A bidirectional stretched surface with constant thickness is used to analyse flow. The optimal homotopy analysis method is used. Temperature and concentration exhibit opposing behaviour thanks to a bigger Brownian parameter. Khan et al. described the entropy production and activation energy (AE) components for NF in their paper [36].

1.1 Contribution to the Thesis

In this assessment, a review study of [37] has been presented and then the flow analysis has been extended with Cattaneo-Christov Double Diffusion Model. Previously, Bilal et al. [37] extended the work of [38] by considering non-Darcian MHD Williamson nanofluid in the presence of non-linear thermal radiation across a stratified sheet. First of all, the governing PDEs are converted into the dimentionless ODEs by using the suitable similarity transformations. The MATLAB software is utilized to construst the tables and graphs which illustrate the numerical results. The key findings using CCDDM in our flow model are provided through complete discussions and elaboration. Using the shooting technique, numerical results are generated for the collection of nonlinear coupled ODEs.

1.2 Thesis Outline

The information below gives a quick summary of the thesis contents.

Chapter 2 includes the definitions of a number of fundamental terms, solution methods, guiding concepts, and dimensionless parameters that will be used in later part of this thesis.

Chapter 3 gives a review of "The Non-Darcian MHD Williamson nanofluid entropy optimization across a stratified sheet". The shooting method is used to regenerate the numerical outcomes of the governing flow equations.

Chapter 4 is focused on an extension of model reviewed in Chapter 3.

Chapter 5 includes the concluding remarks of the thesis.

In the **Bibliography**, the relevant references for this thesis are listed.

Chapter 2

Some Basic Terminologies and Method of Solution

The following chapters will make use of several fundamental terminologies, guiding principles and dimensionless parameters that have been defined in this chapter. The numerical computations of the flow problem discussed in the thesis are carrried out by using the shooting method, which is also covered at the end of the chapter.

2.1 Some Basic Terminologies

Definition 2.1.1 [Fluid]

"A fluid is a substance that deforms continuously under the application of a shear (tangential) stress no matter how small the shear stress may be." [39]

Definition 2.1.2 [Fluid Mechanics]

"Fluid mechanics is that branch of science which deals with the behaviour of the fluids (liquids or gases) at rest as well as in motion. Thus this branch of science deals with the static, kinematics and dynamic aspects of the fluids." [40]

Definition 2.1.3 [Fluid Dynamics]

"The term fluid dynamics encompasses the study of the laws of conservation of mass, momentum and energy as they apply to the flow of fluid." [41]

Definition 2.1.4 [Fluid Statics]

"The study of fluid at rest is called fluid statics." [40]

Definition 2.1.5 [Viscosity]

"Viscosity is defined as the property of a fluid which offers resistance to the movement of one layer of fluid over another adjacent layer of the fluid. Mathematically,

$$\mu = \frac{\tau}{\frac{\partial u}{\partial y}},$$

where μ is viscosity coefficient, τ is shear stress and $\frac{\partial u}{\partial y}$ represents the velocity gradient." [40]

Definition 2.1.6 [Kinematic Viscosity]

"The ratio of dynamic viscosity to density is called kinematic viscosity. It is denoted by the Greek symbol ν called **nu**. Mathematically, it can be expressed as,

$$\nu = \frac{viscosity}{density} = \frac{\mu}{\rho}. \tag{2.1}$$

SI unit of Kinematic Viscosity $= m^2 s^{-1}$." [42]

Definition 2.1.7 [Dynamic Viscosity]

"The extent which measures the resistence of fluid tending to cause the fluid to flow is called dynamic viscosity, also known as absolute viscosity. This resistence arises from the attractive forces between the molecules of fluid. Usually liquids and gases have non zero viscosity. It is denoted by the symbol μ and mathematically it can be written as

$$\mu = \frac{Shear\ stress}{Shear\ strain}." \text{ [42]}$$

Definition 2.1.8 [Thermal Conductivity]

"The Fourier heat conduction law states that the heat flow is proportional to the temperature gradient. The coefficient of proportionality is a material parameter known as the thermal conductivity which may be a function of a number of variables." [43]

Definition 2.1.9 [Thermal Diffusivity]

"The rate at which heat diffuses by conducting through a material depends on the

thermal diffusivity and can be defined as,

$$\alpha = \frac{k}{\rho C_p},$$

where α is the thermal diffusivity, k is the thermal conductivity, ρ is the density and C_p is the specifc heat at constant pressure." [44]

Definition 2.1.10 [Magnetohydrodynamics]

"Magnetohydrodynamics (MHD) is concerned with the mutual interaction of fluid flow and magnetic fields. The fluids in question must be electrically conducting and non-magnetic, which limits us to liquid metals, hot ionised gases (plasmas) and strong electrolytes." [45]

Definition 2.1.11 [Entropy]

"The entropy of a system is the amount of thermal energy per unit of temperature that cannot be used to carry out beneficial work. Every system is capable of producing useful energy. However, some energy is lost in the form of heat during this beneficial work as a result of friction and other factors. The term "entropy of the system" refers to this energy loss." [46]

2.2 Classification of Fluid

Definition 2.2.1 [Ideal Fluid]

"A fluid, which is incompressible and has no viscosity, is known as an ideal fluid. Ideal fluid is only an imaginary fluid as all the fluids, which exist, have some viscosity" [40]

Definition 2.2.2 [Real Fluid]

"A fluid, which possesses viscosity, is known as a real fluid. In actual practice, all the fluids are real fluids." [40]

Definition 2.2.3 [Newtonian Fluid]

"Fluids for which the shearing stress is linearly related to the rate of shearing strain are called newtonian fluids." [47]

Definition 2.2.4 [Non-Newtonian Fluid]

"Fluids for which the shearing stress is not linearly related to the rate of shearing strain are called newtonian fluids.

$$\tau_{xy} \propto \left(\frac{du}{dy}\right)^m, \qquad m \neq 1$$
$$\tau_{xy} = k\left(\frac{du}{dy}\right)^m,$$

where k = Flow consistency coefficient, $\frac{du}{dy}$ = Shear rate, and m = Flow behaviour index." [47]

Definition 2.2.5 [Ideal Plastic Fluid]

"A fluid in which the shear stress is more than the yield value and shear stress is directly proportional to the rate of shear strain (or velocity gradient), is known as ideal plastic fluid." [40]

Definition 2.2.6 [Nanofluids]

"Nanofluids are engineered colloids made of a base fluid and nanoparticles. Nanofluids have higher thermal conductivity and single phase heat transfer coefficients than their base fluids metals, oxides, carbides, or carbon nanotubes are the typical nanoparticles which are used in nanofluids and oil, ethylene glycol and water are examples of common base fluids." [40]

Definition 2.2.7 [Magnetohydrodynamics]

"Magnetohydrodynamics (MHD) is concerned with the mutual interaction of fluid flow and magnetic fields. The fluids in question must be electrically conducting and non-magnetic, which limits us to liquid metals, hot ionised gases (plasmas) and strong electrolytes." [48]

2.3 Types of Flow

Definition 2.3.1 [Laminar Flow]

"The highly ordered fluid motion characterzed by smooth layers of fluid is called laminar flow. The flow of high-viscosity fluids such as oil at low velocity is typically

laminar." [42]

Definition 2.3.2 [Turbulent Flow]

"The highly disordered fluid motion that typically occurs at high velocities and is characterized by velocity fluctuations is called turbulent flow. The flow of low-viscosity fluids such as air at high velocity is typically turbulent." [42]

Definition 2.3.3 [Rotational Flow]

"Rotational flow is that type of flow in which the fluid particles while flowing along stream-lines, also rotate about their own axis." [40]

Definition 2.3.4 [Irrotational Flow]

"Irrotational flow is that type of flow in which the fluid particles while flowing along stream-lines, do not rotate about their own axis then this type of flow is called irrotational flow." [40]

Definition 2.3.5 [Compressible Flow]

"Compressible flow is that type of flow in which the density of the fluid changes from point to point or in other words the density (ρ) is not constant for the fluid, Mathematically,

$$\rho \neq k,$$

where k is constant." [40]

Definition 2.3.6 [Incompressible Flow]

"Incompressible flow is that type of flow in which the density is constant for the fluid. Liquids are generally incompressible while gases are compressible, Mathematically,

$$\rho = k,$$

where k is constant." [40]

Definition 2.3.7 [Internal Flow]

"The flow in a pipe or duct is internal flow if the fluid is completely bounded by solid surfaces. Water flow in a pipe, for example, is internal flow." [42]

Definition 2.3.8 [External Flow]

"The flow of an unbounded fluid over a surface such as a plate, a wire, or a pipe is external flow. Airflow over a ball or over an exposed pipe during a windy day is external flow." [42]

Definition 2.3.9 [Steady Flow]

"If the flow characteristics such as depth of flow, velocity of flow, rate of flow at any point in open channel flow do not change with respect to time, the flow is said to be steady flow. Mathematically,

$$\frac{\partial Q}{\partial t} = 0,$$

where Q is any fluid property." [40]

Definition 2.3.10 [Unsteady Flow]

"If at any point in open channel flow, the velocity of flow, depth of flow or rate of flow changes with respect to time, the flow is said to be unsteady. Mathematically,

$$\frac{\partial Q}{\partial t} \neq 0,$$

where Q is any fluid property." [40]

2.4 Modes of Heat Transfer

Definition 2.4.1 [Heat Transfer]

"Heat transfer is a branch of engineering that deals with the transfer of thermal energy from one point to another within a medium or from one medium to another due to the occurrence of a temperature difference." [49]

Definition 2.4.2 [Conduction]

"The conduction mode of heat transport occurs either because of an exchange of energy from one molecule to another, without the actual motion of the molecules or because of the motion of the free electrones if they are present. Therefore, this form of heat transport depends heavily on the properties of the medium and takes place in solids, liquids and gases if a difference in temperature exists." [50]

Definition 2.4.3 [Convection]

"The transfer of heat from one region to another due to macroscopic motion of molecules in a liquid or gas, added to the energy transfer by conduction within

the fluid, is called heat transfer by convection. Convection may be free, force or mixed." [50]

Definition 2.4.4 [Thermal Radiation]

"Thermal radiation is defined as radiant (electromagnetic) energy emitted by a medium and is solely to the temperature of the medium." [47]

2.5 Dimensionless Numbers

Definition 2.5.1 [Eckert Number]

"It is the dimensionless number used in continuum mechanics. It describes the relation between flows and the boundary layer enthalpy difference and it is used for characterized heat dissipation. Mathematically,

$$Ec = \frac{u^2}{C_p \nabla T}$$

where u is an appropriate fluid velocity, C_p denotes the specific heat and δT, the temperature difference is the driving force for heat transfer." [39]

Definition 2.5.2 [Prandtl Number]

"It is the ratio between the momentum diffusivity ν and thermal diffusivity α. Mathematically, it can be defined as

$$Pr = \frac{\nu}{\alpha} = \frac{\frac{\mu}{\rho}}{\frac{k}{C_p \rho}} = \frac{\mu C_p}{k}$$

where μ represents the dynamic viscosity, Cp denotes the specific heat and k stands for thermal conductivity. The relative thickness of thermal and momentum boundary layer is controlled by Prandtl number. For small Pr, heat distributed rapidly corresponds to the momentum." [39]

Definition 2.5.3 [Skin Friction Coefficient]

"The steady flow of an incompressible gas or liquid in a long pipe of internal D. The mean velocity is denoted by u_w. The skin friction coefficient can be defined

as

$$C_f = \frac{2\tau_0}{\rho u_w^2},$$

where τ_0 denotes the wall shear stress and ρ is the density." [51]

Definition 2.5.4 [Weissenberg Number]

"The Weissenberg number is typically defined as,

$$We = \frac{\lambda u}{L},$$

where u and L are a characteristic velocity and length scale for the flow. The Weissenberg number indicates the relative importance of fluid elasticity for a given flow problem." [39]

Definition 2.5.5 [Nusselt Number]

"The hot surface is cooled by a cold fluid stream. The heat from the hot surface, which is maintained at a constant temperature, is diffused through a boundary layer and convected away by the cold stream. Mathematically,

$$Nu = \frac{qL}{k},$$

where q stands for the convection heat transfer, L for the characteristic length and k stands for thermal conductivity." [52]

Definition 2.5.6 [Sherwood Number]

"It is the nondimensional quantity which show the ratio of the mass transport by convection to the transfer of mass by diffusion. Mathematically:

$$Sh = \frac{kL}{D}$$

Here, L is characteristics length, D is the mass diffusivity and k is the mass transfer" coeffcient." [53]

Definition 2.5.7 [Reynolds Number]

"It is defined as the ratio of inertia force of a flowing fluid and the viscous force of the fluid. Mathematically,

$$Re = \frac{VL}{\nu},$$

where V denotes the free stream velocity, L is the characteristic length and ν stands for kinematic viscosity." [40]

2.6 Governing Laws

Definition 2.6.1 [Continuity Equation]

"The principle of conservation of mass can be stated as the time rate of change of mass is fixed volume is equal to the net rate of flow of mass across the surface. Mathematically, it can be written as

$$\frac{\partial \rho}{\partial t} + \nabla.(\rho \mathbf{v}) = 0, \text{ [54]}$$

where t is the time, ρ is the density of the medium, v the velocity vector, and ∇ is the nabla or del operator. If the fluid is an incompressible, the conservation of mass will be expressed by

$$\nabla.\mathbf{v} = 0."$$

Definition 2.6.2 [Momentum Equation]

"The momentum equation states that the time rate of change of linear momentum of a given set of particles is equal to the vector sum of all the external forces acting on the particles of the set, provided Newtons Third Law of action and reaction governs the internal forces. Mathematically, it can be written as:

$$\frac{\partial}{\partial t}(\rho \mathbf{u}) + \nabla.[(\rho \mathbf{u})\mathbf{u}] = \nabla.\mathbf{T} + \rho g." \text{ [54]}$$

Definition 2.6.3 [Energy Equation]

"The law of conservation of energy states that the time rate of change of the total energy is equal to the sum of the rate of work done by the applied forces and change of heat content per unit time.

$$\frac{\partial \rho}{\partial t} + \nabla.\rho \mathbf{u} = -\nabla.\mathbf{q} + Q + \phi,$$

where ϕ is the dissipation function." [54]

2.7 Shooting Method

The shooting method converts a boundary value problem into a set of initial value problems. If each ODEs initial condition is known, this system of ODEs can be numerically solved. The problem statement for a BVP with an nth-order ODE contains n boundary conditions, some of which are supplied at the domain's beginning and some at the end. The boundary conditions provided at the first point of the domain are utilised as initial conditions for the system. The boundary conditions provided at the domain's first point are utilised as the system's initial conditions when the nth-order ODE is turned into a system of n first-order ODEs. We make educated guesses about the additional initial conditions needed to solve the system. The system is then solved, and the boundary conditions at the domain's end point are compared to the result at that point. If the numerical solution is not precise enough, the system is solved again with new initial values determined using Newton's Iterative technique. Until the numerical solution at the domain's endpoint complies with the specified boundary conditions, this process is repeated. A thorough explanation of the shooting procedure in the event of a second-order BVP have beend discussed below.
Consider the following nonlinear boundary value problem

$$\left.\begin{aligned} U''(x) &= U(x)U'(x) + 2U^2(x) \\ U(0) &= 0, \qquad U(S) = G. \end{aligned}\right\} \tag{2.2}$$

In order to reduce the order of the above BVP, consider the following notations.

$$U = Z_1, \qquad U' = Z_1' = Z_2, \qquad U'' = Z_2'. \tag{2.3}$$

After utilizing the above mentioned notations, (2.2) is reduced into the following system of first order ODEs.

$$Z_1' = Z_2, \qquad Z_1(0) = 0, \tag{2.4}$$

$$Z_2' = Z_1 Z_2 + 2Z_1^2, \qquad Z_2(0) = e, \tag{2.5}$$

where e is the starting condition that is lacking but can be inferred using Newton's approach. The Runge-Kutta method of order four will be used to numerically solve the aforementioned IVP. It is necessary to choose the missing condition e in such a way that

$$Z_1(S, e) = G. \tag{2.6}$$

For convenience, now onward $Z_1(S, e)$ will be denoted by $Z_1(e)$.
Let us further denote $Z_1(e) - G$ by $H(e)$, so that

$$H(e) = 0. \tag{2.7}$$

The following Newton's iterative formula can be used to solve the aforementioned equation

$$e^{n+1} = e^n - \frac{H(e^n)}{\frac{\partial H(e^n)}{\partial e}},$$

or

$$e^{n+1} = e^n - \frac{Z_1(e^n) - G}{\frac{\partial Z_1(e^n)}{\partial e}}. \tag{2.8}$$

To find $\frac{\partial Z_1(e^n)}{\partial e}$, introduce the following notations

$$\frac{\partial Z_1}{\partial e} = Z_3, \quad \frac{\partial Z_2}{\partial e} = Z_4. \tag{2.9}$$

Newton's iterative formula given below can be used to solve the aforementioned equation

$$e^{n+1} = e^n - \frac{Z_1(e) - J}{Z_3(e)}. \tag{2.10}$$

We now obtain a different system of ODEs by differentiating the two first order ODE system (2.4)-(2.5) with respect to e

$$Z_3' = Z_4, \qquad Z_3(0) = 0. \tag{2.11}$$

$$Z_4' = Z_3 Y_2 + Z_1 Z_4 + 4 Z_1 Z_3, \qquad Z_4(0) = 1. \tag{2.12}$$

Writing all the four ODEs (2.4), (2.5), (2.11) and (2.12) together, we get the following initial value problem

$$\begin{aligned} Z_1' &= Z_2, & Z_1(0) &= 0 \\ Z_2' &= Z_1 Z_2 + 2 Z_1^2, & Z_2(0) &= e \\ Z_3' &= Z_4, & Z_3(0) &= 0 \\ Z_4' &= Z_3 Z_2 + Z_1 Z_4 + 4 Z_1 Z_3, & Z_4(0) &= 1. \end{aligned}$$

Runge-Kutta method of order 4 will be used to numerically solve the combined above system. The following is the set of halting criteria for the Newton's technique:

$$\mid Z_1(e) - G \mid < \epsilon,$$

where ϵ is an arbitrarily small positive number.

Chapter 3

Non-Darcian MHD Williamson Nanofluid for the Entropy Analysis in the Presence of Nonlinear Thermal Radiation across a Stratified Sheet

3.1 Introduction

In this chapter, a comprehensive review of the work done by Bilal et al. [37] has been presented. The non-linear PDEs governing the flow model are converted into a system of dimensionless ODEs with the use of appropriate similarity transformations. With the help of the shooting technique, the ODEs have been solved using the MATLAB software. The numerical computations for the analysis of the impact of the variation of various dimentionless parameters on $f'(\eta)$, $\theta(\eta)$, $\phi(\eta)$ and on the rate of entropy generation N_G has been discussed in the last part of this chapter. Tables and graphs have been used to present the numerical results for the clear visualization of the reader.

3.2 Description of Problem

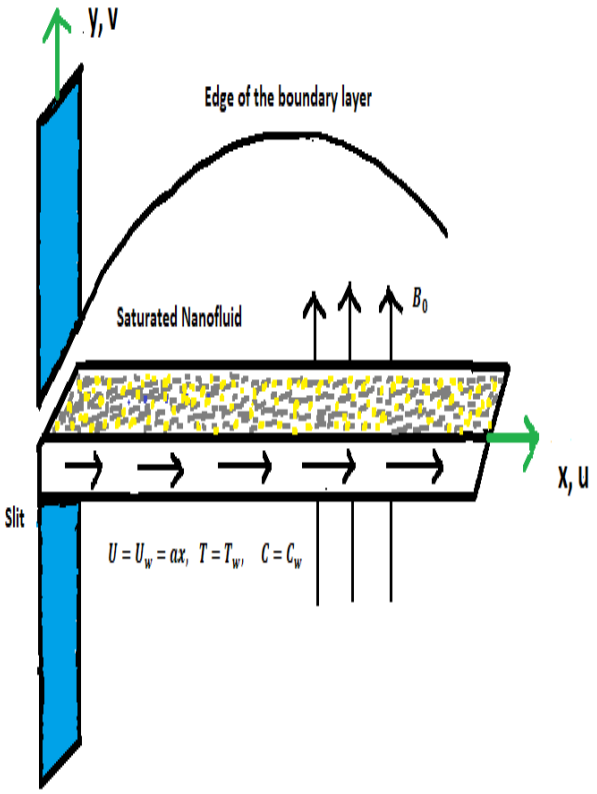

FIGURE 3.1: Geometry of physical model

A stratified sheet has been used to study a two dimentional non-Darcian MHD Williamson nanofluid flow. The irreversibilities of thermal conductivity, Joule dissipation, and the Ohmic effect are utilized to examine the production of entropy. The sheet is supposed to be stretching down the x-axis with a velocity of $u = U_w(x) = ax$, where a is a positive constant. Figure 3.1 shows the physical flow model. The x-axis in the figure is taken in the direction of the stretching velocity, and the y-axis is taken perpendicular to it. While $C_\infty = C_0 + Ex$ is used as the ambient concentration, $T_\infty = T_0 + Bx$ represents the ambient temperature.

The wall's temperature and concentration have been taken as, $T_w = T_0 + Ax$ and $C_w = C_0 + Dx$ respectively.

3.2.1 The Governing PDEs

The set of equations which govern the flow pattern are as follows:

$$\frac{\partial u}{\partial x} + \frac{\partial v}{\partial y} = 0, \tag{3.1}$$

$$u\frac{\partial u}{\partial x} + v\frac{\partial u}{\partial y} = \nu\frac{\partial^2 u}{\partial y^2} + \sqrt{2}\nu\gamma\frac{\partial u}{\partial y}\frac{\partial^2 u}{\partial y^2} - \frac{\sigma}{\rho}{B_0}^2 u - \frac{\nu}{k^*}u - \frac{C_F}{\sqrt{k^*}}u^2, \tag{3.2}$$

$$(\rho C_p)_f\left(u\frac{\partial T}{\partial x} + v\frac{\partial T}{\partial y}\right) = k\frac{\partial^2 T}{\partial y^2} + (\rho C_p)_S\left[D_B\frac{\partial T}{\partial y}\frac{\partial C}{\partial Y} + \frac{D_T}{T_\infty}(\frac{\partial T}{\partial y})^2\right] + \sigma{B_0}^2u^2 + \mu_0\left(\frac{\partial u}{\partial y}\right)^2 + \mu_0\gamma\left(\frac{\partial u}{\partial y}\right)^3 - \frac{\partial q_r}{\partial y}, \tag{3.3}$$

$$u\frac{\partial C}{\partial x} + v\frac{\partial C}{\partial y} = D_B\frac{\partial^2 C}{\partial y^2} + \frac{D_T}{T_\infty}\frac{\partial^2 T}{\partial y^2} - k_1(C - C_\infty). \tag{3.4}$$

The boundary conditions corresponding to the flow model are given below.

$$\left.\begin{aligned} &u = U_w(x) = ax, \quad v = 0, \quad T = T_w, \quad C = C_w, \quad at \quad y = 0, \\ &u \to 0, \quad T \to T_\infty, \quad C \to C_\infty \quad as \quad y \to \infty. \end{aligned}\right\} \tag{3.5}$$

3.2.2 Similarity Transformations

The following analogies will be utilized to transform the nonlinear PDEs into a system of dimensionless ODEs.

$$\left.\begin{aligned} &u = axf'(\eta), \qquad v = -\sqrt{a\nu}f(\eta), \qquad \eta = \sqrt{\frac{a}{\nu}}y, \\ &\theta(\eta) = \frac{T - T_\infty}{T_w - T_0}, \qquad \phi(\eta) = \frac{C - C_\infty}{C_w - C_0}, \end{aligned}\right\} \tag{3.6}$$

where $T = T_w = T_0 + Ax$, $T_\infty = T_0 + Bx$, $C = C_w = C_0 + Dx$, $C_\infty = C_0 + Ex$. Here A, B, C, D and E are the dimentional constants having unit K/m. From

(3.6), T can be written as

$$\begin{aligned} T &= (T_w - T_0)\theta(\eta) + T_\infty \\ &= Ax\theta(\eta) + (T_0 + Bx) \\ &= (T_0 + Bx)\left[\frac{Ax}{T_0 + Bx}\theta(\eta) + 1\right] \\ &= T_\infty\left(\frac{Ax}{Bx(\frac{T_0}{Bx} + 1)}\theta(\eta) + 1\right) \\ &= T_\infty\left(\frac{\theta(\eta)}{N_2(N_3 + 1)} + 1\right), \end{aligned} \tag{3.7}$$

where the temperature ratios N_2 and N_3 are formulated as:

$$N_2 = \frac{B}{A}, \quad N_3 = \frac{T_0}{Bx}.$$

The radiative heat flux q_r can be expressed as

$$\begin{aligned} q_r &= -\frac{4\sigma^*}{3k^*}\frac{\partial T^4}{\partial y} \\ &= -\frac{16\sigma^*}{3k^*}T^3\frac{\partial T}{\partial y}, \end{aligned} \tag{3.8}$$

where the absorption coefficient is k^* and the Stefan-Boltzman constant is σ^*. A Taylor series can be used to expand T^4 about T_∞ if the temperature difference is relatively modest.

$$T^4 = T_\infty^4 + 4T_\infty^3(T - T_\infty) + 6T_\infty^2(T - T_\infty)^2 + ...$$

Leaving aside the higher order terms, we have

$$T^4 = T_\infty^4 + 4T_\infty^3(T - T_\infty)$$

$$\begin{aligned} &= T_\infty^4 + 4T_\infty^3 T - 4T_\infty^4 \\ &= -3T_\infty^4 + 4T_\infty^3 T \\ &= 4T_\infty^3 T - 3T_\infty^4. \end{aligned}$$

Now differentiating both side of (3.8) w.r.t. to y,

$$\begin{aligned}\frac{\partial q_r}{\partial y} &= \frac{\partial}{\partial y}\left(-\frac{16\sigma^*}{3k^*}T^3\frac{\partial T}{\partial y}\right)\\ &= -\frac{16\sigma^*}{3k^*}\frac{\partial}{\partial y}\left(T^3\frac{\partial T}{\partial y}\right)\\ &= -\frac{16\sigma^*}{3k^*}\left(T^3\frac{\partial^2 T}{\partial y^2}+3T^2\left(\frac{\partial T}{\partial y}\right)^2\right).\end{aligned}$$

Now, by using the expression of T from (3.7), the above will be reduced to

$$\begin{aligned}\frac{\partial q_r}{\partial y} = -\frac{16\sigma^*}{3k^*}\Bigg[&T_\infty^3\left(\frac{\theta(\eta)}{N_2(N_3+1)}+1\right)^3(Ax\theta''(\eta)\frac{a}{\nu})\\ &+3T_\infty^2\left(\frac{\theta(\eta)}{N_2(N_3+1)}+1\right)^2\frac{a(Ax)^2}{\nu}(\theta'(\eta))^2\Bigg].\end{aligned} \tag{3.9}$$

3.2.3 Physical Quantities of Interest

Below are the skin friction coefficient, Nusselt number, and Sherwood number in their dimensional form. In the next section of this chapter, when we explore the solution to our flow problem, the dimensionless version of these parameters will be derived and employed.

$$\left.\begin{aligned}C_{fx} &= \frac{-2(\tau_w)_{y=0}}{\rho u_w^2(x)}\\ Nu_x &= \frac{xq_w}{k(T_w-T_\infty)}\\ Sh_x &= \frac{xq_m}{D_B(C_w-C_\infty)}\end{aligned}\right\} \tag{3.10}$$

3.2.4 Entropy Generation Modeling

Physically speaking, entropy is a disorder of a system and surroundings. Entropy generally develops in a variety of systems, notably those involving flow-driven force, Joule heating, and fluid viscous force. Therefore, entropy is also known as the number of irreversibilities. Because of this, heat cannot be completely changed

into work. In dimensional form, the entropy generation is written as:

$$S_G = \frac{k}{T_\infty^2}\left[\left(\frac{\partial T}{\partial y}\right)^2 + \frac{16\sigma^* T^3}{3kk^*}\left(\frac{\partial T}{\partial y}\right)^2\right] + \frac{RD_A}{C_\infty}\left(\frac{\partial C}{\partial y}\right)^2 + \frac{\sigma}{T_\infty}B_0^2u^2 + \frac{RD_A}{C_\infty}\left(\frac{\partial C}{\partial y}\right)\left(\frac{\partial T}{\partial y}\right) + \frac{\mu_0}{T_\infty}\left[\left(\frac{\partial u}{\partial y}\right)^2 + \gamma\left(\frac{\partial u}{\partial y}\right)^3\right]. \tag{3.11}$$

3.3 Conversion of Mathematical Model into Dimentionless Form

3.3.1 The Governing ODEs

The detailed procedure for the conversion of (3.1) to (3.4) into the dimentionless form has been discussed below.

$$\frac{\partial u}{\partial x} = \frac{\partial}{\partial x}\Big(axf'(\eta)\Big) = af'(\eta) \tag{3.12}$$

$$\frac{\partial v}{\partial y} = \frac{\partial}{\partial y}\Big(-\sqrt{a\nu}f(\eta)\Big) = -af'(\eta) \tag{3.13}$$

The continuity equation (3.1) can easily be seen satisfied by adding (3.12) and (3.13) as follows:

$$\frac{\partial u}{\partial x} + \frac{\partial v}{\partial y} = af'(\eta) - af'(\eta) = 0.$$

Moreover,

$$\begin{aligned} u\frac{\partial u}{\partial x} + v\frac{\partial u}{\partial y} &= axf'(\eta).af'(\eta) - \sqrt{a\nu}f(\eta)\frac{\partial}{\partial y}(axf'(\eta)) \\ &= axf'(\eta).af'(\eta) - \sqrt{a\nu}f(\eta).axf''(\eta)\frac{\partial}{\partial y}(\eta) \\ &= axf'(\eta)\Big(af'(\eta)\Big) - \sqrt{a\nu}f(\eta)\Big(axf''(\eta)\sqrt{\frac{a}{\nu}}\Big). \end{aligned}$$

After simplifying, we get the left side of the momentun equation (3.2) as follows:

$$u\frac{\partial u}{\partial x}+v\frac{\partial u}{\partial y}=a^2xf'^2(\eta)-a^2xf(\eta)f''(\eta). \tag{3.14}$$

In order to reform the right side of the momentum equation, the following derivatives will be helpful

$$\begin{aligned}\nu\frac{\partial^2 u}{\partial y^2}&=\nu\frac{\partial}{\partial y}\left(axf''(\eta)\sqrt{\frac{a}{\nu}}\right)\\&=\nu ax f'''(\eta)\sqrt{\frac{a}{\nu}}\sqrt{\frac{a}{\nu}}\\&=\nu ax\frac{a}{\nu}f'''(\eta)=a^2xf'''(\eta)\end{aligned} \tag{3.15}$$

$$\begin{aligned}\Rightarrow\sqrt{2}\nu\gamma\frac{\partial u}{\partial y}\frac{\partial^2 u}{\partial y^2}&=\sqrt{2}\nu\gamma\left((axf''(\eta))\sqrt{\frac{a}{\nu}}\right)\left(\frac{a^2x}{\nu}f'''(\eta)\right)\\&=\left(\sqrt{2}\gamma\frac{a^3x^2\sqrt{a}}{\sqrt{\nu}}\right)f''(\eta)f'''(\eta)\end{aligned} \tag{3.16}$$

Furthermore,

$$\frac{\sigma}{\rho}B_0^2u=\frac{\sigma}{\rho}B_0^2axf'(\eta), \tag{3.17}$$

$$\frac{\nu}{k^*}u=\frac{\nu}{k^*}axf'(\eta), \tag{3.18}$$

$$\frac{C_F}{\sqrt{k^*}}u^2=\frac{C_F}{\sqrt{k^*}}a^2x^2f'^2(\eta). \tag{3.19}$$

As a result, the right side of (3.2) gets the form:

$$a^2xf'''+\left(\sqrt{2}\gamma\frac{a^3x^2\sqrt{a}}{\sqrt{\nu}}\right)f''f'''-\frac{\sigma}{\rho}B_0^2axf'-\frac{\nu}{k^*}axf'-\frac{C_F}{\sqrt{k^*}}a^2x^2f'^2. \tag{3.20}$$

By equating (3.14) and (3.20), we get

$$\begin{aligned}a^2xf'^2-a^2xff''=a^2xf'''+\left(\sqrt{2}\gamma\frac{a^3x^2\sqrt{a}}{\sqrt{\nu}}\right)f''f'''-\frac{\sigma}{\rho}B_0^2axf'\\-\frac{\nu}{k^*}axf'-\frac{C_F}{\sqrt{k^*}}a^2x^2f'^2\end{aligned}$$

$$\Rightarrow f'^2 - ff'' = f''' + \sqrt{2}\gamma\frac{ax\sqrt{a}}{\sqrt{\nu}}f''f''' - \frac{\sigma}{a\rho}B_0^2 f' - \frac{\nu}{ak^*}f' - \frac{C_F}{\sqrt{k^*}}xf'^2$$

$$\Rightarrow f''' - f'^2(\eta) + ff'' + \sqrt{2}\gamma\frac{ax\sqrt{a}}{\sqrt{\nu}}f''f''' - \frac{\sigma}{a\rho}B_0^2 f' - \frac{\nu}{ak^*}f' - \frac{C_F}{\sqrt{k^*}}xf'^2 = 0$$

$$\Rightarrow f''' = f'^2 - ff'' - Wef''f''' + Mf' + \lambda f' + Frf'^2. \tag{3.21}$$

In (3.21), Fr represents the inertial coefficient, We the Weissenberg number and M the magnetic parameter. The dimentionless parameters used in the above expression are formulated as follows:

$$We = \sqrt{\frac{2a^3}{\nu}}\gamma x, \qquad M = \left(\frac{\sigma B_0^2}{\rho a}\right), \qquad \lambda = \frac{\nu}{ak^*}, \qquad Fr = \frac{xC_F}{\sqrt{k^*}}.$$

For the conversion of energy equation (3.3), the following procedure will be helpful.

$$\theta(\eta) = \frac{T - T_\infty}{T_w - T_0}.$$

$$\Rightarrow T = T_\infty + (T_w - T_0)\theta(\eta).$$

We also know that

$$\begin{aligned}
&T_\infty = T_0 + Bx,\\
&T_w - T_0 = Ax.\\
\because\ &T = (T_0 + Bx) + (Ax)\theta(\eta).\\
\therefore\ &\frac{\partial T}{\partial x} = \frac{\partial}{\partial x}\Big((T_0 + Bx) + (Ax)\theta(\eta)\Big)\\
&\qquad = B + A\theta(\eta).\\
\Rightarrow\ &u\frac{\partial T}{\partial x} = axf'(\eta)\Big(B + A\theta(\eta)\Big)\\
&\qquad = Baxf'(\eta) + aAxf'(\eta)\theta(\eta).
\end{aligned} \tag{3.22}$$

Furthermore,

$$\begin{aligned}
\Rightarrow \frac{\partial T}{\partial y} &= \frac{\partial}{\partial y}\Big((T_0 + Bx) + (Ax)\theta(\eta)\Big)\\
&= Ax\theta'(\eta)\frac{\partial}{\partial y}\Big(\eta\Big)
\end{aligned}$$

$$= Ax\theta'(\eta)\sqrt{\frac{a}{\nu}}. \tag{3.23}$$

$$\begin{aligned}\Rightarrow v\frac{\partial T}{\partial y} &= v\left(Ax\theta'(\eta)\sqrt{\frac{a}{\nu}}\right)\\ &= (-\sqrt{a\nu}f'(\eta))\left(Ax\theta'(\eta)\sqrt{\frac{a}{\nu}}\right)\\ &= -aAxf(\eta)\theta'(\eta).\end{aligned} \tag{3.24}$$

By adding (3.22) and (3.24), we get

$$\begin{aligned}u\frac{\partial T}{\partial x} + v\frac{\partial T}{\partial y} &= Baxf'(\eta) + aAxf'(\eta)\theta(\eta) - aAxf(\eta)\theta'(\eta).\\ \Rightarrow (\rho C_P)_f\left(u\frac{\partial T}{\partial x} + v\frac{\partial T}{\partial y}\right) &= (\rho C_P)_f\left(Baxf' + aAxf'\theta) - aAxf\theta'\right).\end{aligned} \tag{3.25}$$

Now, the following procedure will help us to compute the right side of the energy equation.

$$\begin{aligned}\frac{\partial T}{\partial y} &= Ax\sqrt{\frac{a}{\nu}}\theta'(\eta).\\ \Rightarrow \frac{\partial}{\partial y}\left(\frac{\partial T}{\partial y}\right) &= \frac{\partial}{\partial y}\left(Ax\sqrt{\frac{a}{\nu}}\theta'(\eta)\right).\\ \Rightarrow \frac{\partial^2 T}{\partial y^2} &= Ax\theta''(\eta)\frac{a}{\nu}.\\ \Rightarrow k\frac{\partial^2 T}{\partial y^2} &= \frac{kaAx}{\nu}\theta''(\eta).\end{aligned} \tag{3.26}$$

From (3.6), we can write

$$C = C_\infty + (C_w - C_\infty)\phi(\eta).$$

Since

$$C_\infty = C_0 + Ex,$$

$$C_w = C_\infty + Dx,$$

therefore,

$$\begin{aligned}
&C = C_0 + Ex + Dx\phi(\eta).\\
\Rightarrow \frac{\partial C}{\partial y} &= \frac{\partial}{\partial y}\bigg(C_0 + Ex + Dx\phi(\eta)\bigg)\\
&= Dx\phi'(\eta)\frac{\partial}{\partial y}(\eta)\\
&= Dx\sqrt{\frac{a}{\nu}}\phi'(\eta).\\
\Rightarrow \frac{\partial C}{\partial y}\frac{\partial T}{\partial y} &= Dx\sqrt{\frac{a}{\nu}}\phi'(\eta)Ax\sqrt{\frac{a}{\nu}}\theta'(\eta)\\
&= (Ax)(Dx)\frac{a}{\nu}\theta'(\eta)\phi'(\eta).\\
\Rightarrow D_B\bigg(\frac{\partial C}{\partial y}\frac{\partial T}{\partial y}\bigg) &= D_B\bigg((Ax)(Dx)\frac{a}{\nu}\theta'(\eta)\phi'(\eta)\bigg).
\end{aligned}$$

By using the formulation of D_B, we get

$$\begin{aligned}
D_B\bigg(\frac{\partial C}{\partial y}\frac{\partial T}{\partial y}\bigg) &= \frac{Nb\nu(\rho C_P)_f}{(\rho C_P)_S Dx}\bigg((Ax)(Dx)\frac{a}{\nu}\theta'(\eta)\phi'(\eta)\bigg)\\
&= \frac{Nb(\rho C_P)_f}{(\rho C_P)_S}\bigg(aAx\theta'(\eta)\phi'(\eta)\bigg).
\end{aligned} \tag{3.27}$$

As computed earlier,

$$\begin{aligned}
&\frac{\partial T}{\partial y} = Ax\sqrt{\frac{a}{\nu}}\theta'(\eta).\\
\Rightarrow \bigg(\frac{\partial T}{\partial y}\bigg)^2 &= \bigg(Ax\sqrt{\frac{a}{\nu}}\theta'(\eta)\bigg)^2\\
&= (Ax)^2\frac{a}{\nu}\theta'^2(\eta).\\
\Rightarrow \frac{D_T}{T_\infty}\bigg(\frac{\partial T}{\partial y}\bigg)^2 &= \frac{D_T}{T_\infty}\bigg((Ax)^2\frac{a}{\nu}\theta'^2(\eta)\bigg).
\end{aligned} \tag{3.28}$$

By using the value of the parameter D_T, we get

$$\begin{aligned}
\frac{D_T}{T_\infty}\bigg(\frac{\partial T}{\partial y}\bigg)^2 &= \frac{Nt\nu(\rho C_P)_f T_\infty}{(\rho C_P)_S AxT_\infty}\bigg((Ax)^2\frac{a}{\nu}\theta'^2(\eta)\bigg)\\
&= \frac{Nt(\rho C_P)_f}{(\rho C_P)_S}\bigg(aAx\theta'^2(\eta)\bigg).
\end{aligned} \tag{3.29}$$

By adding (3.27) and (3.29), we get

$$D_B\left(\frac{\partial C}{\partial y}\frac{\partial T}{\partial y}\right)+\frac{D_T}{T_\infty}\left(\frac{\partial T}{\partial y}\right)^2=\frac{Nb(\rho C_P)_f}{(\rho C_P)_S}\left(aAx\theta'\phi'\right)+\frac{Nt(\rho C_P)_f}{(\rho C_P)_S}\left(aAx\theta'^2\right).$$

$$\Rightarrow(\rho C_P)_S\left[D_B\left(\frac{\partial C}{\partial y}\frac{\partial T}{\partial y}\right)+\frac{D_T}{T_\infty}\left(\frac{\partial T}{\partial y}\right)^2\right]=(\rho C_P)_S\left[\frac{Nb(\rho C_P)_f}{(\rho C_P)_S}\left(aAx\theta'\phi'\right)+\frac{Nt(\rho C_P)_f}{(\rho C_P)_S}\left(aAx\theta'^2\right)\right].$$

$$\Rightarrow(\rho C_P)_S\left[D_B\left(\frac{\partial C}{\partial y}.\frac{\partial T}{\partial y}\right)+\frac{D_T}{T_\infty}\left(\frac{\partial T}{\partial y}\right)^2\right]=Nb(\rho C_p)_f\left(aAx\theta'\phi'\right)+Nt(\rho C_p)_f\left(aAx\theta'^2\right). \tag{3.30}$$

By using the formula of B_0^2 and u, we get

$$\sigma B_0^2u^2=\sigma\frac{M\rho a}{\sigma}\left(axf')(\eta)\right)^2$$
$$=a^3M\rho x^2f'^2(\eta), \tag{3.31}$$
$$\mu_0\left(\frac{\partial u}{\partial y}\right)^2=\mu_0\left(\frac{\partial}{\partial y}(axf'(\eta))\right)^2$$
$$=\mu_0\left(axf''(\eta))\frac{\partial}{\partial y}(\eta)\right)^2$$
$$=\mu_0\left(axf''(\eta))\sqrt{\frac{a}{\nu}}\right)^2$$
$$=\frac{\mu_0a^3x^2}{\nu}f''^2(\eta). \tag{3.32}$$
$$\Rightarrow\mu_0\gamma\left(\frac{\partial u}{\partial y}\right)^3=\mu_0\gamma\left(\frac{\partial}{\partial y}(axf'(\eta))\right)^3$$
$$=\mu\gamma\left(axf''(\eta))\frac{\partial}{\partial y}(\eta)\right)^3$$
$$=\frac{\mu_0\gamma a^{\frac{9}{2}}x^3}{\nu^{\frac{3}{2}}}f'''^3(\eta). \tag{3.33}$$

From (3.9),

$$\frac{\partial q_r}{\partial y} = -\frac{16\sigma^*}{3k^*}\left[T_\infty^3\left(\frac{\theta(\eta)}{N_2(N_3+1)}+1\right)^3(Ax\theta''(\eta)\frac{a}{\nu}) + 3T_\infty^2\left(\frac{\theta(\eta)}{N_2(N_3+1)}+1\right)^2\frac{a(Ax)^2}{\nu}(\theta'(\eta))^2\right].$$

After expanding and simplifying the expression, we get

$$\begin{aligned}
\Rightarrow \frac{\partial q_r}{\partial y} &= -\frac{16\sigma^*}{3k^*}\frac{aAxT_\infty^3}{\nu}\left[\left(\frac{1}{N_2(N_3+1)}\right)^3\theta^3(\eta)\theta''(\eta)+\theta''(\eta)\right.\\
&\quad+3\left(\frac{1}{N_2(N_3+1)}\right)^2\theta^2(\eta)\theta''(\eta)+3\left(\frac{1}{N_2(N_3+1)}\right)\theta(\eta)\theta''(\eta)\\
&\quad+3\left(\frac{1}{N_2(N_3+1)}\right)^2\theta^2(\eta)\theta'^2(\eta)+3\left(\frac{1}{N_2(N_3+1)}\right)\theta'^2(\eta)\\
&\quad\left.+6\left(\frac{1}{N_2(N_3+1)}\right)^2\theta(\eta)\theta'^2(\eta)\right].\\
\Rightarrow -\frac{\partial q_r}{\partial y} &= \frac{16\sigma^*}{3k^*}\frac{aAxT_\infty^3}{\nu}\left[\left(\frac{1}{N_2(N_3+1)}\right)^3\theta^3(\eta)\theta''(\eta)+\theta''(\eta)\right.\\
&\quad+3\left(\frac{1}{N_2(N_3+1)}\right)^2\theta^2(\eta)\theta''(\eta)+3\left(\frac{1}{N_2(N_3+1)}\right)\theta(\eta)\theta''(\eta)\\
&\quad+3\left(\frac{1}{N_2(N_3+1)}\right)^2\theta^2(\eta)\theta'^2(\eta)+3\left(\frac{1}{N_2(N_3+1)}\right)\theta'^2(\eta)\\
&\quad\left.+6\left(\frac{1}{N_2(N_3+1)}\right)^2\theta(\eta)\theta'^2(\eta)\right]. \qquad (3.34)
\end{aligned}$$

Adding (3.26), (3.30), (3.31), (3.32), (3.33) and (3.34), we get

$$\begin{aligned}
&k\frac{\partial^2 T}{\partial y^2}+(\rho C_p)_S\left[D_B\frac{\partial T}{\partial y}\frac{\partial C}{\partial y}+\frac{D_T}{T_\infty}\left(\frac{\partial T}{\partial y}\right)^2\right]+\sigma {B_0}^2u^2+\mu_0\left(\frac{\partial u}{\partial y}\right)^2+\mu_0\gamma\left(\frac{\partial u}{\partial y}\right)^3\\
&-\frac{\partial q_r}{\partial y}=\frac{kaAx}{\nu}\theta''(\eta)+Nb(\rho C_p)_f\left(aAx\theta'(\eta)\phi'(\eta)\right)+Nt(\rho C_p)_f\left(aAx\theta'^2(\eta)\right)\\
&+a^3M\rho x^2f'^2(\eta)+\frac{\mu_0a^3x^2}{\nu}f''^2(\eta)+\frac{\mu_0\gamma a^{\frac{9}{2}}x^3}{\nu^{\frac{3}{2}}}f''^3(\eta)\\
&+\frac{16\sigma^*}{3k^*}\frac{aAxT_\infty^3}{\nu}\left[\left(\frac{1}{N_2(N_3+1)}\right)^3\theta^3(\eta)\theta''(\eta)+\theta''(\eta)\right.\\
&+3\left(\frac{1}{N_2(N_3+1)}\right)^2\theta^2(\eta)\theta''(\eta)+3\left(\frac{1}{N_2(N_3+1)}\right)\theta(\eta)\theta''(\eta)
\end{aligned}$$

$$
\begin{aligned}
&+3\left(\frac{1}{N_2(N_3+1)}\right)^2\theta^2(\eta)\theta'^2(\eta)\\
&+3\left(\frac{1}{N_2(N_3+1)}\right)\theta'^2(\eta)+6\left(\frac{1}{N_2(N_3+1)}\right)^2\theta(\eta)\theta'^2(\eta)\Bigg]\\
&=\frac{kaAx}{\nu}\theta''(\eta)+Nb(\rho C_p)_f\left(aAx\theta'(\eta)\phi'(\eta)\right)+Nt(\rho C_p)_f\left(aAx\theta'^2(\eta)\right)\\
&+a^3M\rho x^2f'^2(\eta)+\frac{\mu_0a^3x^2}{\nu}f''^2(\eta)+\frac{\mu_0\gamma a^{\frac{9}{2}}x^3}{\nu^{\frac{3}{2}}}f''^3(\eta)\\
&+\frac{16\sigma^*}{3k^*}\frac{aAxT_\infty^3}{\nu}\Bigg[\left(\frac{1}{N_2(N_3+1)}\right)^3\theta^3(\eta)\theta''(\eta)+\theta''(\eta)\\
&+3\left(\frac{1}{N_2(N_3+1)}\right)^2\theta^2(\eta)\theta''(\eta)+3\left(\frac{1}{N_2(N_3+1)}\right)\theta(\eta)\theta''(\eta)\\
&+3\left(\frac{1}{N_2(N_3+1)}\right)^2\theta^2(\eta)\theta'^2(\eta)\\
&+3\left(\frac{1}{N_2(N_3+1)}\right)\theta'^2(\eta)+6\left(\frac{1}{N_2(N_3+1)}\right)^2\theta(\eta)\theta'^2(\eta)\Bigg].
\end{aligned}
\tag{3.35}
$$

By equating (3.25) and (3.35), we get

$$
\begin{aligned}
&(\rho C_P)_f\left(Baxf'(\eta)+aAxf'(\eta)\theta(\eta)-aAxf(\eta)\theta'(\eta)\right)=\frac{kaAx}{\nu}\theta''(\eta)\\
&+Nb(\rho C_p)_f\left(aAx\theta'(\eta)\phi'(\eta)\right)+Nt(\rho C_p)_f\left(aAx\theta'^2(\eta)\right)+a^3M\rho x^2f'^2(\eta)\\
&+\frac{\mu_0a^3x^2}{\nu}f''^2(\eta)+\frac{\mu_0\gamma a^{\frac{9}{2}}x^3}{\nu^{\frac{3}{2}}}f''^3(\eta)\\
&+\frac{16\sigma^*}{3k^*}\frac{aAxT_\infty^3}{\nu}\Bigg[\left(\frac{1}{N_2(N_3+1)}\right)^3\theta^3(\eta)\theta''(\eta)+\theta''(\eta)\\
&+3\left(\frac{1}{N_2(N_3+1)}\right)^2\theta^2(\eta)\theta''(\eta)+3\left(\frac{1}{N_2(N_3+1)}\right)\theta(\eta)\theta''(\eta)\\
&+3\left(\frac{1}{N_2(N_3+1)}\right)^2\theta^2(\eta)\theta'^2(\eta)\\
&+3\left(\frac{1}{N_2(N_3+1)}\right)\theta'^2(\eta)+6\left(\frac{1}{N_2(N_3+1)}\right)^2\theta(\eta)\theta'^2(\eta)\Bigg].
\end{aligned}
$$

$$
\begin{aligned}
&\Rightarrow \frac{kaAx}{\nu}\theta''(\eta) - (\rho C_P)_f\Bigg(Baxf'(\eta) + aAxf'(\eta)\theta(\eta) - aAxf(\eta)\theta'(\eta)\Bigg)\\
&\quad + Nb(\rho C_p)_f\Bigg(aAx\theta'(\eta)\phi'(\eta)\Bigg) + Nt(\rho C_p)_f\Bigg(aAx\theta'^2(\eta)\Bigg) + a^3M\rho x^2f'^2(\eta)\\
&\quad + \frac{\mu_0 a^3x^2}{\nu}f''^2(\eta) + \frac{\mu_0\gamma a^{\frac{9}{2}}x^3}{\nu^{\frac{3}{2}}}f''^3(\eta)\\
&\quad + \frac{16\sigma^*}{3k^*}\frac{aAxT_\infty^3}{\nu}\Bigg[\Bigg(\frac{1}{N_2(N_3+1)}\Bigg)^3\theta^3(\eta)\theta''(\eta) + \theta''(\eta)\\
&\quad + 3\Bigg(\frac{1}{N_2(N_3+1)}\Bigg)^2\theta^2(\eta)\theta''(\eta) + 3\Bigg(\frac{1}{N_2(N_3+1)}\Bigg)\theta(\eta)\theta''(\eta)\\
&\quad + 3\Bigg(\frac{1}{N_2(N_3+1)}\Bigg)^2\theta^2(\eta)\theta'^2(\eta)\\
&\quad + 3\Bigg(\frac{1}{N_2(N_3+1)}\Bigg)\theta'^2(\eta) + 6\Bigg(\frac{1}{N_2(N_3+1)}\Bigg)^2\theta(\eta)\theta'^2(\eta)\Bigg] = 0.\\
&\Rightarrow \theta''(\eta) - \frac{\nu(\rho C_P)_f}{k}\frac{B}{A}f'(\eta) - \frac{\nu(\rho C_P)_f}{k}f'(\eta)\theta(\eta) + \frac{\nu(\rho C_P)_f}{k}f(\eta)\theta'(\eta)\\
&\quad + \frac{Nb\nu(\rho C_p)_f}{k}\theta'(\eta)\phi'(\eta) + \frac{Nt\nu(\rho C_p)_f}{k}\theta'^2(\eta) + \frac{a^2M\rho x^2}{kAx}f'^2(\eta) + \frac{\mu_0 a^2x^2}{kAx}f''^2(\eta)\\
&\quad + \frac{\mu_0\gamma a^{\frac{7}{2}}x^3}{\nu^{\frac{1}{2}}kAx}f''^3(\eta) + \frac{16\sigma^*}{3k^*}\frac{T_\infty^3}{k}\Bigg[\Bigg(\frac{1}{N_2(N_3+1)}\Bigg)^3\theta^3(\eta)\theta''(\eta) + \theta''(\eta)\\
&\quad + 3\Bigg(\frac{1}{N_2(N_3+1)}\Bigg)^2\theta^2(\eta)\theta''(\eta) + 3\Bigg(\frac{1}{N_2(N_3+1)}\Bigg)\theta(\eta)\theta''(\eta)\\
&\quad + 3\Bigg(\frac{1}{N_2(N_3+1)}\Bigg)^2\theta^2(\eta)\theta'^2(\eta)\\
&\quad + 3\Bigg(\frac{1}{N_2(N_3+1)}\Bigg)\theta'^2(\eta) + 6\Bigg(\frac{1}{N_2(N_3+1)}\Bigg)^2\theta(\eta)\theta'^2(\eta)\Bigg] = 0.
\end{aligned}
$$

By using the definitions of different dimentionless parameters in the above expression, we will get the more compact form as the following.

$$
\begin{aligned}
&\theta''(\eta) + Pr\Bigg[f(\eta)\theta'(\eta) - N_2f'(\eta) - f'(\eta)\theta(\eta) + Nb\Bigg(\theta'(\eta)\phi'(\eta) + \frac{N_t}{Nb}\theta'^2(\eta)\Bigg)\\
&\quad + MEcf'^2(\eta) + Ecf''^2(\eta) + \frac{WeEc}{\sqrt{2}}f''^3(\eta)\Bigg] + \frac{4}{3}Rd\Bigg[\Bigg(\frac{1}{N_2(N_3+1)}\Bigg)^3\theta^3(\eta)\theta''(\eta)
\end{aligned}
$$

$$+\theta''(\eta)+3\left(\frac{1}{N_2(N_3+1)}\right)^2\theta^2(\eta)\theta''(\eta)+3\left(\frac{1}{N_2(N_3+1)}\right)\theta(\eta)\theta''(\eta)$$
$$+3\left(\frac{1}{N_2(N_3+1)}\right)^2\theta^2(\eta)\theta'^2(\eta)$$
$$+3\left(\frac{1}{N_2(N_3+1)}\right)\theta'^2(\eta)+6\left(\frac{1}{N_2(N_3+1)}\right)^2\theta(\eta)\theta'^2(\eta)\Bigg]=0.$$

Let $A_1=\frac{1}{N_2(N_3+1)}$, then the above equation becomes

$$\theta''(\eta)+Pr\Bigg[f(\eta)\theta'(\eta)-N_2f'(\eta)-f'(\eta)\theta(\eta)+Nb\left(\theta'(\eta)\phi'(\eta)+\frac{Nt}{Nb}\theta'^2(\eta)\right)$$
$$+MEcf'^2(\eta)+Ecf''^2(\eta)+\frac{WeEc}{\sqrt{2}}f''^3(\eta)\Bigg]+\frac{4}{3}Rd\Bigg[A_1^3\theta^3(\eta)\theta''(\eta)+\theta''(\eta)$$
$$+3A_1^2\theta^2(\eta)\theta''(\eta)+3A_1\theta(\eta)\theta''(\eta)$$
$$+3A_1^2\theta^2(\eta)\theta'^2(\eta)+3A_1\theta'^2(\eta)+6A_1^2\theta(\eta)\theta'^2(\eta)\Bigg]=0. \tag{3.36}$$

In (3.36), Pr represents the Prandtl number, Ec the Eckert number, We the Weissenberg number, M the magnetic parameter, Nt the thermophoresis parameter, Nb the Brownian motion parameter, N_2 the temperature ratio and Rd represents the thermal radiation parameter. The dimentionless parameters used in the above equation are formulated as:

$$\left.\begin{aligned}
&Pr=\frac{\nu(\rho C_P)_f}{k},\quad Ec=\frac{a^2x^2}{C_P(Ax)},\\
&We=\sqrt{\frac{2a^3}{\nu}}\gamma x,\quad M=\frac{\sigma B_0^2}{\rho a},\\
&N_2=\frac{B}{A},\quad Nt=\frac{(\rho C_P)_S D_T(T_w-T_0)}{\nu(\rho C_P)_f T_\infty},\\
&Nb=\frac{(\rho C_P)_S D_B(C_w-C_0)}{\nu(\rho C_P)_f}.
\end{aligned}\right\} \tag{3.37}$$

Now, the conversion of concentration equation (3.4) will be discussed in detail

$$\begin{aligned} C &= C_0 + Ex + (Dx)\phi(\eta) \\ \Rightarrow \frac{\partial C}{\partial x} &= \frac{\partial}{\partial x}\Big(C_0 + Ex + (Dx)\phi(\eta)\Big) = E + D\phi(\eta) \\ \Rightarrow u\frac{\partial C}{\partial x} &= axf'(\eta)\Big(E + D\phi(\eta)\Big) \\ &= aExf'(\eta) + aDxf'(\eta)\phi(\eta). \end{aligned} \tag{3.38}$$

Now,

$$\begin{aligned} \frac{\partial C}{\partial y} &= \frac{\partial}{\partial y}\Big(C_0 + Ex + (Dx)\phi(\eta)\Big) = Dx\phi'(\eta)\frac{\partial}{\partial y}(\eta) = Dx\phi'(\eta)\sqrt{\frac{a}{\nu}}. \\ \Rightarrow v\frac{\partial C}{\partial y} &= (-\sqrt{a\nu}f(\eta))\Big(Dx\phi'(\eta)\sqrt{\frac{a}{\nu}}\Big) \\ &= -aDxf(\eta))\phi'(\eta). \end{aligned} \tag{3.39}$$

By adding (3.38) and (3.39), we will get the left side of the concentration equation

$$u\frac{\partial C}{\partial x} + v\frac{\partial C}{\partial y} = aExf'(\eta) + aDxf'(\eta)\phi(\eta) - aDxf(\eta))\phi'(\eta). \tag{3.40}$$

The following conversion will help us to reform the right side of the concentration equation.

$$\begin{aligned} \frac{\partial^2 C}{\partial y^2} &= \frac{\partial}{\partial y}\Big(Dx\sqrt{\frac{a}{\nu}}\phi'(\eta)\Big) = Dx\sqrt{\frac{a}{\nu}}\phi''(\eta)\sqrt{\frac{a}{\nu}} \\ &= Dx\frac{a}{\nu}\phi''(\eta). \\ \Rightarrow D_B\Big(\frac{\partial^2 C}{\partial y^2}\Big) &= D_B\Big(Dx\frac{a}{\nu}\phi''(\eta)\Big) \end{aligned} \tag{3.41}$$

From (3.26),

$$\begin{aligned} \frac{\partial^2 T}{\partial y^2} &= \frac{aAx}{\nu}\theta''(\eta). \\ \Rightarrow \frac{D_T}{T_\infty}\Big(\frac{\partial^2 T}{\partial y^2}\Big) &= \frac{D_T}{T_\infty}\Big(\frac{aAx}{\nu}\theta''(\eta)\Big). \end{aligned} \tag{3.42}$$

We know that

$$C - C_\infty = (C_w - C_0)\phi(\eta).$$
$$\Rightarrow -k_1(C - C_\infty) = -ak\bigg((C_w - C_0)\bigg)\phi(\eta). \tag{3.43}$$

By using (3.41)-(3.43), we get the right side of the concentration equation

$$D_B\bigg(\frac{\partial^2 C}{\partial y^2}\bigg) + \frac{D_T}{T_\infty}\frac{\partial^2 T}{\partial y^2} - k_1(C - C_\infty) = D_B\bigg(Dx\frac{a}{\nu}\phi''(\eta)\bigg) + \frac{D_T}{T_\infty}\bigg(\frac{aAx}{\nu}\theta''(\eta)\bigg) - ak\bigg(C_w - C_0\phi(\eta)\bigg). \tag{3.44}$$

By equating (3.40) and (3.44), we get

$$aExf' + aDxf'\phi - aDxf\phi' = D_B\bigg(Dx.\frac{a}{\nu}\phi''\bigg) + \frac{D_T}{T_\infty}\bigg(\frac{aAx}{\nu}\theta''\bigg) - ak(C_w - C_0)\phi.$$
$$\Rightarrow D_B\bigg(Dx\frac{a}{\nu}\phi''\bigg) + \frac{D_T}{T_\infty}\bigg(\frac{aAx}{\nu}\theta''\bigg) - aDxf'\phi - aExf' + aDxf\phi'$$

$$- ak(C_w - C_0)\phi = 0.$$

$$\Rightarrow \phi'' + \frac{\frac{D_T}{T_\infty}\bigg(\frac{aAx}{\nu}\bigg)}{D_B.Dx\bigg(\frac{a}{\nu}\bigg)}\theta'' - \frac{aDx}{D_B.Dx\bigg(\frac{a}{\nu}\bigg)}f'\phi - \frac{aEx}{D_BDx\bigg(\frac{a}{\nu}\bigg)}f'$$
$$+ \frac{aDx}{D_B.Dx\bigg(\frac{a}{\nu}\bigg)}f\phi' - \frac{ak(Dx)}{D_BDx\bigg(\frac{a}{\nu}\bigg)}\phi = 0.$$
$$\Rightarrow \phi'' + \frac{(\rho C_P)_S D_T Ax}{(\rho C_P)_f \nu T_\infty}\frac{\nu(\rho C_P)_f}{D_B Dx(\rho C_P)_S}\theta'' - \frac{\alpha\nu}{\alpha D_B}f'\phi(\eta) - \frac{\alpha\nu E}{\alpha D_B D}f'$$
$$+ \frac{\nu\alpha}{D_B\alpha}f\phi' - \frac{\alpha\nu k}{\alpha D_B}\phi = 0.$$
$$\Rightarrow \phi'' + \frac{Nt}{Nb}\theta'' - \bigg(\frac{\alpha\nu}{\alpha D_B}f'\phi + \frac{\alpha\nu E}{\alpha D_B D}f' - \frac{\nu\alpha}{D_B\alpha}f\phi'\bigg) - \frac{\alpha\nu k}{\alpha D_B}\phi = 0$$
$$\Rightarrow \phi'' + \frac{Nt}{Nb}\theta'' - \frac{\alpha\nu}{D_B\alpha}\bigg(f'\phi + N_1 f' - f\phi'\bigg) - \frac{\alpha\nu k}{\alpha D_B}\phi = 0.$$
$$\Rightarrow \phi'' + \frac{Nt}{Nb}\theta'' - LePr\bigg(f'\phi + N_1 f' - f(\eta)\phi'\bigg) - LePrk\phi = 0. \tag{3.45}$$

In the above equation (3.45), Pr represents the Prandtl number, Le the Lewis number, k the chemical reaction parameter, N_1 the solutal stratification parameter, Nt the thermophoresis parameter and Nb represents the Brownian motion parameter. Most of the dimentionless parameters used in the above expression are already formulated in (3.37) but few are formulated as:

$$Le = \frac{\alpha}{D_B}, \qquad N_1 = \frac{E}{D}. \tag{3.46}$$

The boundary conditions corresponding to PDEs at $y = 0$ are transformed into the dimensionaless form through the following procedure.

$$\begin{aligned}
&u = U_w(x) = ax, && at \;\; y = 0.\\
&u = axf'(\eta).\\
\Rightarrow\; &axf'(\eta) = ax. && at \;\; \eta = 0.\\
\Rightarrow\; &f'(\eta) = 1. && at \;\; \eta = 0.\\
\Rightarrow\; &f'(\eta) = 1. && at \;\; \eta = 0.\\
&v = 0, && at \;\; y = 0.\\
&v = -\sqrt{a\nu}f(\eta).\\
\Rightarrow\; &-\sqrt{a\nu}f(\eta) = 0. && at \;\; \eta = 0.\\
\Rightarrow\; &f(\eta) = 0. && at \;\; \eta = 0.\\
\Rightarrow\; &f(\eta) = 0. && at \;\; \eta = 0.\\
&T = Tw && at \;\; y = 0.\\
\Rightarrow\; &\theta(\eta)(T_w - T_0) + T_\infty = T. && at \;\; \eta = 0.\\
\Rightarrow\; &\theta(\eta)(T_w - T_0) = T_w - T_\infty. && at \;\; \eta = 0.\\
\Rightarrow\; &\theta(\eta)(Ax) = (T_0 + Ax) - (T_0 + Bx). && at \;\; \eta = 0.\\
\Rightarrow\; &\theta(\eta) = \frac{1}{Ax}\Big(T_0 + Ax - T_0 - Bx\Big). && at \;\; \eta = 0.\\
\Rightarrow\; &\theta(\eta) = 1 - \frac{B}{A}. && at \;\; \eta = 0.\\
\Rightarrow\; &\theta(\eta) = 1 - N_2. && at \;\; \eta = 0.\\
\Rightarrow\; &\theta(\eta) = 1 - N_2. && at \;\; \eta = 0.
\end{aligned}$$

$$
\begin{aligned}
& C = Cw, && at \;\; y = 0. \\
\Rightarrow\; & \phi(\eta)(C_w - C_0) + C_\infty = C. && at \;\; \eta = 0. \\
\Rightarrow\; & \phi(\eta)(C_w - C_0) = C_w - C_\infty. && at \;\; \eta = 0. \\
\Rightarrow\; & \phi(\eta)(Dx) = (C_0 + Dx) - (C_0 + Ex). && at \;\; \eta = 0. \\
\Rightarrow\; & \phi(\eta) = \frac{1}{Dx}\Big(C_0 + Dx - C_0 - Ex\Big). && at \;\; \eta = 0. \\
\Rightarrow\; & \phi(\eta) = 1 - \frac{E}{D}. && at \;\; \eta = 0. \\
\Rightarrow\; & \phi(\eta) = 1 - N_1. && at \;\; \eta = 0. \\
\Rightarrow\; & \phi(\eta) = 1 - N_1. && at \;\; \eta = 0.
\end{aligned}
$$

Now, the boundary conditions corresponding to PDEs with $y \to \infty$ are transformed into the dimensionaless form through the following procedure.

$$
\begin{aligned}
& u \to 0, && as \;\; y \to \infty. \\
& u = axf'(\eta) && \\
\Rightarrow\; & axf'(\eta) \to 0. && as \;\; \eta \to \infty. \\
\Rightarrow\; & f'(\eta) \to 0. && as \;\; \eta \to \infty. \\
\Rightarrow\; & f'(\eta) \to 0. && as \;\; \eta \to \infty. \\
& T \to T_\infty, && as \;\; y \to \infty. \\
& T = \theta(\eta)(T_w - T_0) + T_\infty. && \\
\Rightarrow\; & \theta(\eta)(T_w - T_0) + T_\infty \to T_\infty. && as \;\; \eta \to \infty. \\
\Rightarrow\; & \theta(\eta)(Ax) \to 0. && as \;\; \eta \to \infty. \\
\Rightarrow\; & \theta(\eta) \to 0. && as \;\; \eta \to \infty. \\
& C \to C_\infty, && as \;\; y \to \infty. \\
& C = \phi(\eta)(C_w - C_0) + C_\infty && \\
\Rightarrow\; & \phi(\eta)(C_w - C_0) + C_\infty \to C_\infty. && as \;\; \eta \to \infty. \\
\Rightarrow\; & \phi(\eta)(Dx) \to 0. && as \;\; \eta \to \infty. \\
\Rightarrow\; & \phi(\eta) \to 0. && as \;\; \eta \to \infty.
\end{aligned}
$$

By combining (3.21), (3.36) and (3.45), the dimensionless form of the governing model is given below.

$$f''' - f'^2 + ff'' + Wef''f''' - Mf' - \lambda f' - Frf'^2 = 0, \tag{3.47}$$

$$\theta'' + Pr\left[f\theta' - N_2 f' - f'\theta + Nb\left(\theta'\phi' + \frac{Nt}{Nb}\theta'^2\right) + MEcf'^2 + Ecf''^2 + \frac{WeEc}{\sqrt{2}}f''^3\right] + \frac{4}{3}Rd\left[A_1^3\theta^3\theta'' + \theta'' + 3A_1^2\theta^2\theta'' + 3A_1\theta\theta'' + 3A_1^2\theta^2\theta'^2 + 3A_1\theta'^2 + 6A_1^2\theta\theta'^2\right] = 0, \tag{3.48}$$

$$\phi'' + \frac{Nt}{Nb}\theta'' - LePr\left(f'\phi + N_1 f' - f\phi'\right) - LePrk\phi = 0. \tag{3.49}$$

The dimentionless form of BCs corresponding to (3.5) are given below.

$$\left.\begin{aligned} &f(\eta) = 0, \quad f'(\eta) = 1, \quad \theta(\eta) = 1 - N_2, \quad \phi(\eta) = 1 - N_1, \quad at \quad \eta = 0, \\ &f'(\eta) \to 0, \quad \theta(\eta) \to 0, \quad \phi(\eta) \to 0 \quad as \quad \eta \to \infty. \end{aligned}\right\} \tag{3.50}$$

3.3.2 Physical Quantities of Interest

3.3.2.1 Skin Friction Coefficient

The dimentional form of coefficient of skin friction is given as:

$$C_{fx} = \frac{-2(\tau_w)_{y=0}}{\rho u_w^2(x)}. \tag{3.51}$$

In order to obtain the dimentionless form of C_{fx}, the following calculations will be helpful:

$$\tau_w = -\mu\left[\frac{\partial u}{\partial y} + \frac{\gamma}{\sqrt{2}}\left(\frac{\partial u}{\partial y}\right)^2\right]_{y=0}. \tag{3.52}$$

From (3.6),

$$\Rightarrow \frac{\partial u}{\partial y} = (axf''(\eta))\sqrt{\frac{a}{\nu}}.$$

By using the above derivative in (3.52), we get

$$\tau_w = -\mu\left[(axf''(\eta))\sqrt{\frac{a}{\nu}} + \frac{\gamma}{\sqrt{2}}\left((axf''(\eta))\sqrt{\frac{a}{\nu}}\right)^2\right]_{\eta=0}.$$

By using the value of $u_w(x)$ and τ_w in (3.51), we get

$$\begin{aligned} C_{fx} &= \frac{-2}{\rho(ax)^2}\left[-\mu\left[\frac{a^{\frac{3}{2}}x}{\nu^{\frac{1}{2}}}f''(\eta) + \frac{\gamma}{\sqrt{2}}\left(\frac{a^3x^2}{\nu}f''^2(\eta)\right)\right]\right]_{\eta=0} \\ &= \frac{2\mu}{\rho a^2x^2}\left[\frac{a^{\frac{3}{2}}x}{\nu^{\frac{1}{2}}}f''(\eta) + \frac{\gamma}{\sqrt{2}}\left(\frac{a^3x^2}{\nu}f''^2(\eta)\right)\right]_{\eta=0} \end{aligned}$$

Since $\frac{\mu}{\rho} = \nu$, therefore

$$\begin{aligned} C_{fx} &= \frac{2\nu}{a^2x^2}\left[\frac{a^{\frac{3}{2}}x}{\nu^{\frac{1}{2}}}f''(\eta) + \frac{\gamma}{\sqrt{2}}\left(\frac{a^3x^2}{\nu}f''^2(\eta)\right)\right]_{\eta=0} \\ &= \frac{2\nu}{a^2x^2}.\frac{a^{\frac{3}{2}}x}{\nu^{\frac{1}{2}}}\left[f''(\eta) + \frac{\gamma}{\sqrt{2}}\left(\frac{\frac{a^3x^2}{\nu}}{\frac{a^{\frac{3}{2}}x}{\nu^{\frac{1}{2}}}}f''^2(\eta)\right)\right]_{\eta=0} \\ &= \frac{2}{\left(\frac{a^{\frac{1}{2}}x}{\nu^{\frac{1}{2}}}\right)}\left[f''(\eta) + \frac{1}{2}\left(\sqrt{\frac{2a^3}{\nu}}\gamma x\right)f''^2(\eta)\right]_{\eta=0} \\ &= \frac{2}{(Re_x)^{\frac{1}{2}}}\left[f''(\eta) + \frac{1}{2}Wef''^2(\eta)\right]_{\eta=0}. \end{aligned}$$

Hence, the dimentionless form of coefficient of skin friction is

$$\Rightarrow C_{fx}(Re_x)^{\frac{1}{2}} = 2f''(0) + Wef''^2(0), \tag{3.53}$$

where Re represents the Reynolds number defined as $Re = \sqrt{\frac{a}{\nu}}x$.

3.3.2.2 Nusselt Number

The dimentional form of the local Nusselt number is defined as the following

$$Nu_x = \frac{xq_w}{k(T_w - T_\infty)}, \tag{3.54}$$

where q_w is formulated as

$$\begin{aligned} q_w &= -\left(k + \frac{16T_\infty^3\sigma^*}{3k^*}\right)\left(\frac{\partial T}{\partial y}\right)_{y=0}. \\ &= -\left(k + \frac{16T_\infty^3\sigma^*}{3k^*}\right)\left(Ax.\sqrt{\frac{a}{\nu}}\theta'(\eta)\right)_{\eta=0}. \end{aligned}$$

By using the above q_w in (3.54), we get

$$\begin{aligned} Nu_x &= \frac{x\Big[-\left(k + \frac{16T_\infty^3\sigma^*}{3k^*}\right)\left(Ax.\sqrt{\frac{a}{\nu}}\theta'(\eta)\right)_{\eta=0}\Big]}{k(T_w - T_\infty)} \\ &= \frac{xk\Big[-\left(1 + \frac{16T_\infty^3\sigma^*}{3k^*k}\right)\left(Ax\sqrt{\frac{a}{\nu}}\theta'(\eta)\right)_{\eta=0}\Big]}{k(Ax - Bx)} \\ \Rightarrow Nu_x(Re_x)^{\frac{-1}{2}} &= \frac{-\left(1 + \frac{16T_\infty^3\sigma^*}{3k^*k}\right)(Re_x)^{\frac{1}{2}}\left(\theta'(\eta)\right)_{\eta=0}}{(1 - \frac{B}{A})}. \end{aligned}$$

Hence, the dimentionless form of the local Nesselt number will be

$$Nu_x(Re_x)^{-\frac{1}{2}} = \frac{\theta'(0) + \frac{4}{3}Rd\ \theta'(0)}{(N_2 - 1)}, \tag{3.55}$$

where

$$Rd = \frac{4T_\infty^3\sigma^*}{k^*k}, \qquad N_2 = \frac{B}{A}, \qquad (Re_x)^{\frac{1}{2}} = \sqrt{\frac{a}{\nu}}x.$$

3.3.2.3 Sherwood Number

The dimentional form of Sherwood number is defined as following:

$$Sh_x = \frac{xq_m}{D_B(C_w - C_\infty)}, \tag{3.56}$$

where

$$\begin{aligned} q_m &= -D_B\left(\frac{\partial C}{\partial y}\right)_{y=0} \\ &= -D_B\left(Dx\sqrt{\frac{a}{\nu}}\phi'(0)\right). \end{aligned}$$

By using the above q_m in (3.56), we get

$$\begin{aligned} Sh_x &= \frac{x\Big[-D_B\Big(Dx\sqrt{\frac{a}{\nu}}\phi'(0)\Big)\Big]}{D_B(C_w - C_\infty)} \\ &= \frac{-x\Big(Dx\sqrt{\frac{a}{\nu}}\phi'(0)\Big)}{(Dx - Ex)} \\ &= \frac{-(Re_x)^{\frac{1}{2}}\phi'(0)}{(1-\frac{E}{D})}. \\ \Rightarrow Sh_x(Re_x)^{-\frac{1}{2}} &= \frac{-\phi'(0)}{(1-\frac{E}{D})}. \end{aligned}$$

Hence, the dimentionless form of the Sherwood number will be

$$Sh_x(Re_x)^{-\frac{1}{2}} = \frac{-\phi'(0)}{(1-N_1)}, \tag{3.57}$$

where

$$N_1 = \frac{E}{D}, \qquad (Re_x)^{\frac{1}{2}} = \sqrt{\frac{a}{\nu}}x.$$

From (3.53), (3.55) and (3.57), the expression for the dimentionless form of the skin friction coefficient, Nusselt Number and Sherwood Number are given below,

$$\left.\begin{aligned} C_{fx}(Re_x^{\frac{1}{2}}) &= 2f''(0) + Wef''^2(0), \\ Nu_x(Re_x)^{\frac{-1}{2}} &= \frac{\theta'(0) + \frac{4}{3}Rd\ \theta'(0)}{(N_2 - 1)}, \\ Sh_x(Re_x)^{-\frac{1}{2}} &= \frac{-\phi'(0)}{(1-N_1)}. \end{aligned}\right\} \tag{3.58}$$

3.3.3 Entropy Generation

In order to obtain the dimentionless form of (3.11), the following calculations will be helpful:

From (3.28),

$$\left(\frac{\partial T}{\partial y}\right)^2 = (T_w - T_0)^2(\frac{a}{\nu})\theta'^2(\eta).$$

From (3.6),

$$\left(\frac{\partial C}{\partial y}\right)^2 = (C_w - C_0)^2\left(\frac{a}{\nu}\right)\phi'^2(\eta)$$
$$\Rightarrow \left(\frac{\partial u}{\partial y}\right)^2 = a^2x^2\left(\frac{a}{\nu}\right)f''^2(\eta)$$
$$\Rightarrow \left(\frac{\partial u}{\partial y}\right)^3 = a^3x^3.\left(\frac{a}{\nu}\right)^{\frac{3}{2}}f''^3(\eta).$$

From (3.7) and (3.37),

$$B_0^2 = \frac{M\rho a}{\sigma}, \qquad T = T_\infty\left(\frac{\theta(\eta)}{N_2(N_3+1)} + 1\right).$$

Hence (3.11) gets the following form:

$$\begin{aligned}
S_G &= \frac{k}{T_\infty^2}\left[(T_w - T_0)^2\frac{a}{\nu}\theta'^2 + \frac{16\sigma^*}{3kk^*}\left(T_\infty\left(\frac{\theta}{N_2(N_3+1)} + 1\right)\right)^3\right.\\
&\quad \left.\left((T_w - T_0)^2\frac{a}{\nu}\theta'^2\right)\right] + \frac{RD_A}{C_\infty}\left((C_w - C_0)^2\frac{a}{\nu}\phi'^2\right) + \frac{\sigma}{T_\infty}\left(\frac{M\rho a}{\sigma}\right)\left(axf'\right)^2\\
&\quad + \frac{RD_A}{T_\infty}\left((C_w - C_0)\sqrt{\frac{a}{\nu}}\phi'\right)\left((T_w - T_0)\sqrt{\frac{a}{\nu}}\theta'\right)\\
&\quad + \frac{\mu_0}{T_\infty}\left[a^2x^2\left(\frac{a}{\nu}\right)f''^2 + \gamma\left(a^3x^3.\left(\frac{a}{\nu}\right)^{\frac{3}{2}}f''^3\right)\right].\\
&= \frac{k}{T_\infty^2}(T_w - T_0)^2\frac{a}{\nu}\left[1 + \frac{4}{3}Rd\left(\frac{\theta}{N_2(N_3+1)} + 1\right)^3\right]\theta'^2 + \frac{M\rho a}{T_\infty}a^2x^2f'^2\\
&\quad + \frac{RD_A}{C_\infty}\left((C_w - C_0)^2\frac{a}{\nu}\phi'^2\right) + \frac{RD_A}{T_\infty}\left((C_w - C_0)(T_w - T_0)\frac{a}{\nu}\theta'\phi'\right.\\
&\quad \left. + \frac{\mu_0}{T_\infty}\left[a^2x^2\left(\frac{a}{\nu}\right)f''^2 + \gamma\left(a^3x^3\left(\frac{a}{\nu}\right)^{\frac{3}{2}}f''^3\right)\right].\right.\\
\Rightarrow \frac{T_\infty\nu}{k(T_w - T_0)a}S_G &= \frac{(T_w - T_0)}{T_\infty}\left[1 + \frac{4}{3}Rd\left(\frac{\theta}{N_2(N_3+1)} + 1\right)^3\right]\theta'^2\\
&\quad + \frac{1}{\frac{k(T_w-T_0)a}{T_\infty\nu}}\frac{RD_A}{C_\infty}\left((C_w - C_0)^2\frac{a}{\nu}\phi'^2\right) + \frac{1}{\frac{k(T_w-T_0)a}{T_\infty\nu}}\frac{M\rho a}{T_\infty}a^2x^2f'^2\\
&\quad + \frac{1}{\frac{k(T_w-T_0)a}{T_\infty\nu}}\frac{RD_A}{T_\infty}\left((C_w - C_0)(T_w - T_0)\frac{a}{\nu}\theta'\phi'\right.\\
&\quad \left. + \frac{1}{\frac{k(T_w-T_0)a}{T_\infty\nu}}\frac{\mu_0}{T_\infty}\left[a^2x^2\left(\frac{a}{\nu}\right)f''^2 + \gamma\left(a^3x^3\left(\frac{a}{\nu}\right)^{\frac{3}{2}}f''^3\right)\right].\right.
\end{aligned}$$

After simplifying the above expression, we get the dimentionless form of the entropy generation as follows.

$$N_G(\eta) = \beta_1 \left[1 + \frac{4}{3}Rd\left(\frac{\theta(\eta)}{N_2(N_3+1)} + 1\right)^3\right]\theta'^2(\eta) + L\frac{\beta_2}{\beta_1}\phi'^2(\eta) + MBrf'^2(\eta) + L\theta'(\eta)\phi'(\eta) + Brf''^2(\eta) + \frac{BrWe}{\sqrt{2}}f''^3(\eta), \tag{3.59}$$

where Br stands for Brinkman number, L for the diffusion parameter, $N_G(\eta)$ describes the rate of entropy generation, β_1 signifies the temperature difference parameter, and β_2 stands for the concentration difference. The following formulations are used for the dimensionless parameters in (3.59):

$$\left.\begin{aligned} N_G &= \frac{T_\infty \nu}{k(T_w - T_0)a}S_G, \quad \beta_1 = \frac{T_w - T_0}{T_\infty}, \quad \beta_2 = \frac{C_w - C_0}{C_\infty}, \\ L &= \frac{RD_A(C_w - C_0)}{k}, \quad Br = \frac{a^2\mu_0 x^2}{k(T_w - T_0)}. \end{aligned}\right\} \tag{3.60}$$

3.4 Solution Methodology

In order to solve the ordinary differential equation (3.21), the shooting technique has been used by considering the following notations.

$$f = S_1, \qquad f' = S_1' = S_2, \qquad f'' = S_1'' = S_2' = S_3, \qquad f''' = S_3'.$$

By using the above mentioned notations, the momentum equation is converted into the following system of first order ODEs.

$$\begin{aligned} S_1' &= S_2, & S_1(0) &= 0. \\ S_2' &= S_3, & S_2(0) &= 1. \\ S_3' &= \frac{1}{(1 + WeS_3)}\left[{S_2}^2 - S_1S_3 + MS_2 + \lambda S_2 - Fr{S_2}^2\right], & S_3(0) &= r. \end{aligned}$$

The Runge-Kutta method of order four is used in order to solve the above initial value problem. By taking into account the problems domain, which is $[0, \eta_\infty]$,

and choosing η_∞ so that no discernible changes result from going beyond, one can achieve an approximative numerical solution. The selection of missing condition r is carried out in such a way that the following condition must hold:

$$S_2(\eta_\infty, r) = 0.$$

In order to find the value of the missing condition r in a systematic way, the Newton's iterative method will be used. The method used the following itterative scheme for finding the missing conditions.

$$r^{(n+1)} = r^{(n)} - \left(\frac{S_2(\eta_\infty, r)}{\frac{\partial}{\partial r}(S_2(\eta_\infty, r))} \right)^{(n)}.$$

Let us further introduce the new notations that will be helpful for finding the numerical solution of ODEs.

$$\frac{\partial S_1}{\partial r} = S_4, \quad \frac{\partial S_2}{\partial r} = S_5, \quad \frac{\partial S_3}{\partial r} = S_6.$$

The above mentioned notations will change the form of Newton's itterative scheme as follows.

$$r^{(n+1)} = r^{(n)} - \left(\frac{S_2(\eta_\infty, r)}{S_5(\eta_\infty, r)} \right)^{(n)}.$$

Now, differentiating the system of three first order ordinary differential equations w.r.t. to the missing condition r, we get another system of three first order ordinary differential equations as follows.

$$\begin{aligned}
S_4' &= S_5, && S_4(0) = 0.\\
S_5' &= S_6, && S_5(0) = 0.\\
S_6' &= \frac{1}{(1+WeS_3)^2}\Big[(1+WeS_3)(2S_2S_5 - S_1S_3 \\
&\quad - S_3S_4 + MS_5 + \lambda S_5 - Fr(2S_2S_5)) - ({S_2}^2 - S_1S_3 \\
&\quad + MS_2 + \lambda S_2 - Fr{S_2}^2)(WeS_6)\Big], && S_6(0) = 1.
\end{aligned}$$

The stopping criteria for the Newtons itterative technique is given below:

$$\mid S_2(\eta_\infty, r) \mid < \epsilon,$$

where $\epsilon > 0$ is an arbitrarily small positive number. The value of ϵ has been taken as 10^{-9}.

The ordinary differentional equations (3.36) and (3.45) are coupled in θ and ϕ. For numerical solution of these coupled ODEs, we will use the shooting method by assuming that the value of function f is known. For this, we utilize the following notations.

$$\theta(\eta) = W_1, \qquad \theta'(\eta) = W_1' = W_2, \qquad \theta''(\eta) = W_1{}'' = W_2',$$
$$\phi(\eta) = W_3, \qquad \phi'(\eta) = W_3' = W_4, \qquad \phi''(\eta) = W_3{}'' = W_4'.$$

$$F_1 = \frac{1}{\left[1 + \frac{4}{3}Rd\Big(1 + (A_1W_1)^3 + 3(A_1W_1)^2 + 3(A_1W_1)\Big)\right]},$$

$$F_2 = -Pr\left[fW_2 - f'W_1 - N_2f' + Nb\left(W_2W_4 + \frac{Nt}{Nb}W_2^2\right) + MEcf'^2 + Ecf''^2 + \frac{WeEc}{\sqrt{2}}f''^3\right] - \frac{4}{3}Rd\left[3(A_1W_1W_2)^2 + 3A_1W_2^2 + 6(A_1W_2)^2W_1\right],$$

$$F_3 = \frac{-\frac{4}{3}Rd\left[A_1^3 3W_1^2W_5 + 6A_1^2W_1W_5 + 3A_1W_5\right]}{(F_1)^2},$$

$$F_4 = -Pr\left[fW_6 - f'W_5 + Nb\left(W_2W_8 + W_4W_6 + \frac{Nt}{Nb}2W_2W_6\right)\right] - \frac{4}{3}Rd\Big[3A_1^3(2W_1^2W_2W_6 + 2W_2^2W_1W_5) + 6A_1W_2W_6 + 6A_1^2(2W_1W_2W_6 + W_2^2W_5)\Big],$$

$$F_5 = \frac{-\frac{4}{3}Rd\left[A_1^3 3W_1^2W_9 + 6A_1^2W_1W_9 + 3A_1W_9\right]}{(F_1)^2},$$

$$F_6 = -Pr\left[fW_{10} - f'W_9 + Nb\left(W_2W_{12} + W_4W_{10} + \frac{Nt}{Nb}2W_2W_{10}\right)\right]$$
$$-\frac{4}{3}Rd\Big[3A_1^3(2W_1^2W_2W_10 + 2W_2^2W_1W_9) + 6A_1W_2W_{10}$$
$$+ 6A_1^2(2W_1W_2W_{10} + W_2^2W_9)\Big].$$

As a result, the coupled ODEs (3.36) and (3.45) are converted into the following system of 1st order ODEs.

$$\begin{aligned}
W_1' &= W_2, & W_1(0) &= 1 - N_2.\\
W_2' &= F_1F_2, & W_2(0) &= p.\\
W_3' &= W_4, & W_3(0) &= 1 - N_1.\\
W_4' &= LePr(W_3f' + N_1f' - W_4f) & & \\
&\quad + LePrKW_3 - (Nt/Nb)(F1F2), & W_4(0) &= q.
\end{aligned}$$

The Runge-Kutta method of order four is used in order to solve the above initial value problem. The selection of the missing conditions p and q is carried out in such a way that the following conditions must hold.

$$(W_1(p,q))_{\eta_\infty} = 0, \qquad (W_3(p,q))_{\eta_\infty} = 0.$$

In order to find the values of the missing conditions p and q in a systematic way, the Newton's itterative method will be used. The method used the following iterative scheme for finding missing conditions.

$$\begin{bmatrix} p \\ q \end{bmatrix}^{(n+1)} = \begin{bmatrix} p \\ q \end{bmatrix}^{(n)} - \left(\begin{bmatrix} \frac{\partial W_1(p,q)}{\partial p} & \frac{\partial W_1(p,q)}{\partial q} \\ \frac{\partial W_3(p,q)}{\partial p} & \frac{\partial W_3(p,q)}{\partial q} \end{bmatrix}^{-1} \begin{bmatrix} W_1 \\ W_3 \end{bmatrix} \right)^{(n)}$$

Let us further introduce the new notations that will be helpful for finding the numerical solution of ODEs.

$$\frac{\partial W_1}{\partial p} = W_5, \quad \frac{\partial W_2}{\partial p} = W_6 \quad \frac{\partial W_3}{\partial p} = W_7 \quad \frac{\partial W_4}{\partial p} = W_8,$$
$$\frac{\partial W_1}{\partial q} = W_9 \quad \frac{\partial W_2}{\partial q} = W_{10} \quad \frac{\partial W_3}{\partial q} = W_{11} \quad \frac{\partial W_4}{\partial q} = W_{12}.$$

The above mentioned notations will change the form of Newton's iterative scheme as follows.

$$\begin{bmatrix} p \\ q \end{bmatrix}^{(n+1)} = \begin{bmatrix} p \\ q \end{bmatrix}^{(n)} - \left(\begin{bmatrix} W_5 & W_9 \\ W_7 & W_{11} \end{bmatrix}^{-1} \begin{bmatrix} W_1 \\ W_3 \end{bmatrix} \right)^{(n)}.$$

Now, differentiating the system of four first ODEs w.r.t. to the missing conditions p and q respectively. We will get another system of eight first order ODEs as follows.

$$\begin{aligned}
W_5' &= W_6, && W_5(0) = 0.\\
W_6' &= F_1F_4 + F_3F_2, && W_6(0) = 1.\\
W_7' &= W_8 && W_7(0) = 0.\\
W_8' &= LePr(W_7f' - W_8f) + LePrKW_7 \\
&\quad - (Nt/Nb)(F_1F_4 + F_3F_2), && W_8(0) = 0.\\
W_9' &= W_{10}, && W_9(0) = 0.\\
W_{10}' &= F_1F_6 + F_5F_2, && W_{10}(0) = 0.\\
W_{11}' &= W_{12}, && W_{11}(0) = 1.\\
W_{12}' &= LePr(W_{11}f' - W_{12}f) + LePrKW_{11} \\
&\quad - (Nt/Nb) * (F_1F_6 + F_5F_2), && W_{12}(0) = 0.
\end{aligned}$$

The stoping criteria for shooting method is given below:

$$\max\{\mid W_1(\eta_\infty) \mid, \mid W_3(\eta_\infty) \mid\} < \epsilon,$$

where $\epsilon > 0$ is an arbitrarily small positive number. The value of ϵ has been taken as 10^{-9}.

3.5 Numerical Results and Discussion

In this section, the numerical results for momentum, energy, concentration Equation for the physical quantities for non-Darcian MHD Williamson nanofluid have been discussed through tables and graphs. The numercical data that has been shown through tables and graphs is actually produced by varying the influence of different physical quantities used in the ODEs. The dimentionless factors that have direct effect on velocity, conentration and temperature of nanofluid flowing over the sheet are Prandtl number (Pr), Eckert number (Ec), magnetic parameter (M), Solutal stratification parameter (N_1), Brownian motion parameter (Nb), inertial coefficient (Fr), Lewis number (Le), thermophoresis parameter (Nt), Weissenberg number (We), thermal radiation parameter (Rd), chemical reaction parameter (k) and some temperature ratios N_2 and N_3. At the end of this section, the phenomenon of entropy generation corresponding to (3.59) is explained through graphs due to the fluctuation of numerous dimentionless parameters.

3.5.1 Numerical Data for Skin Friction Coefficient

Table 3.1 shows the impact of variation of different dimentionless parameters on the skin friction coefficient $C_f(Re_x)^{\frac{1}{2}}$. The numerical results for skin friction coefficient presented in the following table have been obtained by using shooting technique in the MATLAB software. The table shows that due to an increment in the value of the magnetic parameter (M), porosity parameter (λ) and inertial coefficient (Fr), the value of the skin friction coefficient decreases. Similarly, as the value of Weissenberg number (We) increases, a decline in the value of skin friction coefficient has been noted. Table 3.1 also contains an interval I_f where from an initial guess for missing condition for the velocity profile can be choosen.

TABLE 3.1: Results of $C_f(Re_x)^{\frac{1}{2}}$ for various parameters

M	We	λ	Fr	$C_f(Re_x)^{\frac{1}{2}}$	I_f
0.3	0.3	0.2	0.1	-2.30701	[-1,4]
0.5				-2.43594	[0,4]
0.7				-2.55552	[-1,5]
0.9				-2.66702	[-1,6]
	0.35			-2.26569	[-1,6]
	0.40			-2.21929	[0,5]
	0.45			-2.16399	[-1,7]
		0.3		-2.37274	[-1,4]
		0.4		-2.43594	[-1,4]
		0.5		-2.49681	[-1,4]
			0.2	-2.34984	[-1,5]
			0.3	-2.39166	[-1,4]
			0.4	-2.43251	[-2,4]

3.5.2 Numerical Data for Nusselt and Sherwood Numbers

The following table presents the influence of variation in different dimentionless parameters on Nusselt and Sherwood numbers. Table 3.2 also contains the intervals I_θ and I_ϕ for the missing condistions, where from we can choose the missing conditions easily and get a convergent numerical solution.

TABLE 3.2: Results of $Nu(Re_x)^{-\frac{1}{2}}$ *and* $Sh(Re_x)^{-\frac{1}{2}}$ when $N_1 = 0.8$, $N_2 = 0.8$, $N_3 = 1.0$, $k = 0.1$, $Le = 1.0$, $We = 0.3$.

Ec	M	Nt	Pr	Rd	$Nu(Re_x)^{-\frac{1}{2}}$	$Sh(Re_x)^{-\frac{1}{2}}$	I_θ	I_ϕ
0.4	0.3	0.5	0.3	0.3	0.78027	0.80627	[-0.2, 0.3]	[-0.3, 0.3]
0.5					0.70038	0.85922	[-0.3, 0.3]	[-0.2, 0.5]
0.6					0.62047	0.91218	[-0.3, 0.3]	[-0.3, 0.4]
0.7					0.54056	0.96516	[-0.3, 0.3]	[-0.3, 0.4]
	0.4				0.73048	0.81115	[-0.2, 0.3]	[-0.3, 0.3]
	0.5				0.68383	0.81616	[-0.2, 0.3]	[-0.3, 0.3]
	0.6				0.63999	0.82125	[-0.2, 0.3]	[-0.2, 0.4]
		0.6			0.77966	0.73094	[-0.2, 0.3]	[-0.2, 0.3]
		0.7			0.77904	0.65577	[-0.2, 0.3]	[-0.3, 0.3]
		0.8			0.77842	0.58075	[-0.3, 0.3]	[-0.3, 0.3]
			0.4		0.96678	1.01683	[-0.4, 0.3]	[-0.4, 0.4]
			0.5		1.14242	1.22301	[-0.4, 0.3]	[-0.4, 0.4]
			0.6		1.30690	1.42565	[-0.4, 0.3]	[-0.4, 0.4]
				0.4	0.78352	0.84690	[-0.3, 0.2]	[-0.4, 0.4]
				0.5	0.78872	0.87998	[-0.2, 0.2]	[-0.4, 0.4]
				0.6	0.79538	0.90742	[-0.2, 0.2]	[-0.4, 0.5]

The following points elaborate the key findings from the Table 3.2.

- An increment in the value of the Eckert number results a decrement in Nusselt number but an increment in the Sherwood number.

- Enhancing the value of the magnetic parameter, the Nusselt number decreases but the Sherwood number increases though slowly.

- An increment in the value of the Prandtl number results an increment in both Nusselt and Sherwood numbers.

- An increment in the value of the Nusselt number and Sherwood number has been observed against the increase in the value of thermal radiation parameter.

- Due to an increase in the value of the thermophoeresis parameter, the Nusselt number decreases slowly whereas the value of the Sherwood number decreases rapidly.

3.5.3 Velocity Profile

An increment in the value of the magnetic parameter results a decline in the velocity profile and this phenomenon can be visulized from Figure 3.2. As the parameter M physically induces a resistive force in the conduction fluid that's why in Figure 3.2, a drop in the fluid velocity is seen as a result of this produced resistive force. Similarly, as the value of Weissenberg number increases, a decline in the velocity profile is notable and this can be seen through Figure 3.3. The Weissenberg number, which describes the relationship between the relaxation time and the time scale of fluid flow, states that as We increases, the relaxation period lengthens, allowing for greater flow resistance. As a result, the thickness of the associated boundary layer grows, causing the fluid's velocity to decline. Figure 3.4 depicts that due to an increasing value of the inertial coefficient, the velcoity profile decreases and similar phenomenon can be seen for porosity parameter through Figure 3.5.

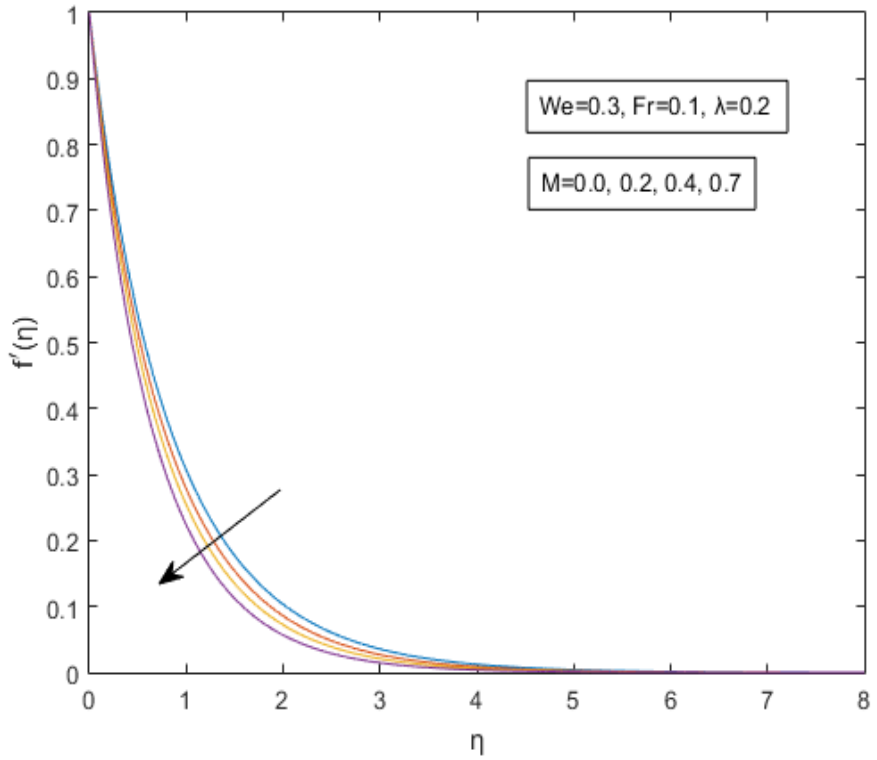

FIGURE 3.2: Effect of M on $f'(\eta)$

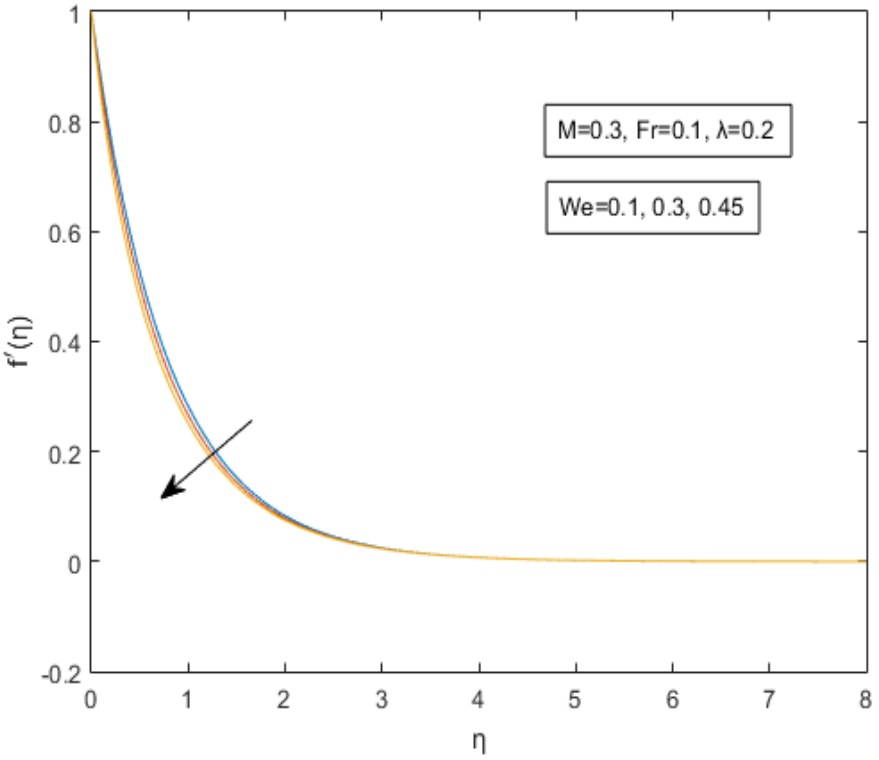

FIGURE 3.3: Effect of We on $f'(\eta)$

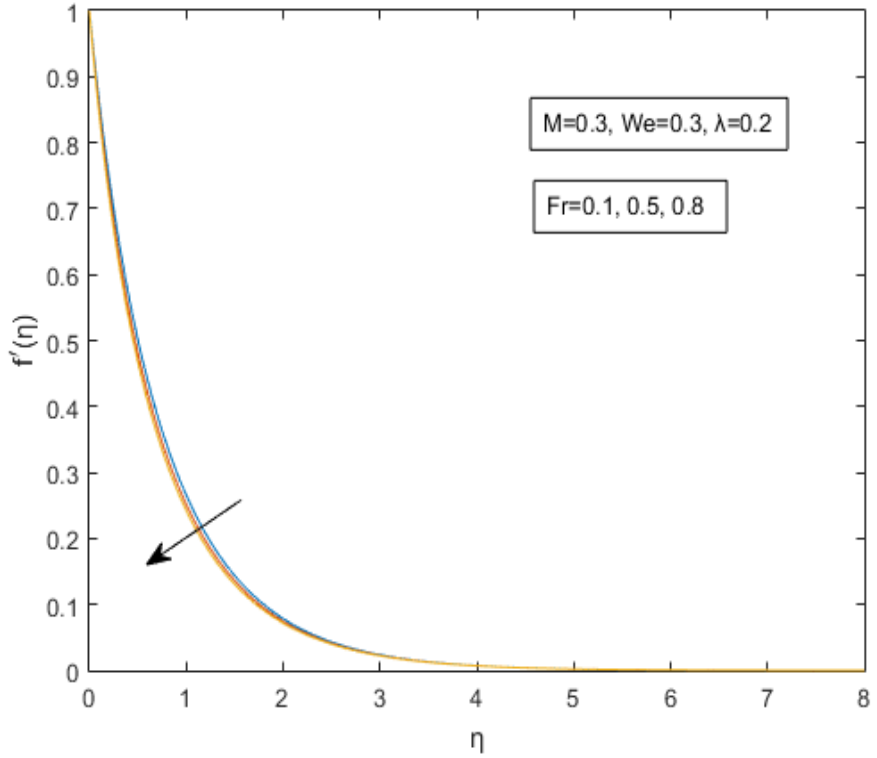

FIGURE 3.4: Effect of Fr on $f'(\eta)$

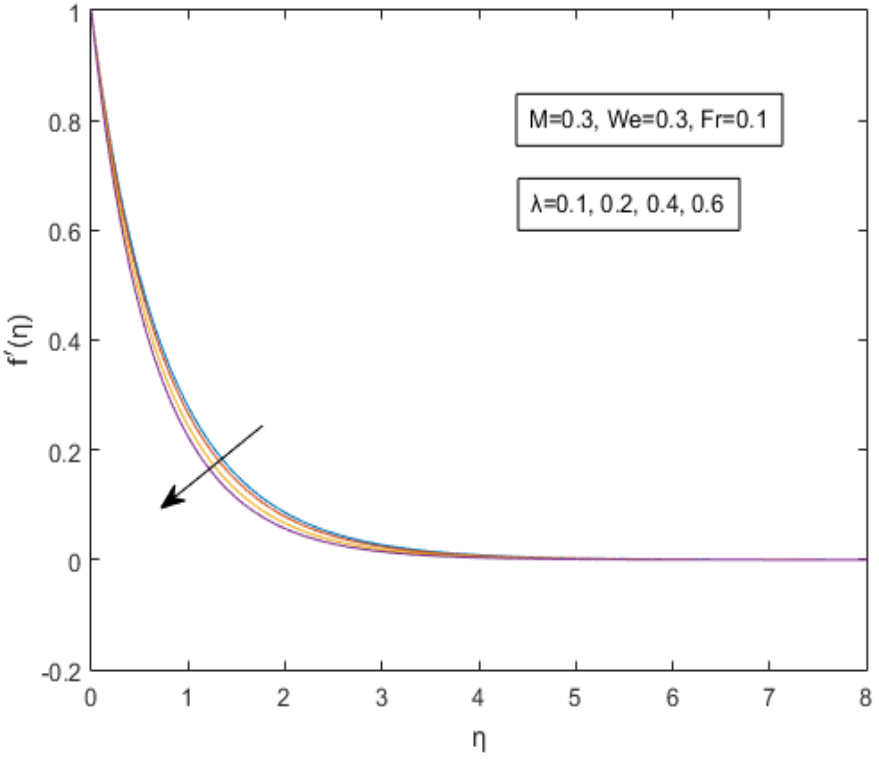

FIGURE 3.5: Effect of λ on $f'(\eta)$

3.5.4 Temperature Profile

The following key observations have been recorded on the basis of the graphs of temperature profiles plotted against different dimentionless parameters belonging.

- The temperature distribution rises by a minor increase in the magnetic parameter. Physically, a resistive force is created in the fluid's direction of flow, and this force contributes to the rise in the temperature profile (See Figure 3.6).
- The temperature profile exhibits an increasing behaviour when the Brownian motion parameter rises. In general, a rise in Nb causes fluid particle motion to increase dramatically, which increases the kinetic energy of the fluid particles and raises the temperature distribution as a result (See Figure 3.7).
- An increasing behaviour in the temperature profile is seen as the thermophoresis parameter increases. Physically, as Nt increases, the nanoparticles are attracted from hotter to less heated regions, raising the temperature profile of the nanofluid as a whole (See Figure 3.8).
- As the Prandtl number rises, the temperature profile exhibits an abrupt declining behaviour. Since Pr may be expressed as a ratio of the density to thermal diffusivity, raising the value of Pr indicates, the fluid's density rises while the thermal diffusivity is falling, which lowers the temperature (See Figure 3.9).
- The temperature profile increases as the value of the porosity parameter increases (See Figure 3.10).
- The temperature profile decreases as the value of the temperature ratio increases (See Figure 3.11).
- As the value of the thermal radiation parameter increases, the temperature profile rises. In general, when Rd values rise, more heat is transferred to the fluid, which causes an increase in the temperature distribution and the thickness of the thermal boundary layer (See Figure 3.12).

3.5.5 Concentration Profile

On the basis of the graphs of the concentration profiles plotted against solutal stratification and chemical reaction parameter, the following significant conclusions have been noted.

- The concentration profile decreases as the value of the solutal stratification parameter increases (See Figure 3.13)

- When the chemical reaction parameter increases, the concentration profile behaves in a decreasing manner (See Figure 3.14).

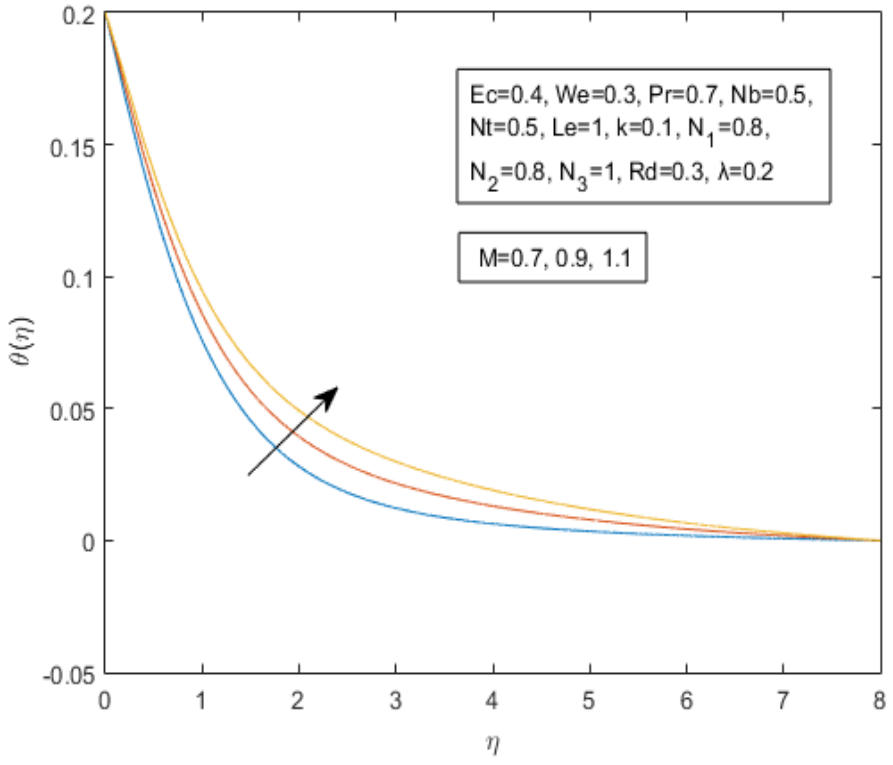

FIGURE 3.6: Effect of M on $\theta(\eta)$

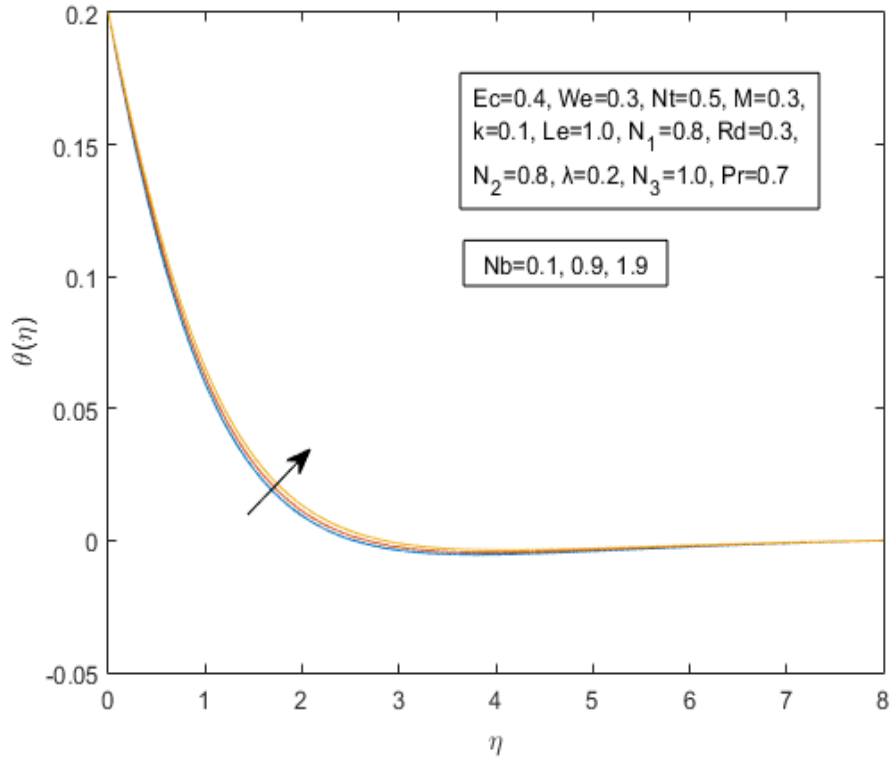

FIGURE 3.7: Effect of Nb on $\theta(\eta)$

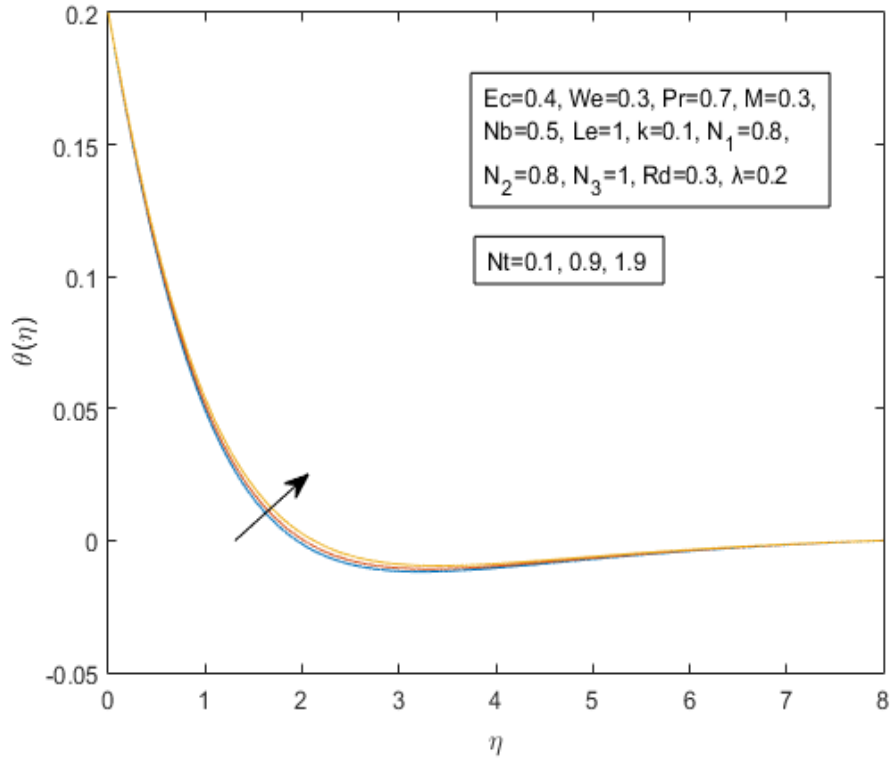

FIGURE 3.8: Effect of Nt on $\theta(\eta)$

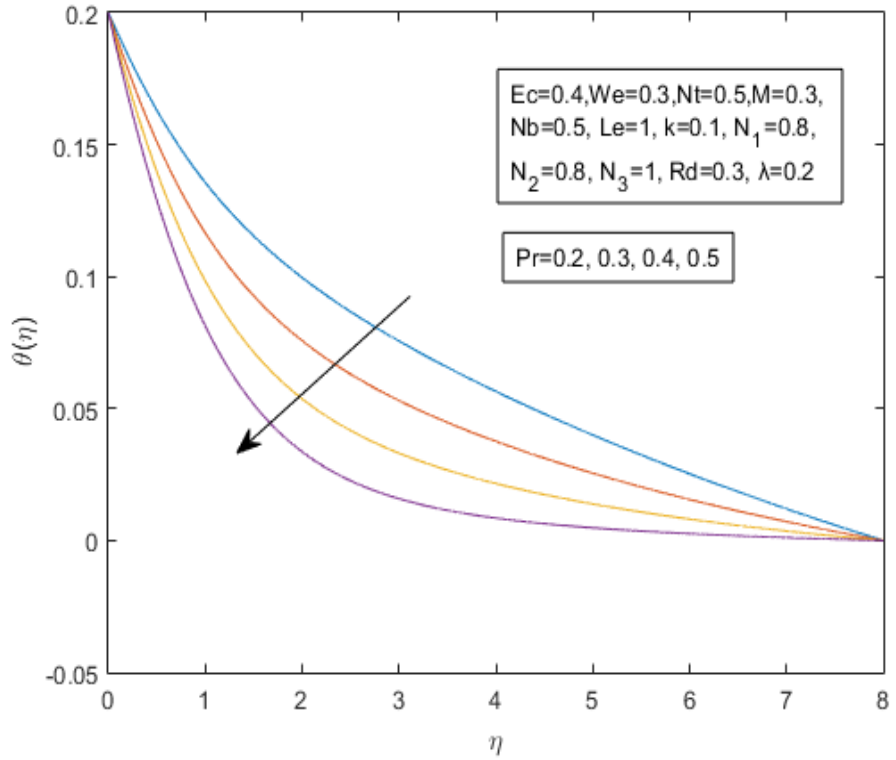

FIGURE 3.9: Effect of Pr on $\theta(\eta)$

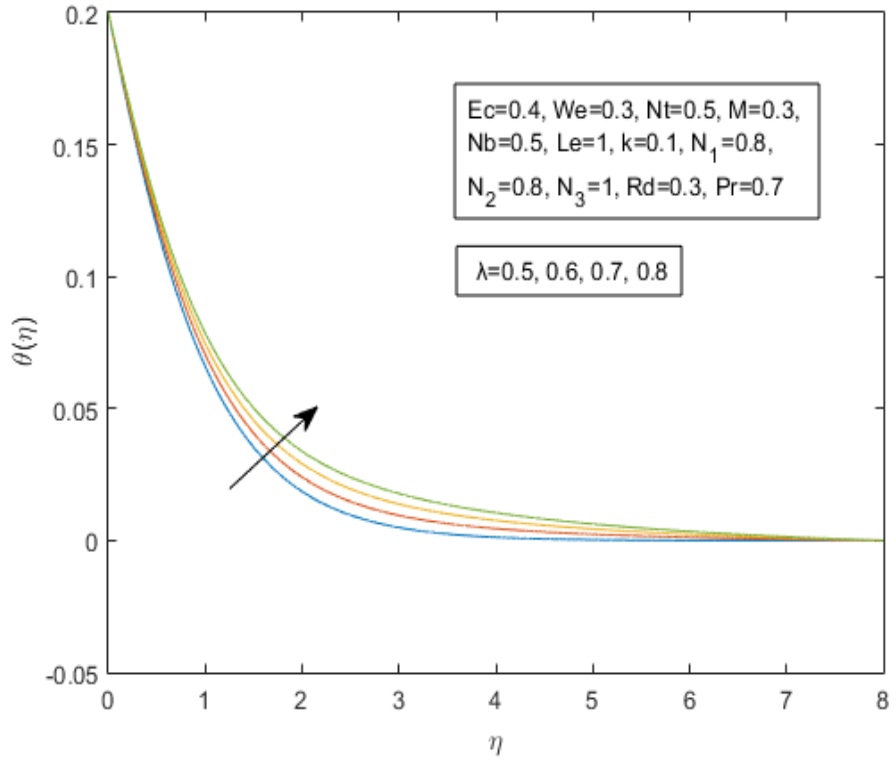

FIGURE 3.10: Effect of λ on $\theta(\eta)$

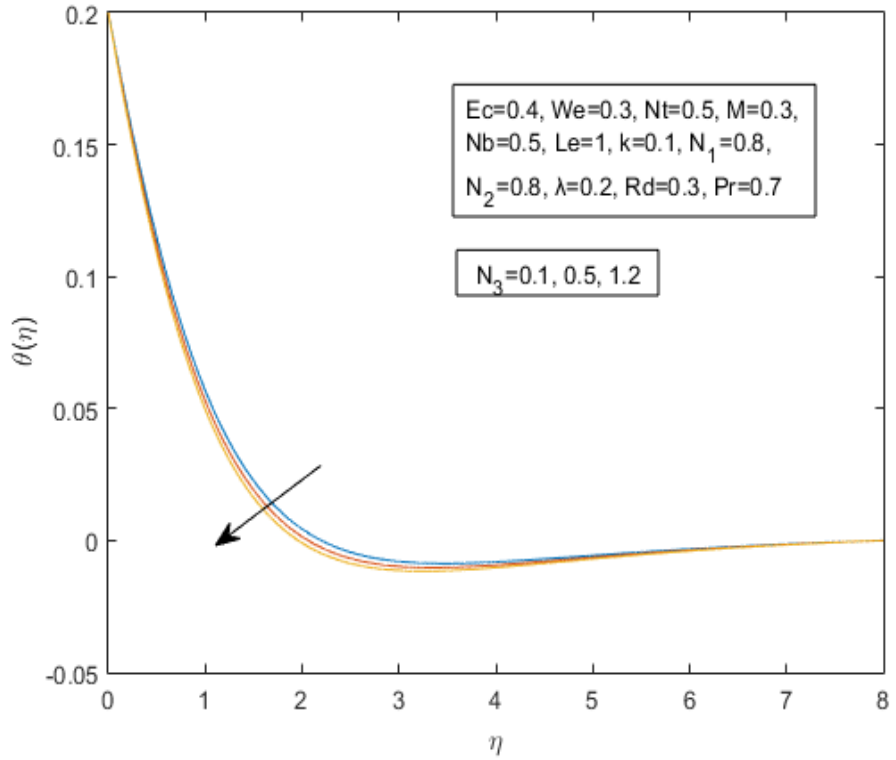

FIGURE 3.11: Effect of N_3 on $\theta(\eta)$

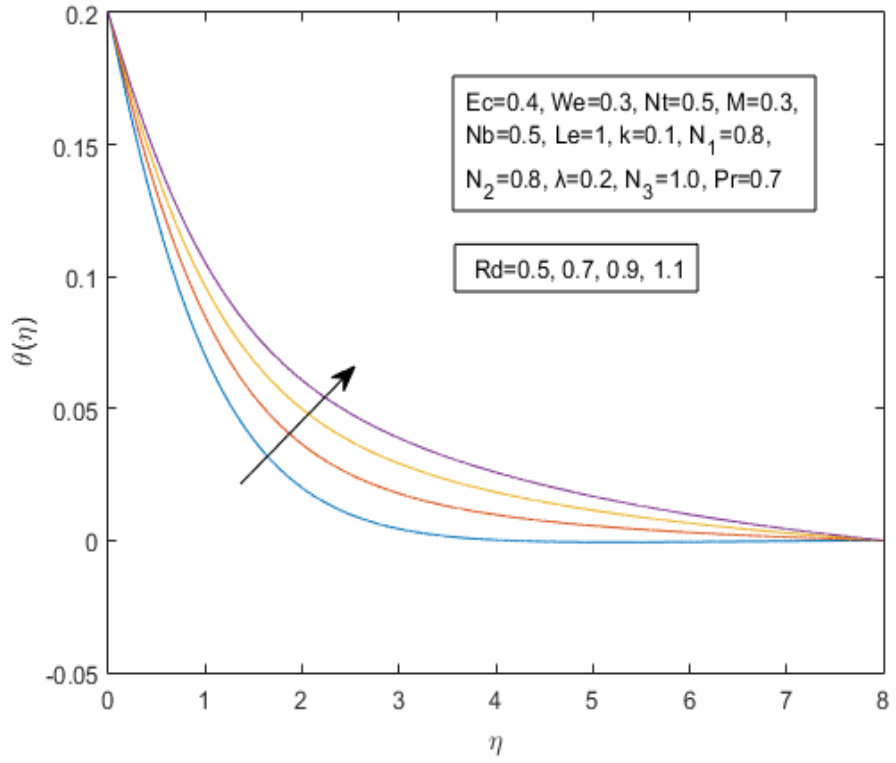

FIGURE 3.12: Effect of Rd on $\theta(\eta)$

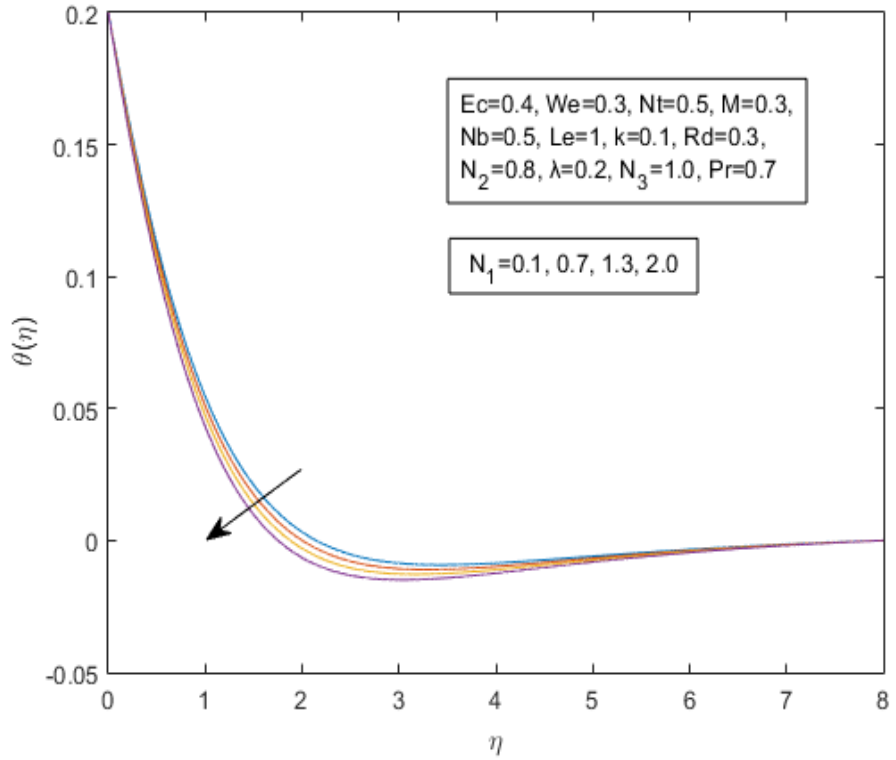

FIGURE 3.13: Effect of N_1 on $\theta(\eta)$

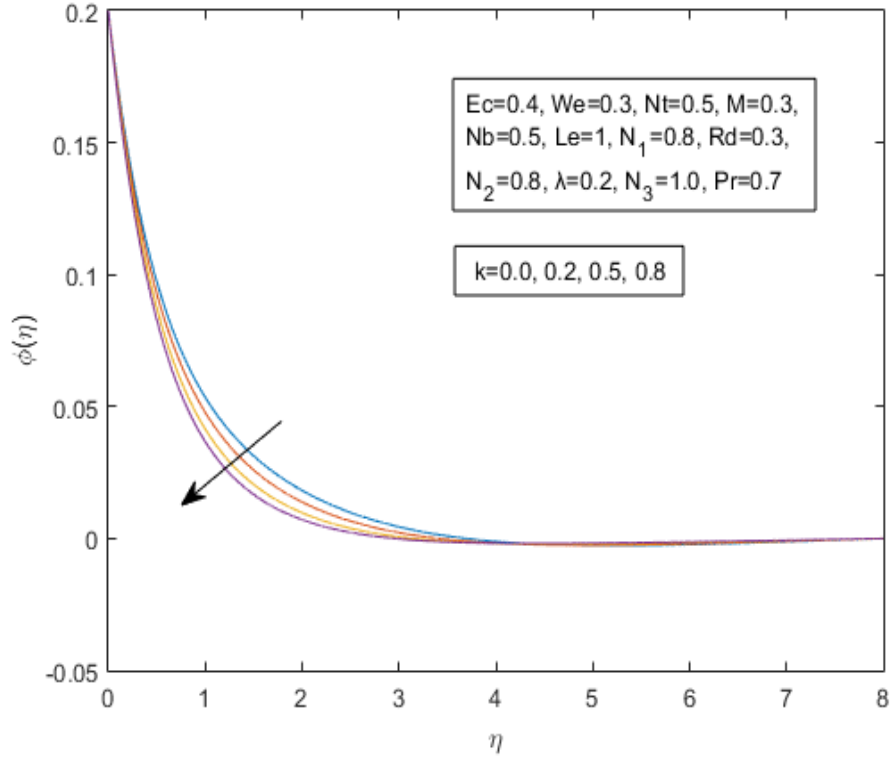

FIGURE 3.14: Effect of k on $\phi(\eta)$

3.5.6 Entropy Generation

Entropy is the system's inability to completely utilize the energy at hand. It is also considered to be a measure of chaos. The progressive impact of the magnetic parameter on N_G is shown in Figure 3.15. It can be seen that entropy is produced in proportion to the magnetic field strength. Figure 3.16 discusses the rate of entropy generation in relation to the Weissenberg number. An increase in the rate of heat transmission is what causes the appearance of entropy development at the microscopic level. Additional factors such as molecular vibration, spin movement, kinetic energy, molecular friction, and internal displacement of molecules, can occur as a result of the motion of heat. These additional factors are what cause the heat loss. The system becomes disordered as a result of these extra movements. The Weissenberg number directly correlates with the relaxation time. As a result, an increase in relaxation time causes fluid's motion to become more difficult, hence raising We. Hence the system's generated abnormalities are diminished.

The impact of Brinkman number Br on the entropy generation N_G can be seen in Figure 3.17. The Brinkman number describes a reduction in the heat transfer rate caused from molecular conduction to viscous heating. Near the sheet, it is observed that the heat transfer caused by viscous effects is outweighed by the quantity of heat released owing to the molecular conduction. The actual cause of the increase in entropy generation and the related diseases is the realization of a significant amount of heat between the layers of the non-Newtonian fluid. The effects of the concentration difference parameter β_2 on the entropy generation are depicted in Figure 3.18. An increment in the temperature ratio N_2, the rate of entropy generation N_G decreases, as seen in Figure 3.19. By increasing the diffusion parameter L, the rate of entropy generation N_G increases, as seen in Figure 3.20.

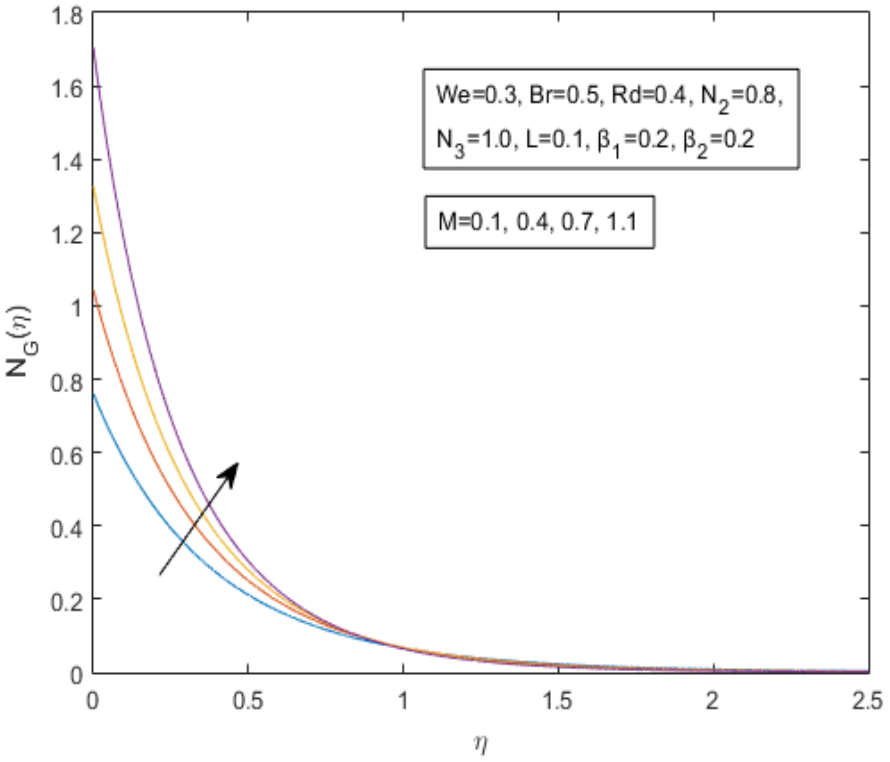

FIGURE 3.15: Effect of M on $N_G(\eta)$

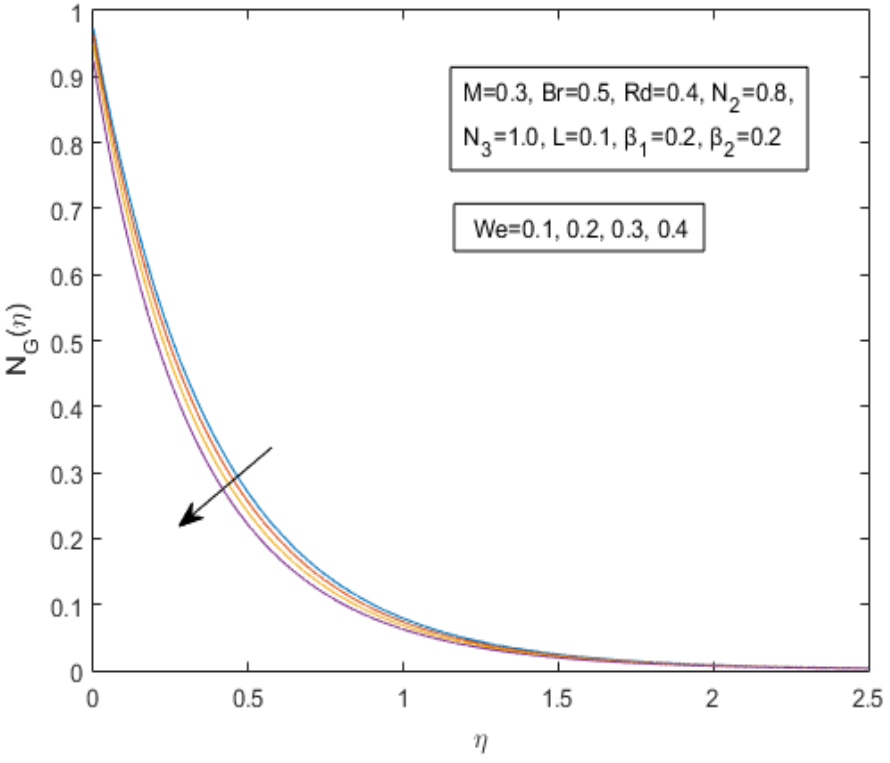

FIGURE 3.16: Effect of We on $N_G(\eta)$

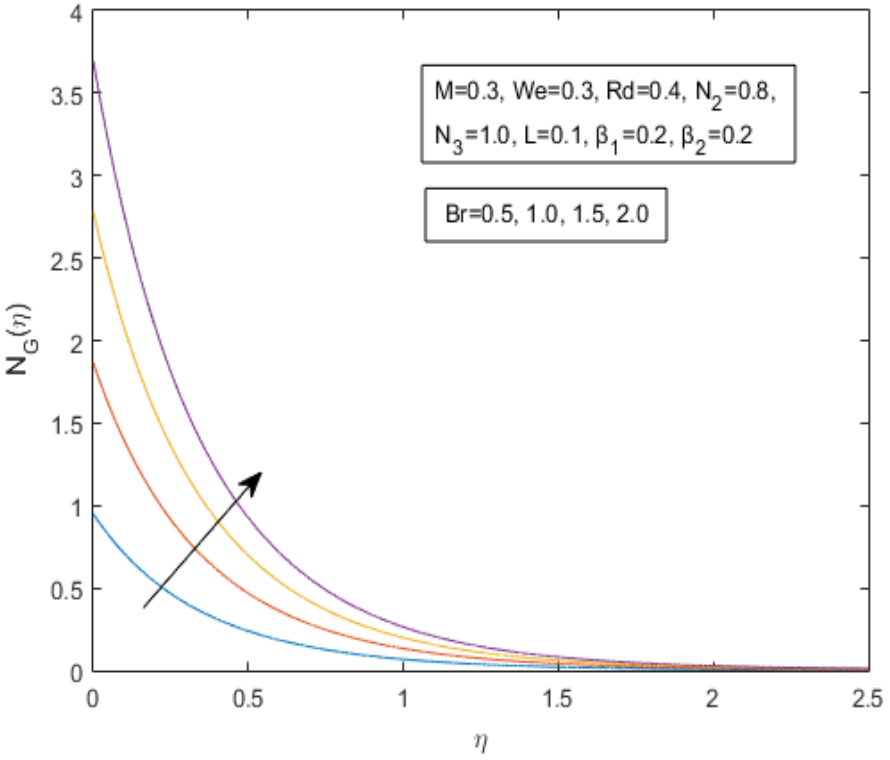

FIGURE 3.17: Effect of Br on $N_G(\eta)$

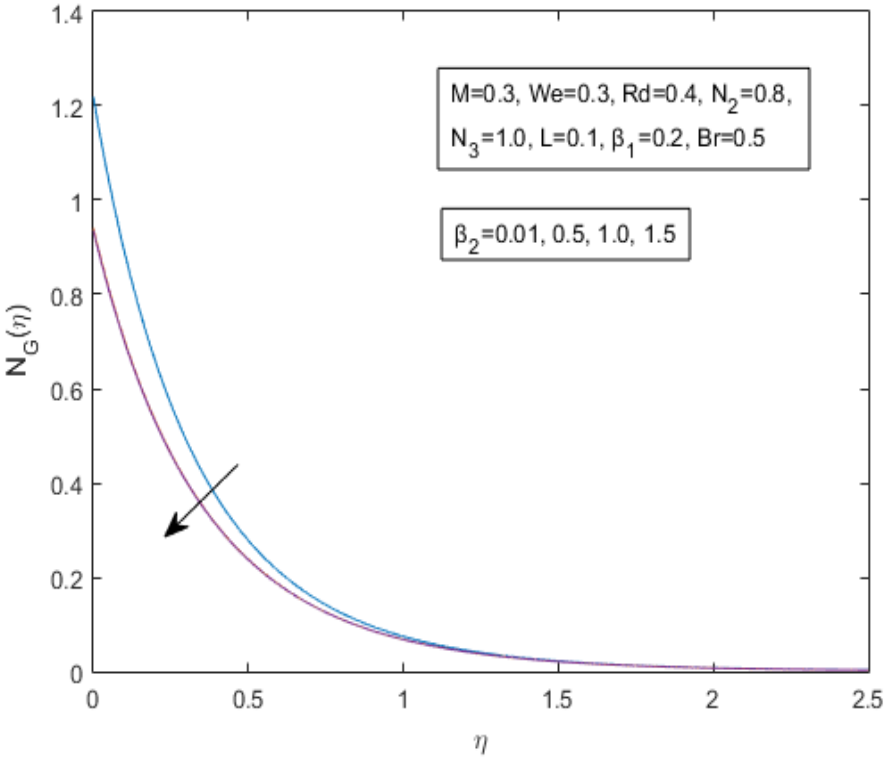

FIGURE 3.18: Effect of β_2 on $N_G(\eta)$

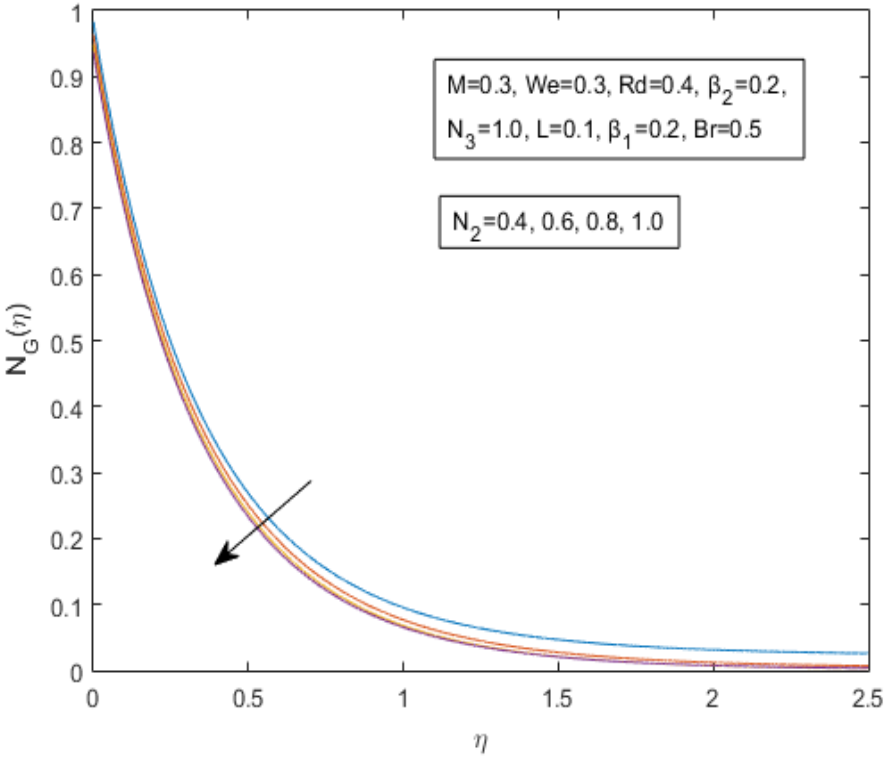

FIGURE 3.19: Effect of N_2 on $N_G(\eta)$

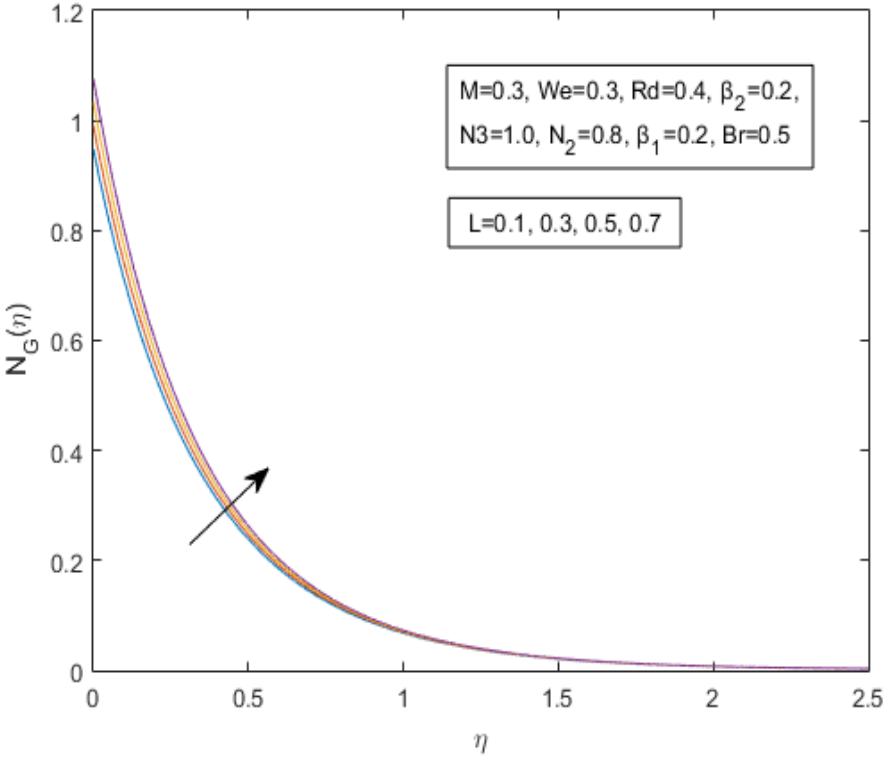

FIGURE 3.20: Effect of L on $N_G(\eta)$

Chapter 4

Cattaneo-Christov Double Diffusion Model for the Entropy Analysis of a Non-Darcian MHD Williamson Nanofluid

4.1 Introduction

This chapter includes an extention of [37] by including the Cattaneo-Christov double diffusion model (CCDDM) in the energy and concentration equations. Using the similarity transformations, the governing nonlinear PDEs are transformed into a system of dimensionless ODEs. The numerical solution of ODEs is obtained by using the shooting technique, which is a numerical technique. The final results for significant parameters affecting $f'(\eta)$, $\theta(\eta)$, $\phi(\eta)$, and entropy optimization, are displayed in tables and graphs.

4.2 Mathematical Formulations

The influence of the Cattaneo-Christov double diffusion model for non-Darcian MHD Williamson nanofluid on the rate of entropy production has been investigated using a stratified sheet. The generation of entropy is examined using the impact of thermal conductivity, Joule dissipation, and the Ohmic effects. The sheet is expected to be stretching in the direction of the x-axis with a velocity $u = u_w(x) = ax$, where a is a positive constant. The physical flow model is shown in Figure 3.1, where the y-axis is taken perpendicular to the stretching velocity and the x-axis is taken towards the stretching velocity. The ambient temperature is represented by $T_\infty = T_0 + Bx$, and the ambient concentration is represented by $C_\infty = C_0 + Ex$. Temperature and concentration at the wall are denoted by $T_w = T_0 + Ax$ and $C_w = C_0 + Dx$, respectively.

4.2.1 The Governing PDEs

The system of PDEs that depicts the flow problem, is given below.

$$\frac{\partial u}{\partial x} + \frac{\partial v}{\partial y} = 0, \tag{4.1}$$

$$u\frac{\partial u}{\partial x} + v\frac{\partial u}{\partial y} = \nu\frac{\partial^2 u}{\partial y^2} + \sqrt{2}\nu\gamma\frac{\partial u}{\partial y}\frac{\partial^2 u}{\partial y^2} - \frac{\sigma}{\rho}{B_0}^2 u - \frac{\nu}{k^*}u - \frac{C_F}{\sqrt{k^*}}u^2, \tag{4.2}$$

$$\begin{aligned}(\rho C_p)_f\left(u\frac{\partial T}{\partial x} + v\frac{\partial T}{\partial y}\right) + \lambda_1\Bigg[\left(u\frac{\partial u}{\partial x} + v\frac{\partial u}{\partial y}\right)\frac{\partial T}{\partial x} + \left(u\frac{\partial v}{\partial x} + v\frac{\partial v}{\partial y}\right)\frac{\partial T}{\partial y}\\ + u^2\frac{\partial^2 T}{\partial x^2} + v^2\frac{\partial^2 T}{\partial y^2} + 2uv\frac{\partial^2 T}{\partial x \partial y}\Bigg] = k\frac{\partial^2 T}{\partial y^2} + (\rho C_p)_S\left[D_B\frac{\partial T}{\partial y}\frac{\partial C}{\partial Y} + \frac{D_T}{T_\infty}(\frac{\partial T}{\partial y})^2\right]\\ + \sigma{B_0}^2u^2 + \mu_0\left(\frac{\partial u}{\partial y}\right)^2 + \mu_0\gamma\left(\frac{\partial u}{\partial y}\right)^3 - \frac{\partial q_r}{\partial y},\end{aligned} \tag{4.3}$$

$$\begin{aligned}u\frac{\partial C}{\partial x} + v\frac{\partial C}{\partial y} + \lambda_2\Bigg[\left(u\frac{\partial u}{\partial x} + v\frac{\partial u}{\partial y}\right)\frac{\partial C}{\partial x} + \left(u\frac{\partial v}{\partial x} + v\frac{\partial v}{\partial y}\right)\frac{\partial C}{\partial y} + u^2\frac{\partial^2 C}{\partial x^2}\\ + v^2\frac{\partial^2 C}{\partial y^2} + 2uv\frac{\partial^2 T}{\partial x \partial y}\Bigg] = D_B\frac{\partial^2 C}{\partial y^2} + \frac{D_T}{T_\infty}\frac{\partial^2 T}{\partial y^2} - k_1(C - C_\infty).\end{aligned} \tag{4.4}$$

The boundary conditions corresponding to the flow pattern are given below.

$$\left.\begin{aligned} &u = U_w(x) = ax, \quad v = 0, \quad C = C_w, \quad T = T_w \quad at \quad y = 0, \\ &u \to 0, \quad T \to T_\infty, \quad C \to C_\infty \quad as \quad y \to \infty. \end{aligned}\right\} \tag{4.5}$$

4.2.2 Similarity Transformations

The following similarity transformations will be used to convert the system of nonlinear PDEs into a system of dimentionless ODEs.

$$\left.\begin{aligned} &u = axf'(\eta), \quad v = -\sqrt{a\nu} f(\eta), \\ &\eta = \sqrt{\frac{a}{\nu}} y, \quad \theta(\eta) = \frac{T - T_\infty}{T_w - T_\infty}, \\ &\phi(\eta) = \frac{C - C_\infty}{C_w - C_\infty}, \end{aligned}\right\} \tag{4.6}$$

where f, θ and ϕ are the velocity, temperature and concentration profiles. Furthermore, T_∞, C_∞, T_w and C_w represent the ambient temperature, ambient concentration, wall temperature and concentration respectively.

4.2.3 Physical Quantities of Interest

The dimentional form of the skin friction coefficient, Nusselt and Sherwood numbers are given below.

$$\left.\begin{aligned} C_{fx} &= \frac{-2(\tau_w)_{y=0}}{\rho u_w^2(x)}, \\ Nu_x &= \frac{xq_w}{k(T_w - T_\infty)}, \\ Sh_x &= \frac{xq_m}{D_B(C_w - C_\infty)}. \end{aligned}\right\} \tag{4.7}$$

4.2.4 Entropy Optimization

The rate of entropy generation E_G for Cattaneo-Christov double diffusion model has been discussed briefly in [55]. The dimentional form of E_G is given below:

$$E_G = \frac{1}{T_\infty^2}\left[k\left(\frac{\partial T}{\partial y}\right)^2 + \frac{16\sigma^* T^3}{3kk^*}k\left(\frac{\partial T}{\partial y}\right)^2\right] + \frac{RD_w}{C_\infty}\left(\frac{\partial C}{\partial y}\right)^2 + \frac{\sigma}{T_\infty}B_0^2u^2\frac{RD_w}{C_\infty}\left(\frac{\partial C}{\partial y}\right)\left(\frac{\partial T}{\partial y}\right) + \frac{1}{T_\infty}\left[\mu_0\left(\frac{\partial u}{\partial y}\right)^2 + \mu_0\gamma\left(\frac{\partial u}{\partial y}\right)^3 + \alpha_1\left(u\frac{\partial u}{\partial y}\frac{\partial^2 u}{\partial x\partial y} + v\frac{\partial u}{\partial y}\frac{\partial^2 u}{\partial y^2}\right) + 2\alpha_2\left(\frac{\partial u}{\partial y}\right)^4\right]. \tag{4.8}$$

4.3 PDEs to ODEs Transformation

4.3.1 Transformation of the Governing PDEs

As in chapter 3, the conversion of (4.1) into the dimentionless form has been discussed in detailed. So the continuity equation (4.1) can be seen satisfied under the same circumstances,

$$\frac{\partial u}{\partial x} + \frac{\partial v}{\partial y} = 0. \tag{4.9}$$

Similarly, as the momentum equation (4.2) is what we have make detailed discussion in chapter 3. So the dimentionaless form of (4.2) under the same conditions can be reffered to (3.21), which is gievn below

$$f'''(\eta) = f'^2(\eta) - f(\eta)f''(\eta) - Wef''(\eta)f'''(\eta) + Mf'(\eta) + \lambda f'(\eta) + Frf'^2(\eta). \tag{4.10}$$

The following procedure will help us to understand the conversion of energy equation (4.3) into the dimentionless form. The findings which are given below have been taken from chapter 3. Instead of doing whole calculations again and again, we can directly utilize those calculations here in ongoing chapter without any hesitation. From (3.25), (3.26), (3.30), (3.31), (3.32), (3.33) and (3.34), we can

write

$$(\rho C_P)_f\left(u\frac{\partial T}{\partial x}+v\frac{\partial T}{\partial y}\right)=(\rho C_P)_f\left(Baxf'(\eta)+aAxf'(\eta)\theta(\eta)-aAxf(\eta)\theta'(\eta)\right), \tag{4.11}$$

$$k\frac{\partial^2 T}{\partial y^2}=\frac{kaAx}{\nu}\theta''(\eta), \tag{4.12}$$

$$(\rho C_P)_S\left[D_B\left(\frac{\partial C}{\partial y}.\frac{\partial T}{\partial y}\right)+\frac{D_T}{T_\infty}\left(\frac{\partial T}{\partial y}\right)^2\right]=Nb(\rho C_p)_f\left(aAx\theta'(\eta)\phi'(\eta)\right)+Nt(\rho C_p)_f\left(aAx\theta'^2(\eta)\right), \tag{4.13}$$

$$\sigma B_0^2u^2=a^3M\rho x^2f'^2(\eta), \tag{4.14}$$

$$\mu_0\left(\frac{\partial u}{\partial y}\right)^2=\frac{\mu_0a^3x^2}{\nu}f''^2(\eta), \tag{4.15}$$

$$\mu_0\gamma\left(\frac{\partial u}{\partial y}\right)^3=\frac{\mu_0\gamma a^{\frac{9}{2}}x^3}{\nu^{\frac{3}{2}}}f''^3(\eta), \tag{4.16}$$

$$\begin{aligned}-\frac{\partial q_r}{\partial y}=\frac{16\sigma^*}{3k^*}\frac{aAxT_\infty^3}{\nu}\Bigg[&\left(\frac{1}{N_2(N_3+1)}\right)^3\theta^3(\eta)\theta''(\eta)+\theta''(\eta)\\&+3\left(\frac{1}{N_2(N_3+1)}\right)^2\theta^2(\eta)\theta''(\eta)+3\left(\frac{1}{N_2(N_3+1)}\right)\theta(\eta)\theta''(\eta)\\&+3\left(\frac{1}{N_2(N_3+1)}\right)^2\theta^2(\eta)\theta'^2(\eta)+3\left(\frac{1}{N_2(N_3+1)}\right)\theta'^2(\eta)\\&+6\left(\frac{1}{N_2(N_3+1)}\right)^2\theta(\eta)\theta'^2(\eta)\Bigg].\end{aligned} \tag{4.17}$$

From (4.6),

$$\theta(\eta)=\frac{T-T_\infty}{T_w-T_\infty},$$

$$\Rightarrow T=T_\infty+(T_w-T_0)\theta(\eta).$$

As we know that,

$$T_\infty=T_0+Bx,$$

$$T_w=T_0+Ax.$$

$$\therefore\ T=T_0+Bx+(Ax)\theta(\eta).$$

$$\Rightarrow \frac{\partial T}{\partial x} = \frac{\partial}{\partial x}\Big(T_0 + Bx + (Ax)\theta(\eta)\Big) = B + A\theta(\eta). \tag{4.18}$$

From (3.14), we know that

$$u\frac{\partial u}{\partial x} + v\frac{\partial u}{\partial y} = a^2 x f'^2(\eta) - a^2 x f(\eta) f''(\eta). \tag{4.19}$$

$$\Rightarrow \left(u\frac{\partial u}{\partial x} + v\frac{\partial u}{\partial y}\right)\frac{\partial T}{\partial x} = a^2 x\Big(f'^2(\eta) - f(\eta)f''(\eta)\Big)\Big(B + A\theta(\eta)\Big). \tag{4.20}$$

From (4.6),

$$\frac{\partial v}{\partial x} = 0, \qquad \frac{\partial v}{\partial y} = -af'(\eta),$$
$$u\frac{\partial v}{\partial x} = 0, \qquad v\frac{\partial v}{\partial y} = a^{\frac{3}{2}}\sqrt{\nu} f(\eta) f'(\eta).$$

$$\therefore\ u\frac{\partial v}{\partial x} + v\frac{\partial v}{\partial y} = a^{\frac{3}{2}}\sqrt{\nu} f(\eta) f'(\eta). \tag{4.21}$$

$$\frac{\partial T}{\partial y} = (T_w - T_0)\sqrt{\frac{a}{\nu}}\theta'(\eta). \tag{4.22}$$

$$\left(u\frac{\partial v}{\partial x} + v\frac{\partial v}{\partial y}\right)\frac{\partial T}{\partial y} = (T_w - T_0)a^2 f(\eta) f'(\eta)\theta'(\eta). \tag{4.23}$$

$$\frac{\partial^2 T}{\partial x^2} = 0.$$

$$u^2\frac{\partial^2 T}{\partial x^2} = 0. \tag{4.24}$$

$$\frac{\partial^2 T}{\partial y^2} = (T_w - T_0)\frac{a}{\nu}\theta''(\eta).$$

$$v^2\frac{\partial^2 T}{\partial y^2} = v^2(T_w - T_0)\frac{a}{\nu}\theta''(\eta) = (T_w - T_0)a^2 f^2(\eta)\theta''(\eta). \tag{4.25}$$

$$2uv\frac{\partial}{\partial x}\left(\frac{\partial T}{\partial y}\right) = 2(axf'(\eta))(-\sqrt{a\nu} f(\eta))\frac{\partial}{\partial x}\left((T_w - T_0)\sqrt{\frac{a}{\nu}}\theta'(\eta)\right)$$
$$= 2(axf'(\eta))(-\sqrt{a\nu} f(\eta))\left(A\sqrt{\frac{a}{\nu}}\theta'(\eta)\right).$$
$$\Rightarrow 2uv\frac{\partial^2 T}{\partial x \partial y} = -2a^2 Axf(\eta)f'(\eta)\theta'(\eta). \tag{4.26}$$

By adding (4.20), (4.23), (4.24), (4.25) and (4.26), we get

$$\left[\left(u\frac{\partial u}{\partial x}+v\frac{\partial u}{\partial y}\right)\frac{\partial T}{\partial x}+\left(u\frac{\partial v}{\partial x}+v\frac{\partial v}{\partial y}\right)\frac{\partial T}{\partial y}+u^2\frac{\partial^2 T}{\partial x^2}+v^2\frac{\partial^2 T}{\partial y^2}\right.$$
$$\left.+2uv\frac{\partial^2 T}{\partial x\partial y}\right]=\left[a^2x\Big(f'^2(\eta)-f(\eta)f''(\eta)\Big)\Big(B+A\theta(\eta)\Big)\right.$$
$$\left.+(T_w-T_0)a^2f(\eta)f'(\eta)\theta'(\eta)+Axa^2f^2(\eta)\theta''(\eta)-2a^2Axf(\eta)f'(\eta)\theta'(\eta)\right].$$
$$\Rightarrow\lambda_1\left[\left(u\frac{\partial u}{\partial x}+v\frac{\partial u}{\partial y}\right)\frac{\partial T}{\partial x}+\left(u\frac{\partial v}{\partial x}+v\frac{\partial v}{\partial y}\right)\frac{\partial T}{\partial y}+u^2\frac{\partial^2 T}{\partial x^2}+v^2\frac{\partial^2 T}{\partial y^2}\right.$$
$$\left.+2uv\frac{\partial^2 T}{\partial x\partial y}\right]=\lambda_1\left[a^2Bxf'^2(\eta)-a^2Bxf(\eta)f''(\eta)+a^2Axf'^2(\eta)\theta(\eta)\right.$$
$$\left.-a^2Axf(\eta)f''(\eta)\theta(\eta)+a^2Axf^2(\eta)\theta''(\eta)-a^2Axf(\eta)f'(\eta)\theta'(\eta)\right]. \tag{4.27}$$

By utilizing (4.11)-(4.17) and (4.27) in (4.3), we get

$$(\rho C_P)_f\Big(Baxf'(\eta)+aAxf'(\eta)\theta(\eta)-aAxf(\eta)\theta'(\eta)\Big)+\lambda_1\left[a^2Bxf'^2(\eta)\right.$$
$$-a^2Bxf(\eta)f''(\eta)+a^2Axf'^2(\eta)\theta(\eta)-a^2Axf(\eta)f''(\eta)\theta(\eta)$$
$$\left.+a^2Axf^2(\eta)\theta''(\eta)-a^2Axf(\eta)f'(\eta)\theta'(\eta)\right]=\frac{kaAx}{\nu}\theta''(\eta)$$
$$+Nb(\rho C_p)_f\Big(aAx\theta'(\eta)\phi'(\eta)\Big)+Nt(\rho C_p)_f\Big(aAx\theta'^2(\eta)\Big)$$
$$+a^3M\rho x^2f'^2(\eta)+\frac{\mu_0a^3x^2}{\nu}f''^2(\eta)+\frac{\mu_0\gamma a^{\frac{9}{2}}x^3}{\nu^{\frac{3}{2}}}f''^3(\eta)$$
$$+\frac{16\sigma^*}{3k^*}\frac{aAxT_\infty^3}{\nu}\left[\left(\frac{1}{N_2(N_3+1)}\right)^3\theta^3(\eta)\theta''(\eta)+\theta''(\eta)\right.$$
$$+3\left(\frac{1}{N_2(N_3+1)}\right)^2\theta^2(\eta)\theta''(\eta)+3\left(\frac{1}{N_2(N_3+1)}\right)\theta(\eta)\theta''(\eta)$$
$$+3\left(\frac{1}{N_2(N_3+1)}\right)^2\theta^2(\eta)\theta'^2(\eta)+3\left(\frac{1}{N_2(N_3+1)}\right)\theta'^2(\eta)$$
$$\left.+6\left(\frac{1}{N_2(N_3+1)}\right)^2\theta(\eta)\theta'^2(\eta)\right].$$

$$\Rightarrow a^2Ax\lambda_1\left[\frac{B}{A}f'^2(\eta)-\frac{B}{A}f(\eta)f''(\eta)+f'^2(\eta)\theta(\eta)-f(\eta)f''(\eta)\theta(\eta)+f^2(\eta)\theta''(\eta)\right.$$
$$\left.-f(\eta)f'(\eta)\theta'(\eta)\right]=aAx\left[\frac{k}{\nu}\theta''(\eta)-(\rho C_P)_f\left(\frac{B}{A}f'(\eta)+f'(\eta)\theta(\eta)-f(\eta)\theta'(\eta)\right)\right.$$
$$+Nb(\rho C_p)_f\left(\theta'(\eta)\phi'(\eta)\right)+Nt(\rho C_p)_f\left(\theta'^2(\eta)\right)+\frac{a^3M\rho x^2}{aAx}f'^2(\eta)$$
$$+\frac{\mu_0a^3x^2}{aAx\nu}f''^2(\eta)+\frac{\mu_0\gamma a^{\frac{7}{2}}x^3}{Ax\nu^{\frac{3}{2}}}f''^3(\eta)$$
$$+\frac{16\sigma^*}{3k^*}\frac{T_\infty^3}{\nu}\left[\left(\frac{1}{N_2(N_3+1)}\right)^3\theta^3(\eta)\theta''(\eta)+\theta''(\eta)\right.$$
$$+3\left(\frac{1}{N_2(N_3+1)}\right)^2\theta^2(\eta)\theta''(\eta)+3\left(\frac{1}{N_2(N_3+1)}\right)\theta(\eta)\theta''(\eta)$$
$$+3\left(\frac{1}{N_2(N_3+1)}\right)^2\theta^2(\eta)\theta'^2(\eta)$$
$$\left.\left.+3\left(\frac{1}{N_2(N_3+1)}\right)\theta'^2(\eta)+6\left(\frac{1}{N_2(N_3+1)}\right)^2\theta(\eta)\theta'^2(\eta)\right]\right].$$

$$\Rightarrow a\lambda_1\left[N_2f'^2(\eta)-N_2f(\eta)f''(\eta)+f'^2(\eta)\theta(\eta)-f(\eta)f''(\eta)\theta(\eta)+f^2(\eta)\theta''(\eta)\right.$$
$$\left.-f(\eta)f'(\eta)\theta'(\eta)\right]=\frac{k}{\nu}\left[\theta''(\eta)-(\rho C_P)_f\frac{\nu}{k}N_2f'(\eta)-(\rho C_P)_f\frac{\nu}{k}f'(\eta)\theta(\eta)\right.$$
$$+(\rho C_P)_f\frac{\nu}{k}f(\eta)\theta'(\eta)+Nb(\rho C_p)_f\frac{\nu}{k}\theta'(\eta)\phi'(\eta)+Nt(\rho C_p)_f\frac{\nu}{k}\theta'^2(\eta)$$
$$+\frac{a^3M\rho x^2}{aAx}\frac{\nu}{k}f'^2(\eta)+\frac{\mu_0a^2x^2}{Axk}f''^2(\eta)+\frac{\mu_0\gamma a^{\frac{7}{2}}x^3}{Ax\nu^{\frac{1}{2}}k}f''^3(\eta)$$
$$+\frac{4}{3}\frac{4\sigma^*T_\infty^3}{k^*k}\left[\left(\frac{1}{N_2(N_3+1)}\right)^3\theta^3(\eta)\theta''(\eta)+\theta''(\eta)\right.$$
$$+3\left(\frac{1}{N_2(N_3+1)}\right)^2\theta^2(\eta)\theta''(\eta)+3\left(\frac{1}{N_2(N_3+1)}\right)\theta(\eta)\theta''(\eta)$$
$$+3\left(\frac{1}{N_2(N_3+1)}\right)^2\theta^2(\eta)\theta'^2(\eta)$$
$$\left.\left.+3\left(\frac{1}{N_2(N_3+1)}\right)\theta'^2(\eta)+6\left(\frac{1}{N_2(N_3+1)}\right)^2\theta(\eta)\theta'^2(\eta)\right]\right].$$

$$\Rightarrow\frac{\nu a\lambda_1}{k}\left[N_2f'^2(\eta)-N_2f(\eta)f''(\eta)+f'^2(\eta)\theta(\eta)-f(\eta)f''(\eta)\theta(\eta)+f^2(\eta)\theta''(\eta)\right.$$
$$\left.-f(\eta)f'(\eta)\theta'(\eta)\right]=\theta''(\eta)+Pr\left[f(\eta)\theta'(\eta)-N_2f'(\eta)-f'(\eta)\theta(\eta)\right.$$

$$+ Nb\left(\theta'(\eta)\phi'(\eta) + \frac{Nt}{Nb}(\theta'(\eta))^2\right) + MEcf'^2(\eta) + Ecf''^2(\eta) + \frac{WeEc}{\sqrt{2}}f''^3(\eta)\Bigg]$$
$$+ \frac{4}{3}Rd\Bigg[B_1^3\theta^3(\eta)\theta''(\eta) + \theta''(\eta) + 3B_1^2\theta^2(\eta)\theta''(\eta) + 3B_1\theta(\eta)\theta''(\eta)$$
$$+ 3B_1^2\theta^2(\eta)\theta'^2(\eta) + 3B_1\theta'^2(\eta) + 6B_1^2\theta(\eta)\theta'^2(\eta)\Bigg].$$
$$\Rightarrow \left(1 - \lambda_t f^2(\eta) + \frac{4}{3}Rd\Big[1 + B_1^3\theta^3(\eta) + 3B_1^2\theta^2(\eta) + 3B_1\theta(\eta)\Big]\right)\theta''(\eta) - \lambda_t N_2 f'^2(\eta)$$
$$+ \lambda_t N_2 f(\eta)f''(\eta) - \lambda_t f'^2(\eta)\theta(\eta) + \lambda_t f(\eta)f''(\eta)\theta(\eta) + \lambda_t f(\eta)f'(\eta)\theta'(\eta)$$
$$+ Pr\Bigg[f(\eta)\theta'(\eta) - N2f'(\eta) - f'(\eta)\theta(\eta) + Nb\left(\theta'(\eta)\phi'(\eta) + \frac{Nt}{Nb}(\theta'(\eta))^2\right)$$
$$+ MEcf'^2(\eta) + Ecf''^2(\eta) + \frac{WeEc}{\sqrt{2}}f''^3(\eta)\Bigg]$$
$$+ \frac{4}{3}Rd\Big[3B_1^2\theta^2(\eta)\theta'^2(\eta) + 3B_1\theta'^2(\eta) + 6B_1^2\theta(\eta)\theta'^2(\eta)\Big] = 0.$$
$$\Rightarrow \theta''(\eta) = \frac{1}{\left(1 - \lambda_t f^2(\eta) + \frac{4}{3}Rd\Big[1 + B_1^3\theta^3(\eta) + 3B_1^2\theta^2(\eta) + 3B_1\theta(\eta)\Big]\right)}\Bigg[\lambda_t N_2 f'^2$$
$$- \lambda_t N_2 f(\eta)f''(\eta) + \lambda_t f'^2(\eta)\theta(\eta) - \lambda_t f(\eta)f''(\eta)\theta(\eta) - \lambda_t f(\eta)f'(\eta)\theta'(\eta)$$
$$- Pr\Bigg[f(\eta)\theta'(\eta) - N_2 f'(\eta) - f'\theta + Nb\left(\theta'(\eta)\phi'(\eta) + \frac{Nt}{Nb}(\theta'(\eta))^2\right)$$
$$+ MEcf'^2(\eta) + Ecf''^2(\eta) + \frac{WeEc}{\sqrt{2}}f''^3(\eta)\Bigg]$$
$$- \frac{4}{3}Rd\Big[+ 3B_1^2\theta^2(\eta)\theta'^2(\eta) + 3B_1\theta'^2(\eta) + 6B_1^2\theta(\eta)\theta'^2(\eta)\Big]\Bigg]. \tag{4.28}$$

The most of the dimentionless parameters in (4.28) have been explained in (3.37) and (3.60). As we have used Cattaneo-Cristtov heat flux model in (4.3) that's why the new parameter arises, which is gievn below:

$$\lambda_t = \frac{\nu a \lambda_1}{k},$$

where λ_t is Cattaneo-Christov temperature parameter. Similarly, the expression for notation B_1 is given below:

$$B_1 = \frac{1}{N_2(N_3 + 1)}.$$

Now, the conversion of (4.4) into dimentionless form will be discussed in detail. As (4.4) is extended form of (3.4), so the conversions that are already done in Chapter 3 can be used here in order to get the dimentionless form of (4.4). The following process has been taken into account from (3.40) and (3.44) of Chapter 3.

$$u\frac{\partial C}{\partial x}+v\frac{\partial C}{\partial y}=aExf'(\eta)+aDxf'(\eta)\phi(\eta)-aDxf(\eta))\phi'(\eta). \tag{4.29}$$

$$D_B\left(\frac{\partial^2 C}{\partial y^2}\right)+\frac{D_T}{T_\infty}\frac{\partial^2 T}{\partial y^2}-k_1(C-C_\infty)=D_B\left(Dx.\frac{a}{\nu}\phi''(\eta)\right)$$
$$+\frac{D_T}{T_\infty}\left(\frac{aAx}{\nu}\theta''(\eta)\right)-ak\Big(C_w-C_0\Big)\phi(\eta). \tag{4.30}$$

From (4.6),

$$\phi(\eta)=\frac{C-C_\infty}{C_w-C_0}.$$
$$\Rightarrow C=C_\infty+(C_w-C_0)\phi(\eta).$$

As we know that

$$C_\infty=C_0+Ex,$$
$$C_w=C_0+Dx,$$
$$\therefore\ C=(C_0+Ex)+(Dx)\phi(\eta).$$
$$\Rightarrow\frac{\partial C}{\partial x}=\frac{\partial}{\partial x}\Big((C_0+Ex)+(Dx)\theta(\eta)\Big)=E+D\phi(\eta). \tag{4.31}$$

From (3.14),

$$u\frac{\partial u}{\partial x}+v\frac{\partial u}{\partial y}=a^2xf'^2(\eta)-a^2xf(\eta)f''(\eta). \tag{4.32}$$

$$\Rightarrow\left(u\frac{\partial u}{\partial x}+v\frac{\partial u}{\partial y}\right)\frac{\partial C}{\partial x}=a^2x\Big(f'^2(\eta)-f(\eta)f''(\eta)\Big)\Big(E+D\phi(\eta)\Big). \tag{4.33}$$

From (4.6),

$$\frac{\partial v}{\partial x}=0,\qquad\qquad\frac{\partial v}{\partial y}=-af'(\eta),$$

$$u\frac{\partial v}{\partial x}=0, \qquad v\frac{\partial v}{\partial y}=a^{\frac{3}{2}}\sqrt{\nu}f(\eta)f'(\eta).$$

$$\therefore\ u\frac{\partial v}{\partial x}+v\frac{\partial v}{\partial y}=a^{\frac{3}{2}}\sqrt{\nu}f(\eta)f'(\eta). \tag{4.34}$$

$$\frac{\partial C}{\partial y}=(C_w-C_0)\sqrt{\frac{a}{\nu}}\phi'(\eta). \tag{4.35}$$

$$\Rightarrow\left(u\frac{\partial v}{\partial x}+v\frac{\partial v}{\partial y}\right)\frac{\partial C}{\partial y}=(C_w-C_0)a^2f(\eta)f'(\eta)\phi'(\eta). \tag{4.36}$$

$$\frac{\partial^2 C}{\partial x^2}=0.$$

$$u^2\frac{\partial^2 T}{\partial x^2}=0. \tag{4.37}$$

$$\Rightarrow\frac{\partial^2 C}{\partial y^2}=(C_w-C_0)\frac{a}{\nu}\phi''(\eta).$$

$$\Rightarrow v^2\frac{\partial^2 C}{\partial y^2}=v^2(C_w-C_0)\frac{a}{\nu}\phi''(\eta).$$

$$=(C_w-C_0)a^2f^2(\eta)\phi''(\eta). \tag{4.38}$$

$$2uv\frac{\partial}{\partial x}\left(\frac{\partial C}{\partial y}\right)=2(axf'(\eta))(-\sqrt{a\nu}f(\eta))\frac{\partial}{\partial x}\left((C_w-C_0)\sqrt{\frac{a}{\nu}}\phi'(\eta)\right)$$

$$=2(axf'(\eta))(-\sqrt{a\nu}f(\eta))\left(D\sqrt{\frac{a}{\nu}}\phi'(\eta)\right)$$

$$=-2a^2Dxf(\eta)f'(\eta)\phi'(\eta). \tag{4.39}$$

By utilizing (4.33) and (4.36)-(4.39),

$$\lambda_2\Bigg[\left(u\frac{\partial u}{\partial x}+v\frac{\partial u}{\partial y}\right)\frac{\partial C}{\partial x}+\left(u\frac{\partial v}{\partial x}+v\frac{\partial v}{\partial y}\right)\frac{\partial C}{\partial y}+u^2\frac{\partial^2 C}{\partial x^2}+v^2\frac{\partial^2 C}{\partial y^2}$$

$$+2uv\frac{\partial^2 C}{\partial x\partial y}\Bigg]=\lambda_2\Bigg[a^2x(f'^2(\eta)-f(\eta)f''(\eta)).(E+D\phi(\eta))$$

$$+Dxa^2f(\eta)f'(\eta)\phi'(\eta)Dxa^2f^2(\eta)\phi''(\eta)-2a^2Dxf(\eta)f'(\eta)\phi'(\eta)\Bigg].$$

$$=\lambda_2\Bigg[a^2Exf'^2(\eta)-a^2Exf(\eta)f''(\eta)+a^2Dxf'(\eta)^2\phi(\eta)+a^2Dxff'\phi'$$

$$+a^2Dxf^2(\eta)\phi''(\eta)-3a^2Dxf(\eta)f'(\eta)\phi'(\eta)\Bigg]. \tag{4.40}$$

By putting (4.29)-(4.30) and (4.40) in (4.4),

$$aExf'(\eta)+aDxf'(\eta)\phi(\eta)-aDxf(\eta))\phi'(\eta)+\lambda_2\Bigg[a^2Exf'^2(\eta)$$
$$-a^2Exf(\eta)f''(\eta)+a^2Dxf'(\eta)^2\phi(\eta)+a^2Dxf(\eta)f'(\eta)\phi'(\eta)$$
$$+a^2Dxf^2(\eta)\phi''(\eta)-3a^2Dxf(\eta)f'(\eta)\phi'(\eta)\Bigg]=D_B\left(Dx\frac{a}{\nu}\phi''(\eta)\right)$$
$$+\frac{D_T}{T_\infty}\left(\frac{aAx}{\nu}\theta''(\eta)\right)-ak\Big(C_w-C_0\phi(\eta)\Big).$$
$$\Rightarrow D_B\left(Dx.\frac{a}{\nu}\phi''(\eta)\right)+\frac{D_T}{T_\infty}\left(\frac{aAx}{\nu}\theta''(\eta)\right)-ak\Big(C_w-C_0\Big)\phi(\eta)$$
$$-aExf'(\eta)-aDxf'(\eta)\phi(\eta)+aDxf(\eta))\phi'(\eta)-\lambda_2\Bigg[a^2Exf'^2(\eta)$$
$$-a^2Exf(\eta)f''(\eta)+a^2Dxf'(\eta)^2\phi(\eta)+a^2Dxf(\eta)f'(\eta)\phi'(\eta)+a^2Dxf^2\phi''$$
$$-3a^2Dxf(\eta)f'(\eta)\phi'(\eta)\Bigg]=0.$$
$$\Rightarrow\phi''(\eta)+\frac{\frac{D_T}{T_\infty}\left(\frac{aAx}{\nu}\right)}{D_B.Dx\left(\frac{a}{\nu}\right)}\theta''(\eta)-\frac{aDx}{D_B.Dx\left(\frac{a}{\nu}\right)}f'(\eta)\phi(\eta)-\frac{aEx}{D_BDx\left(\frac{a}{\nu}\right)}f'(\eta)$$
$$+\frac{aDx}{D_BDx\left(\frac{a}{\nu}\right)}f(\eta)\phi'(\eta)-\frac{ak(Dx)}{D_BDx\left(\frac{a}{\nu}\right)}\phi(\eta)-\frac{a^2Dx\lambda_2}{D_BDx\left(\frac{a}{\nu}\right)}\Bigg[\frac{E}{D}f'^2(\eta)$$
$$-\frac{E}{D}f(\eta)f''(\eta)+f'(\eta)^2\phi(\eta)+f(\eta)f'(\eta)\phi'(\eta)+f^2(\eta)\phi''(\eta)$$
$$-3f(\eta)f'(\eta)\phi'(\eta)\Bigg]=0.$$
$$\Rightarrow\phi''(\eta)+\frac{(\rho C_P)_SD_T.Ax}{(\rho C_P)_f\nu T_\infty}.\frac{\nu(\rho C_P)_f}{D_BDx(\rho C_P)_S}\theta''(\eta)-\frac{\alpha\nu}{\alpha D_B}f'(\eta)\phi(\eta)-\frac{\alpha\nu}{\alpha D_B}N1f'$$
$$+\frac{\nu\alpha}{D_B\alpha}f(\eta)\phi'(\eta)-\frac{\alpha\nu k}{\alpha D_B}\phi(\eta)-\frac{a\nu\lambda_2}{D_B}\Bigg[N_1f'^2(\eta)-N_1f(\eta)f''(\eta)$$
$$+f'(\eta)^2\phi(\eta)+f^2(\eta)\phi''(\eta)-3f(\eta)f'(\eta)\phi'(\eta)\Bigg]=0.$$
$$\Rightarrow\phi''(\eta)+\frac{Nt}{Nb}\theta''(\eta)-\frac{\alpha\nu}{\alpha D_B}\Big(f'(\eta)\phi(\eta)+N1f'(\eta)-f(\eta)\phi'(\eta)\Big)$$

$$
\begin{aligned}
&- \frac{\alpha\nu k}{\alpha D_B}\phi(\eta) - \lambda_d\Big[N_1 f'^2(\eta) - N_1 f(\eta)f''(\eta) + f'^2(\eta)\phi(\eta) \\
&+ f^2(\eta)\phi''(\eta) - 3f(\eta)f'(\eta)\phi'(\eta)\Big] = 0. \\
\Rightarrow\ &(1-\lambda_d f^2(\eta))\phi''(\eta) = LePr\Big(f'(\eta)\phi(\eta) + N_1 f'(\eta) \\
&+ f(\eta)\phi'(\eta) + k\phi(\eta)\Big) - \frac{Nt}{Nb}\theta''(\eta) + \lambda_d N_1 f'^2(\eta) - \lambda_d N_1 f f'' \\
&+ \lambda_d f'^2(\eta)\phi(\eta) - 3\lambda_d f(\eta)f'(\eta)\phi'(\eta). \\
\Rightarrow\ &\phi''(\eta) = \frac{1}{(1-\lambda_d f^2(\eta))}\Big[LePr\Big(f'(\eta)\phi(\eta) + N_1 f'(\eta) + f(\eta)\phi'(\eta) \\
&\qquad + k\phi(\eta)\Big) - \frac{Nt}{Nb}\theta''(\eta) + \lambda_d N_1 f'^2(\eta) - \lambda_d N_1 f(\eta)f''(\eta) \\
&\qquad + \lambda_d f'(\eta)^2\phi(\eta) - 3\lambda_d f(\eta)f'(\eta)\phi'(\eta)\Big].
\end{aligned} \tag{4.41}
$$

The most of the dimentionless parameters in (4.41) are already defined in (3.37) and (3.60), except N_1, which is given below,

$$N_1 = \frac{E}{D}.$$

Here, a new parameter arsies due to the Cattaneo-Christov diffusion model, which is named as Cattaneo-Christov concentration parameter and formulated as following,

$$\lambda_d = \frac{a\nu\lambda_2}{D_B}.$$

The detailed discussion for the transformation of the boundary conditions (4.5) into dimentionless form have been done in chapter 3. Instead of repeating those calculations again and again, we can directly write those findings from (3.50) as follow

$$
\left.
\begin{aligned}
&f(\eta) = 0, \quad f'(\eta) = 1, \quad \phi(\eta) = 1 - N_1, \quad \theta(\eta) = 1 - N_2 \quad at \quad \eta = 0, \\
&f'(\eta) \to 0, \quad \phi(\eta) \to 0, \quad \theta(\eta) \to 0 \qquad as \quad \eta \to \infty.
\end{aligned}
\right\} \tag{4.42}
$$

From (4.10), (4.28), (4.41) and (4.42), the dimentionless form of the governing model is given below.

$$f''' = f'^2 - f(\eta)f'' - Wef''f''' + Mf' + \lambda f' + Frf'^2, \tag{4.43}$$

$$\begin{aligned}\theta'' = \frac{1}{1-\lambda_t f^2 + \frac{4}{3}Rd\Big[1+B_1^3\theta^3+3B_1^2\theta^2+3B_1\theta\Big]}\Bigg[&\lambda_t N_2 f'^2 \\ &- \lambda_t N_2 f(\eta)f'' + \lambda_t f'^2\theta - \lambda_t f f''\theta - \lambda_t f f'\theta' - Pr\Bigg[f\theta' - N_2 f' \\ &- f'\theta + N_b\Big(\theta'\phi'(\eta) + \frac{Nt}{Nb}(\theta')^2\Big) + MEcf'^2 + Ecf''^2 \\ &+ \frac{WeEc}{\sqrt{2}}f''^3\Bigg] - \frac{4}{3}Rd\Big[+3B_1^2\theta^2\theta'^2 + 3B_1\theta'^2 + 6B_1^2\theta\theta'^2\Big]\Bigg],\end{aligned} \tag{4.44}$$

$$\begin{aligned}\phi'' = \frac{1}{(1-\lambda_d f^2)}\Bigg[&LePr\Big(f'\phi + N_1 f' + f\phi' + k\phi\Big) \\ &- \frac{Nt}{Nb}\theta'' + \lambda_d N_1 f'^2 - \lambda_d N_1 f f'' + \lambda_d f'^2\phi - 3\lambda_d f f'\phi'\Bigg].\end{aligned} \tag{4.45}$$

4.3.2 Entropy Optimization

The computations below will be useful in order to determine the dimensionless form of (4.8). As we know that

$$\begin{aligned} T &= T_\infty + (T_w - T_0)\theta(\eta) \\ \Rightarrow \frac{\partial T}{\partial y} &= (T_w - T_0)(\sqrt{\frac{a}{\nu}})\theta'(\eta) \\ \Rightarrow \left(\frac{\partial T}{\partial y}\right)^2 &= (T_w - T_0)^2(\frac{a}{\nu})\theta'^2(\eta). \\ C &= C_\infty + (C_w - C_0)\phi(\eta) \end{aligned}$$

$$\begin{aligned} \Rightarrow \frac{\partial C}{\partial y} &= (C_w - C_0)\left(\sqrt{\frac{a}{\nu}}\right)\phi'(\eta) \\ \Rightarrow \left(\frac{\partial C}{\partial y}\right)^2 &= (C_w - C_0)^2\left(\frac{a}{\nu}\right)\phi'^2(\eta). \end{aligned}$$

From (4.6),

$$\Rightarrow \frac{\partial u}{\partial y} = ax(\sqrt{\frac{a}{\nu}})f''(\eta). \tag{4.46}$$
$$\Rightarrow \left(\frac{\partial u}{\partial y}\right)^2 = a^2x^2\left(\frac{a}{\nu}\right)f''^2(\eta).$$
$$\Rightarrow \left(\frac{\partial u}{\partial y}\right)^4 = a^4x^4\left(\frac{a^2}{\nu^2}\right)f''^4(\eta)$$
$$\Rightarrow \frac{\partial^2 u}{\partial x \partial y} = a(\sqrt{\frac{a}{\nu}})f''(\eta).$$
$$\frac{\partial^2 u}{\partial y^2} = ax\frac{a}{\nu}f'''(\eta)$$
$$u\frac{\partial u}{\partial y}\frac{\partial^2 u}{\partial x \partial y} = a^3x^2\frac{a}{\nu}f'(\eta)f''^2(\eta).$$
$$v\frac{\partial u}{\partial y}\frac{\partial^2 u}{\partial y^2} = -\frac{a^4x^2}{\nu}f(\eta)f''(\eta)f'''(\eta).$$

From (3.7) and (3.37),

$$B_0^2 = \frac{M\rho a}{\sigma}, \quad T = T_\infty\left(\frac{\theta(\eta)}{N_2(N_3+1)} + 1\right).$$

By using the values in (4.8), we get

$$\begin{aligned} E_G = {} & \frac{1}{T_\infty^2}\left[k + k\frac{16\sigma^*}{3kk^*}\left(T_\infty\left(\frac{\theta}{N_2(N_3+1)} + 1\right)\right)^3\right](T_w - T_0)^2\frac{a}{\nu}\theta'^2 \\ & + \frac{RD_w}{C_\infty}\left((C_w - C_0)^2\frac{a}{\nu}\phi'^2\right) + \frac{\sigma}{T_\infty}\left(\frac{M\rho a}{\sigma}\right)\left(axf'\right)^2 \\ & + \frac{RD_A}{T_\infty}\left((C_w - C_0)\sqrt{\frac{a}{\nu}}\phi'\right)\left((T_w - T_0)\sqrt{\frac{a}{\nu}}\theta'\right) \\ & + \frac{1}{T_\infty}\left[\mu_0\left(a^2x^2.\frac{a}{\nu}f''^2\right) + \mu_0\gamma\left(a^3x^3\left(\frac{a}{\nu}\right)^{\frac{3}{2}}f''^3\right) + \alpha_1\left(a^3x^2\frac{a}{\nu}f'f''^2\right.\right. \\ & \left.\left. - \frac{a^4x^2}{\nu}ff''f'''\right) + 2\alpha_2\left(a^4x^4\left(\frac{a^2}{\nu^2}\right)f''^4\right)\right]. \end{aligned}$$

$$= \frac{k}{T_\infty^2}(T_w - T_0)^2 \frac{a}{\nu}\left[1 + \frac{4}{3}\frac{4\sigma^* T_\infty^3}{kk^*}\left(\frac{\theta}{N_2(N_3+1)} + 1\right)^3\right]\theta'^2$$
$$+ \frac{RD_w}{C_\infty}\left((C_w - C_0)^2 \frac{a}{\nu}\phi'^2\right) + \frac{RD_w}{T_\infty}(C_w - C_0)(T_w - T_0)\frac{a}{\nu}\theta'\phi'$$
$$+ \frac{\mu_0}{T_\infty}\left(a^2x^2\frac{a}{\nu}f''^2\right) + \frac{\mu_0\gamma}{T_\infty}\left(a^3x^3\left(\frac{a}{\nu}\right)^{\frac{3}{2}}f''^3\right) + \frac{M\rho a}{T_\infty}a^2x^2f'^2$$
$$+ \frac{1}{T_\infty}\frac{a^4x^2}{\nu}\alpha_1\left(f'f''^2 - ff''f'''\right) + 2\frac{1}{T_\infty}\frac{a^6x^4}{\nu^2}\alpha_2 f''^4\Bigg].$$

$$\frac{T_\infty\nu}{k(T_w - T_0)a}E_G = \left[1 + \frac{4}{3}\frac{4\sigma^* T_\infty^3}{kk^*}\left(\frac{\theta}{N_2(N_3+1)} + 1\right)^3\right]\theta'^2$$
$$+ \frac{RD_w}{C_\infty}\left((C_w - C_0)^2 \frac{a}{\nu}\phi'^2\right) + \frac{RD_w}{T_\infty}(C_w - C_0)(T_w - T_0)\frac{a}{\nu}\theta'\phi'$$
$$+ \frac{\mu_0}{T_\infty}\left(a^2x^2\frac{a}{\nu}f''^2\right) + \frac{\mu_0\gamma}{T_\infty}\left(a^3x^3\left(\frac{a}{\nu}\right)^{\frac{3}{2}}f''^3\right) + \frac{M\rho a}{T_\infty}a^2x^2f'^2$$
$$+ \frac{1}{T_\infty}\frac{a^4x^2}{\nu}\alpha_1\left(f'f''^2 - ff''f'''\right) + 2\frac{1}{T_\infty}\frac{a^6x^4}{\nu^2}\alpha_2 f''^4\Bigg].$$
$$N_G(\eta) = \tau_1\left[1 + \frac{4}{3}Rd\left(\frac{\theta}{N_2(N_3+1)} + 1\right)^3\right]\theta'^2 + L\frac{\tau_2}{\tau_1}\phi'^2 + L\theta'\phi'$$
$$+ Brf''^2 + MBrf'^2 + \frac{2a^5x^4\alpha_2}{k(T_w - T_0)\nu}f''^4 + \frac{WeBr}{\sqrt{2}}f''^3\Bigg)$$
$$+ \frac{a^3x^2\alpha_1}{k(T_w - T_0)}\left(f'f''^2 - ff''f'''\right).$$

Hence, the dimentionless form of the entropy generation will be

$$N_G(\eta) = \tau_1\left[1 + \frac{4}{3}Rd\left(\frac{\theta(\eta)}{N_2(N_3+1)} + 1\right)^3\right]\theta'^2(\eta) + L\frac{\tau_2}{\tau_1}\phi'^2(\eta) + L\theta'(\eta)\phi'(\eta)$$
$$+ Brf''^2(\eta) + MBrf'^2(\eta) + Xbf''^4(\eta)\frac{WeBr}{\sqrt{2}}f''^3(\eta)$$
$$+ Xr\left(f'(\eta)f''^2(\eta) - f(\eta)f''(\eta)f'''(\eta)\right). \tag{4.47}$$

The dimensionless parameters in (4.47) have been formulated as following:

$$\left.\begin{aligned} N_G(\eta) &= \frac{T_\infty \nu}{k(T_w - T_0)a} E_G, & \tau_1 &= \frac{T_w - T_0}{T_\infty}, \\ L &= \frac{RD_A(C_w - C_0)}{k}, & \tau_2 &= \frac{C_w - C_0}{C_\infty}, \\ Br &= \frac{a^2 \mu_0 x^2}{k(T_w - T_0)}, & Xr &= \frac{a^3 x^2 \alpha_1}{k(T_w - T_0)}, \\ Xb &= \frac{2a^5 x^4 \alpha_2}{k(T_w - T_0)\nu}. \end{aligned}\right\} \tag{4.48}$$

4.4 Numerical Solution

In this segment, a discussion on the numerical solution of the ordinary differential equations (4.43), (4.44) and (4.45) subject to the boundary conditions (4.42) has been presented thoroughly. For the numerical solution of the flow problem, we used the well known shooting technique along with Runge-Kutta method of order four. Furthermore, the tables and graphs for the numerical results corresponding to the flow problem subject to boundary conditions have been generated through MATLAB application. The procedure for the numerical solution of ordinary differential equation (4.43) is already discussed in Chapter 3. The ordinary differentional equations (4.44) and (4.45) are coupled in θ and ϕ. For the numerical solution of these coupled ODEs, we will use shooting method by assuming that the function f is known. For this, we utilize the following notations:

$$\begin{aligned} &\theta(\eta) = V_1, \quad \theta'(\eta) = V_1' = V_2, \quad \theta''(\eta) = V_1'' = V_2', \\ &\phi(\eta) = V_3, \quad \phi'(\eta) = V_3' = V_4, \quad \phi''(\eta) = V_3'' = V_4', \end{aligned}$$

$$D_1 = \frac{1}{\left[1 - \lambda_t f^2 + \frac{4}{3}Rd\Big(1 + (B_1V_1)^3 + 3(B_1V_1)^2 + 3(B_1V_1)\Big)\right]},$$

$$D_2 = \lambda_t N_2 f'^2 - \lambda_t N_2 f f'' + \lambda_t f'^2 V_1 - \lambda_t f f'' V_1 - \lambda_t f f' V_2 - Pr\Bigg[fV_2 - f'V_1 - N_2 f' + Nb\left(V_2 V_4 + \frac{Nt}{Nb} V_2^2\right) + MEcf'^2 + Ecf''^2 + \frac{WeEc}{\sqrt{2}} f''^3\Bigg] - \frac{4}{3} Rd\Big[3(B_1 V_1 V_2)^2 + 3B_1 V_2^2 + 6(B_1 V_2)^2 V_1\Big],$$

$$D_3 = \frac{-\frac{4}{3} Rd\Big[B_1^3 3V_1^2 V_5 + 6B_1^2 V_1 V_5 + 3B_1 V_5\Big]}{(D_1)^2},$$

$$D_4 = \lambda_t f'^2 V_5 - \lambda_t f f'' V_5 - \lambda_t f f' V_6 - Pr\Bigg[fV_6 - f'V_5 + Nb\left(V_2 V_8 + V_4 V_6 + \frac{Nt}{Nb} 2V_2 V_6\right)\Bigg] - \frac{4}{3} Rd\Big[3B_1^3(2V_1^2 V_2 V_6 + 2V_2^2 V_1 V_5) + 6B_1 V_2 V_6 + 6B_1^2(2V_1 V_2 V_6 + V_2^2 V_5\Big],$$

$$D_5 = \frac{-\frac{4}{3} Rd\Big[B_1^3 3V_1^2 V_9 + 6B_1^2 V_1 V_9 + 3B_1 V_9\Big]}{(D_1)^2},$$

$$D_6 = \lambda_t f'^2 V_9 - \lambda_t f f'' V_9 - \lambda_t f f' V_{10} - Pr\Bigg[fV_{10} - f'V_9 + N_b\left(V_2 V_{12} + V_4 V_{10} + \frac{Nt}{Nb} 2V_2 V_{10}\right)\Bigg] - \frac{4}{3} Rd\Big[3V_1^3(2V_1^2 V_2 V_1 0 + 2V_2^2 V_1 V_9) + 6B_1 V_2 V_{10} + 6B_1^2(2V_1 V_2 V_{10} + V_2^2 V_9\Big].$$

As a result, the coupled ODEs (4.44) and (4.45) are converted into the following system of 1st order ODEs.

$$\begin{aligned} V_1' &= V_2, & V_1(0) &= 1 - N_2 \\ V_2' &= D_1 D_2, & V_2(0) &= c \\ V_3' &= V_4, & V_3(0) &= 1 - N_1 \end{aligned}$$

$$V_4' = \frac{1}{(1-\lambda_d f^2)}\Bigg[LePr(V_3 f' + N_1 f' - V_4 f) + LePrKV_3 \\ - (Nt/Nb)(D_1 D_2) + \lambda_d N_1 f'^2 - \lambda_d N_1 f f'' \\ + \lambda_d V_3 f'^2 - \lambda_d f f'' V_3 - \lambda_d f f' V_4\Bigg], \qquad V_4(0) = d.$$

The above initial value problem is solved by using Runge-Kutta method of order four. One can arrive at an approximated numerical solution by considering the problem's domain, $[0, \eta_\infty]$, and selecting η_∞ such that there are no apparent changes when going beyond η_∞. The missing conditions c and d are choosen very carefully, so that the following conditions must hold.

$$(V_1(c,d))_{\eta_\infty} = 0, \qquad (V_3(c,d))_{\eta_\infty} = 0.$$

The Newton's iterative method is used to find the values of the missing conditons c and d in a systematic manner.

$$\begin{bmatrix} c \\ d \end{bmatrix}^{(n+1)} = \begin{bmatrix} c \\ d \end{bmatrix}^{(n)} - \left\{ \begin{bmatrix} \frac{\partial V_1(c,d)}{\partial c} & \frac{\partial V_1(c,d)}{\partial d} \\ \frac{\partial V_3(c,d)}{\partial c} & \frac{\partial V_3(c,d)}{\partial d} \end{bmatrix}^{-1} \begin{bmatrix} V_1 \\ V_3 \end{bmatrix} \right\}^{(n)}.$$

Furthermore, the following notations will be fruitful to apply the above iterative formula

$$\frac{\partial V_1}{\partial c} = V_5 \quad \frac{\partial V_2}{\partial c} = V_6 \quad \frac{\partial V_3}{\partial c} = V_7 \quad \frac{\partial V_4}{\partial c} = V_8, \\ \frac{\partial V_1}{\partial d} = V_9 \quad \frac{\partial V_2}{\partial d} = V_{10} \quad \frac{\partial V_3}{\partial d} = V_{11} \quad \frac{\partial V_4}{\partial d} = V_{12}.$$

The Newton's iterative scheme will then change its form after utilizing the above mentioned notations as follow:

$$\begin{bmatrix} c \\ d \end{bmatrix}^{(n+1)} = \begin{bmatrix} c \\ d \end{bmatrix}^{(n)} - \left\{ \begin{bmatrix} V_5 & V_9 \\ V_7 & V_{11} \end{bmatrix}^{-1} \begin{bmatrix} V_1 \\ V_3 \end{bmatrix} \right\}^{(n)}.$$

Now, we will get another system of eight 1st order ODEs after differentiaiting the above system of four ODEs of 1st order w.r.t. to c and d

$$
\begin{aligned}
V_5' &= V_6, && V_5(0) = 0\\
V_6' &= D_1D_4 + D_3D_2, && V_6(0) = 1\\
V_7' &= V_8, && V_7(0) = 0\\
V_8' &= \frac{1}{(1-\lambda_d f^2)}\Big[LePr(V_7f' - V_8f) + LePrKV_7\\
&\quad - (Nt/Nb)(D_1D_4\\
&\quad + D_3D_2) + \lambda_d V_7 f'^2 - \lambda_d f f'' V_7 - \lambda_d f f' V_8\Big], && V_8(0) = 0\\
V_9' &= V_{10}, && V_9(0) = 0\\
V_{10}' &= D_1D_6 + D_5D_2, && V_{10}(0) = 0\\
V_{11}' &= V_{12}, && V_{11}(0) = 1.
\end{aligned}
$$

$$
\begin{aligned}
V_{12}' &= \frac{1}{(1-\lambda_d f^2)}\Big[LePr(V_{11}f' - V_{12}f) + LePrKV_{11}\\
&\quad - (Nt/Nb)(D_1D_6 + D_5D_2)\\
&\quad + \lambda_d V_{11} f'^2 - \lambda_d f f'' V_{11} - \lambda_d f f' V_{12}\Big], && V_{12}(0) = 0.
\end{aligned}
$$

The following inequality is the stoping cretieria for the shooting method.

$$\max\{\mid V_1(\eta_\infty) \mid, \mid V_3(\eta_\infty) \mid\} < \epsilon,$$

where the value of ϵ has been choosen as 10^{-9}.

4.5 Numercial Results and Discussion

The ongoing segment consists of the discussion related to the numerical solution of the system of ODEs that governs the flow problem in the dimentionless form.

With the aid of tables and graphs, the numerical data for the non-Darcian MHD Williamson Nanofluid with Cattaneo-Christov double diffusion model has been presented. This includes the temperature profile $\theta(\eta)$ and concentration profile $\phi(\eta)$, as well as previously discussed physical parameters. It should also be remembered that the information in tables and graphs really represents the effects of different non-dimensional parameters used in ODEs.

4.5.1 Numerical Results for Nusselt and Sherwood Numbers

The impact of various dimentionless parameters on Nusselt and Sherwood numbers have been discussed in Table 4.1. In Table 4.1, the values of Nusselt and Sherwood numbers corresponding to the variation in chemical reaction parameter, magnetic parameter, Cattaneo-Christov temperature parameter, Cattaneo-Christov concentration parameter, thermal radiation parameter and thermophoresis parameter are provided.

The parameters which are kept fixed are solutal stratification parameter, Brownian motion parameter, Lewis number, Weissenberg number and some temperature ratios N_2 and N_3. In this Table, I_θ and I_ϕ are the intervals where from the missing conditions of the energy and concentration equations can be chosen.

TABLE 4.1: Results of $Nu(Re_x)^{-\frac{1}{2}}$ *and* $Sh(Re_x)^{-\frac{1}{2}}$ when $N_1 = 0.8$, $N_2 = 0.8$, $N_3 = 1.0$, $Pr = 0.7$, $Le = 1.0$, $We = 0.3$.

k	M	λ_t	λ_d	Rd	N_t	$Nu(Re_x)^{-\frac{1}{2}}$	$Sh(Re_x)^{-\frac{1}{2}}$	I_θ	I_ϕ
0.1	0.3	0.1	0.1	0.3	0.5	1.70985	1.74825	[-0.5, 0.2]	[-0.5, 0.3]
0.2						1.70945	1.77680	[-0.3, 0.1]	[-0.4, 0.1]
0.3						1.70904	1.80501	[-0.4, 0.1]	[-0.3, 0.2]
0.4						1.70865	1.83263	[-0.4, 0.1]	[-0.5, 0.2]
	0.4					1.60433	1.75192	[-0.5, 0.2]	[-0.5, 0.3]
	0.5					1.50437	1.75673	[-0.5, 0.2]	[-0.5, 0.3]
	0.6					1.40946	1.76246	[-0.5, 0.1]	[-0.4, 0.3]
		0.98				3.89998	0.51412	[-0.4,-0.1]	[-0.4,-0.1]
		0.96				3.85151	0.54140	[-0.5,-0.1]	[-0.5,-0.2]
		0.94				3.80296	0.56872	[-0.5,-0.1]	[-0.5,-0.1]
			0.98			1.66548	4.04724	[-0.4, 0.1]	[-0.4, 0.2]
			0.96			1.66638	3.99659	[-0.4, 0.1]	[-0.4, 0.3]
			0.94			1.66727	3.94585	[-0.4, 0.2]	[-0.4, 0.2]
				0.4		0.21654	0.36098	[-0.5, 0.2]	[-0.4, 0.3]
				0.5		0.20227	0.37353	[-0.5, 0.2]	[-0.5, 0.3]
				0.6		0.19032	0.38401	[-0.5, 0.2]	[-0.4, 0.3]
					0.6	1.70587	1.58473	[-0.4, 0.2]	[-0.4, 0.4]
					0.7	1.70191	1.42209	[-0.5, 0.1]	[-0.5, 0.2]
					0.8	1.69797	1.26035	[-0.3, 0.2]	[-0.4, 0.3]

The following points express the theme of Table 4.1 more clearly.

- As the value of the chemical reaction parameter k increases, the Nusselt number slowly decreases while the Sherwood number increases.

- The Sherwood number increases gradually whereas the Nusselt number falls quickly as the magnetic parameter is increased.

- A rise in the Cattaneo-Christov temperature parameter λ_t causes a rise in Nusselt number whereas a decline in Sherwood number.
- When the Cattaneo-Christov concentration parameter λ_d increases, Nusselt number slowly decreases and Sherwood number slightly increases.
- When compared to an increase in the value of the thermal radiation parameter, a decrease in the Nusselt number and an increase in the Sherwood number have been observed.
- Due to an increase in the value of the thermophoresis parameter, a modest decline in the Nusselt number and a sharp decline in the Sherwood number, can be observed.

4.5.2 Temperature Profile

Here a thorough discussion on the impact of several dimensionless characteristics on the temperature profile has been conducted. The following observations have been recorded as key findings.

- A slight increase in the magnetic parameter results in an increase in the temperature distribution, as seen in Figure 4.1. Physically, a resistive force in the fluid's direction of flow is produced, and this force causes an increase in the temperature.
- As the value of the porosity parameter λ rises, so does the temperature profile (See Figure 4.2).
- A correlation between the temperature profile and inertial coefficient is shown in Figure 4.3. For a greater inertial coefficient, a growing thermal boundary layer is shown.
- A reduction in the temperature prfile is seen as a result of rising values of the Cattaneo-Christov temperature parameter λ_t (See Figure 4.4).

- As the Prandtl number increases, it is found that the temperature field is droped. This is because an increase in Pr causes a decrease in the rate of heat transmission (See Figure 4.5).

- The temperature profile exhibits an increasing behaviour when the thermophoresis parameter rises. Physically, as Nt rises, the nanoparticles are moved from hotter to cooler areas, increasing the temperature distribution across the nanofluid (See Figure 4.6).

- When the Brownian motion parameter increases, the temperature profile displays an increasing behaviour. In general, a rise in Nb leads to a sharp increase in the fluids motion, which enhances the fluid particles, kinetic energy and, consequently, the temperature distribution (See Figure 4.7).

- The temperature distribution rises as the Eckert number increases. The Eckert number describes the ratio of the kinetic energy to change in enthalpy of the flow. Physically, the kinetic energy of the fluid particles rises as Ec acquires larger values. The temperature of the fluid is increased as a result, increasing the thickness of the thermal boundary layer (See Figure 4.8).

- Figure 4.9 shows that the temperature profile rises as the value of the solutal stratification parameter rises.

- An increment in the value of temperature ratio, results a quick decrement in temperature profile (See Figure 4.10).

- The thermal radiation parameter increases together with the temperature profile. The general rule is that as Rd values grow, more heat is delivered to the fluid, increasing the temperature distribution and the thickness of the thermal boundary layer (See Figure 4.11).

- A reduction in the concentration distribution is observed as λ_d increases in value (See Figure 4.18).

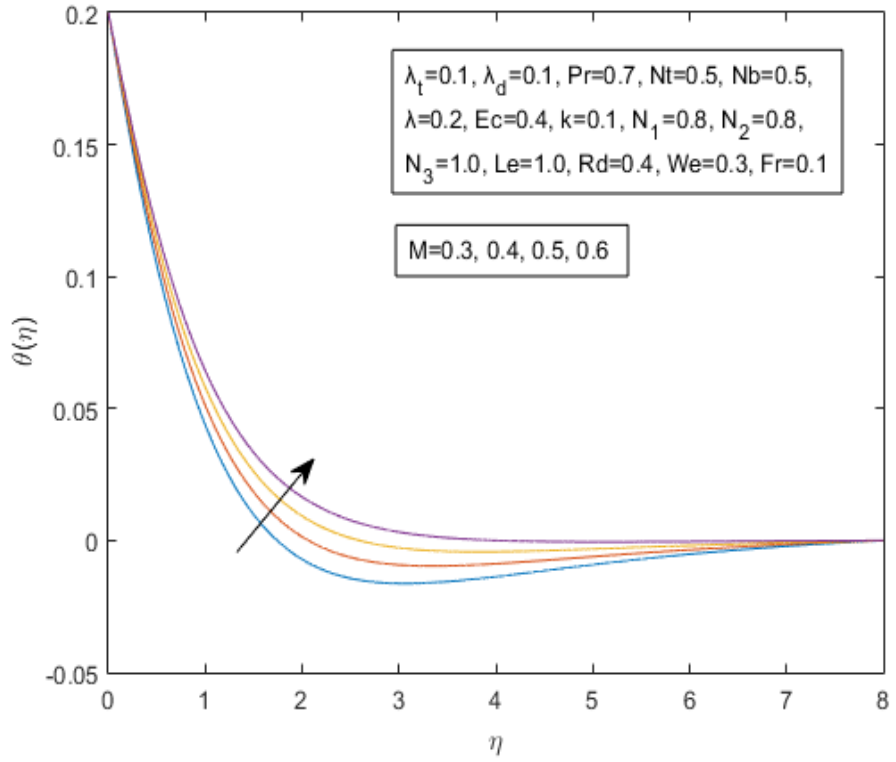

FIGURE 4.1: Influence of M on $\theta(\eta)$

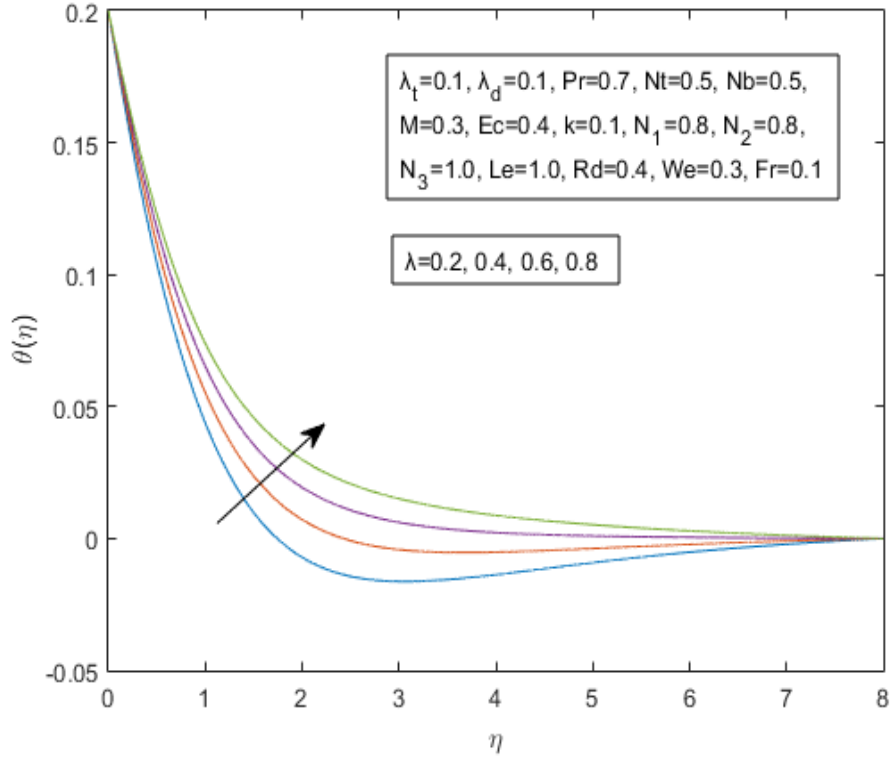

FIGURE 4.2: Influence of λ on $\theta(\eta)$

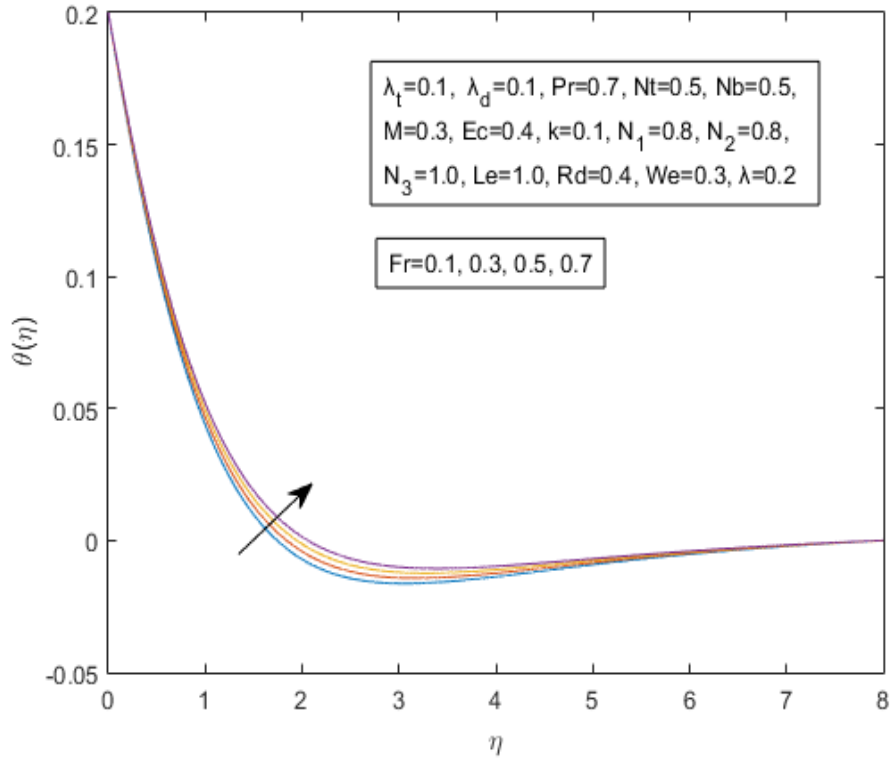

FIGURE 4.3: Impact of Fr on $\theta(\eta)$

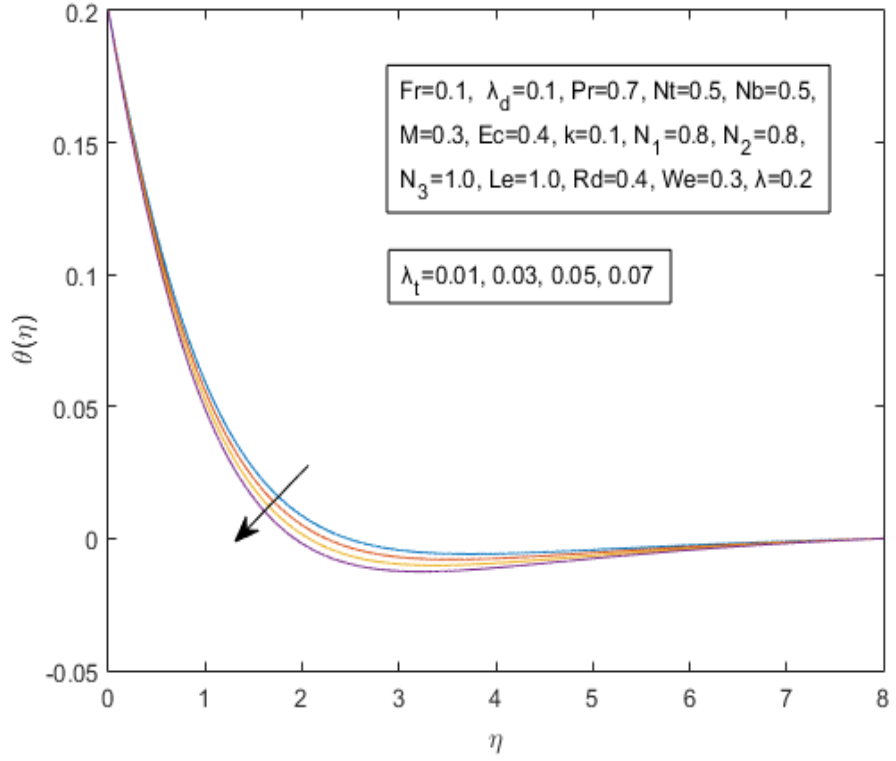

FIGURE 4.4: Influence of λ_t on $\theta(\eta)$

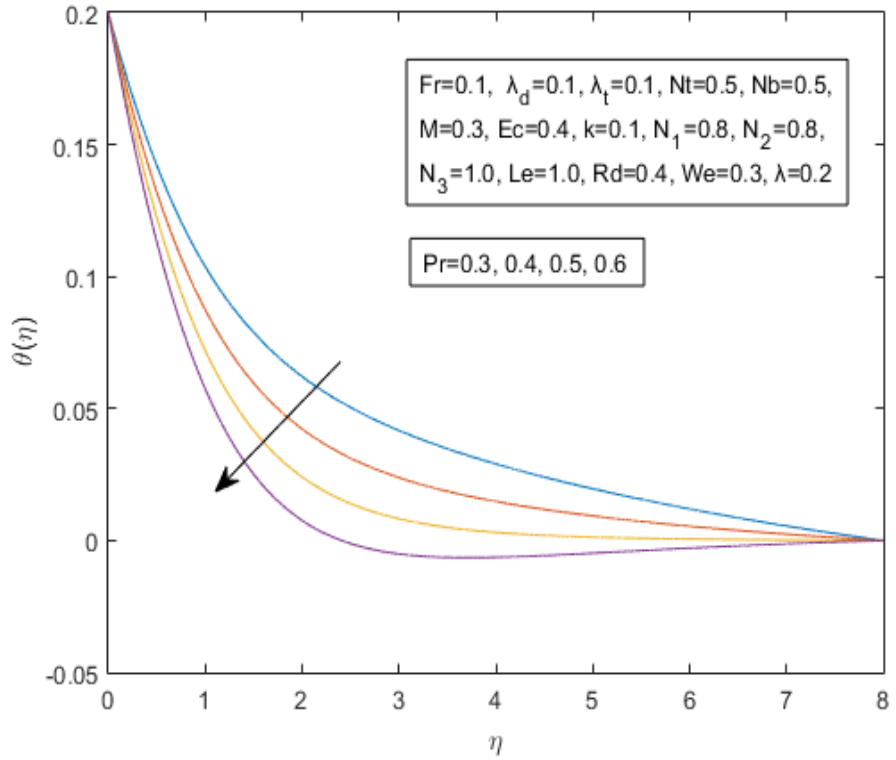

FIGURE 4.5: Influence of Pr on $\theta(\eta)$

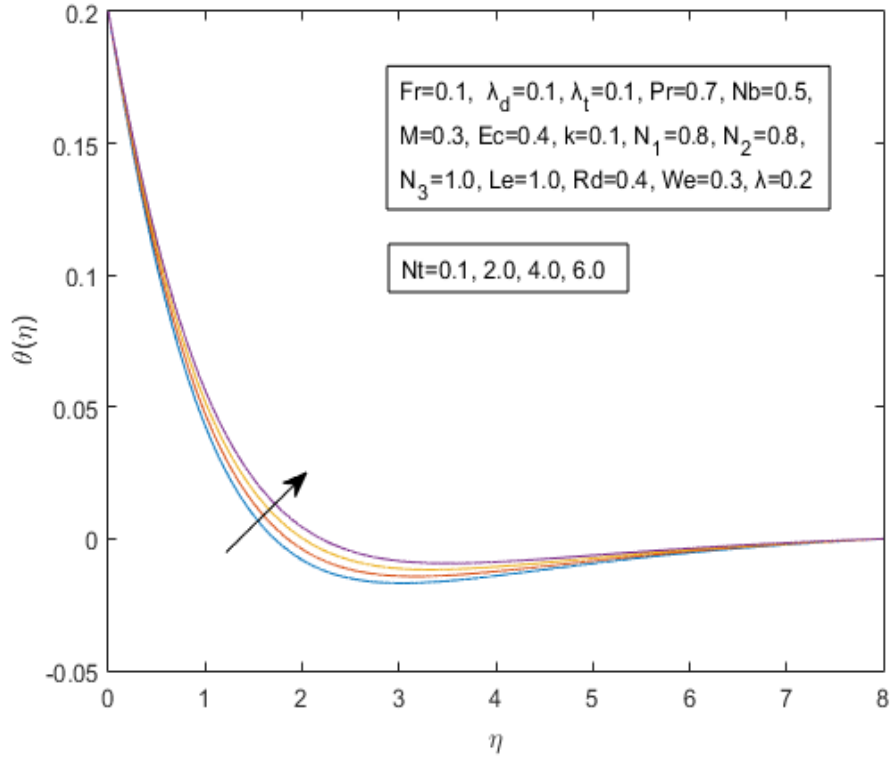

FIGURE 4.6: Influence of Nt on $\theta(\eta)$

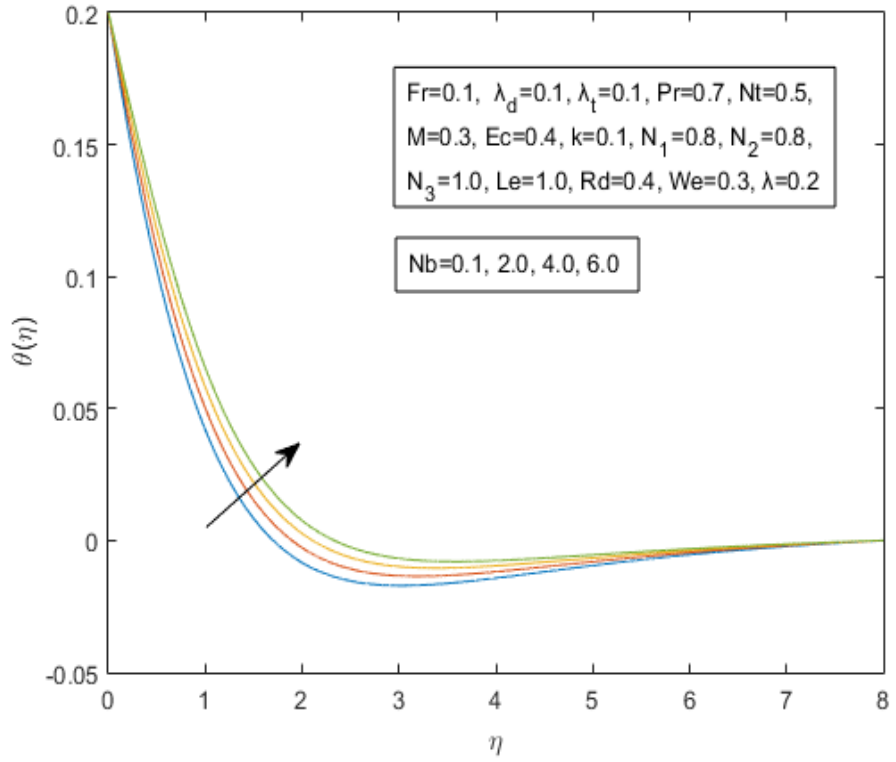

FIGURE 4.7: Influence of Nb on $\theta(\eta)$

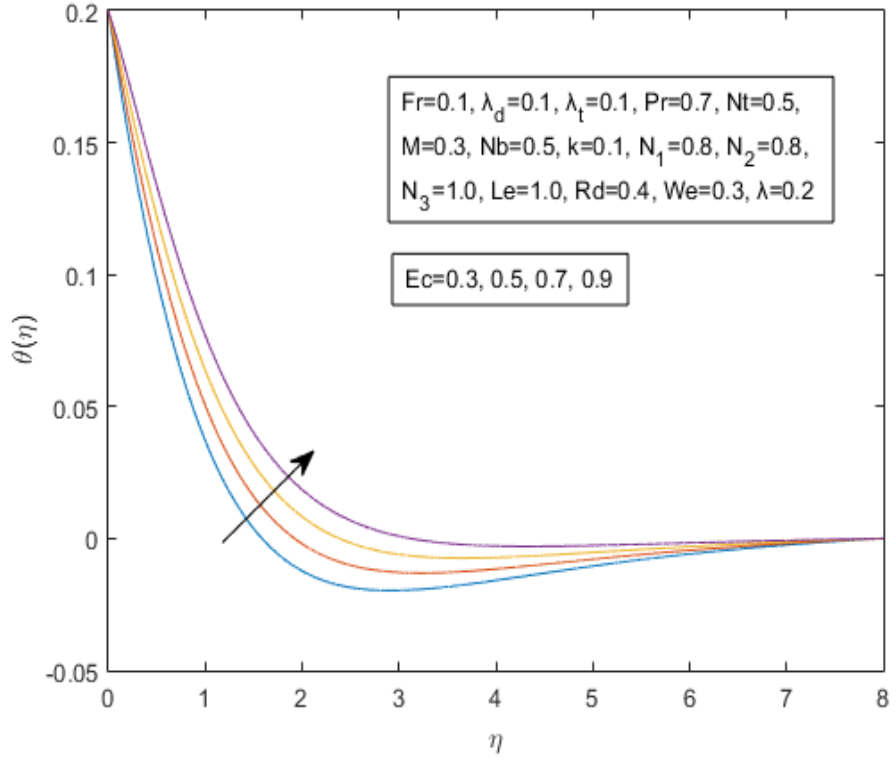

FIGURE 4.8: Influence of Ec on $\theta(\eta)$

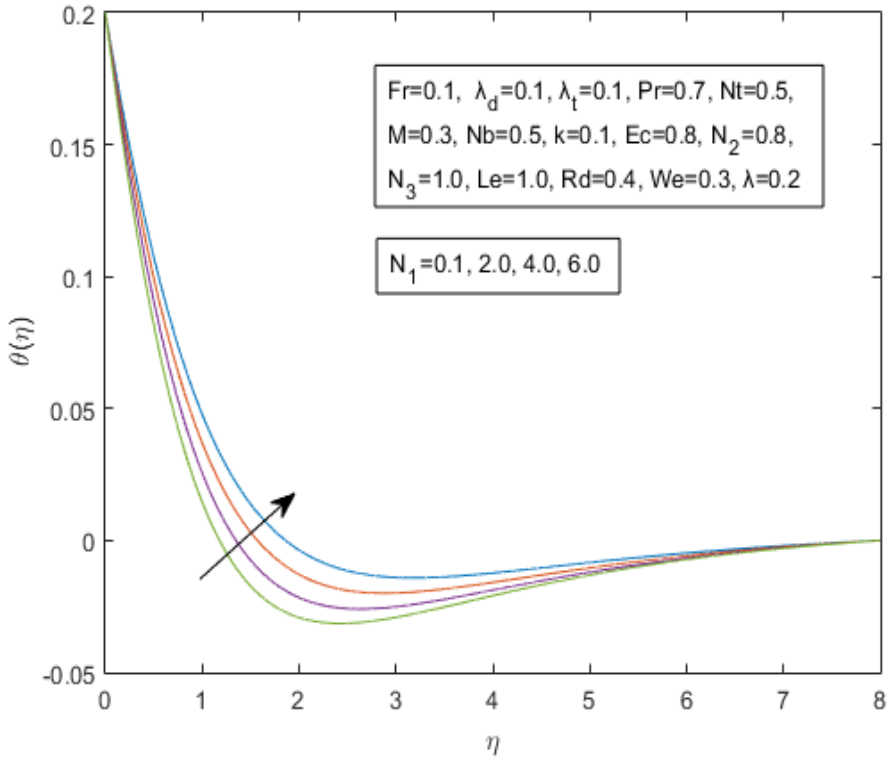

FIGURE 4.9: Influence of N_1 on $\theta(\eta)$

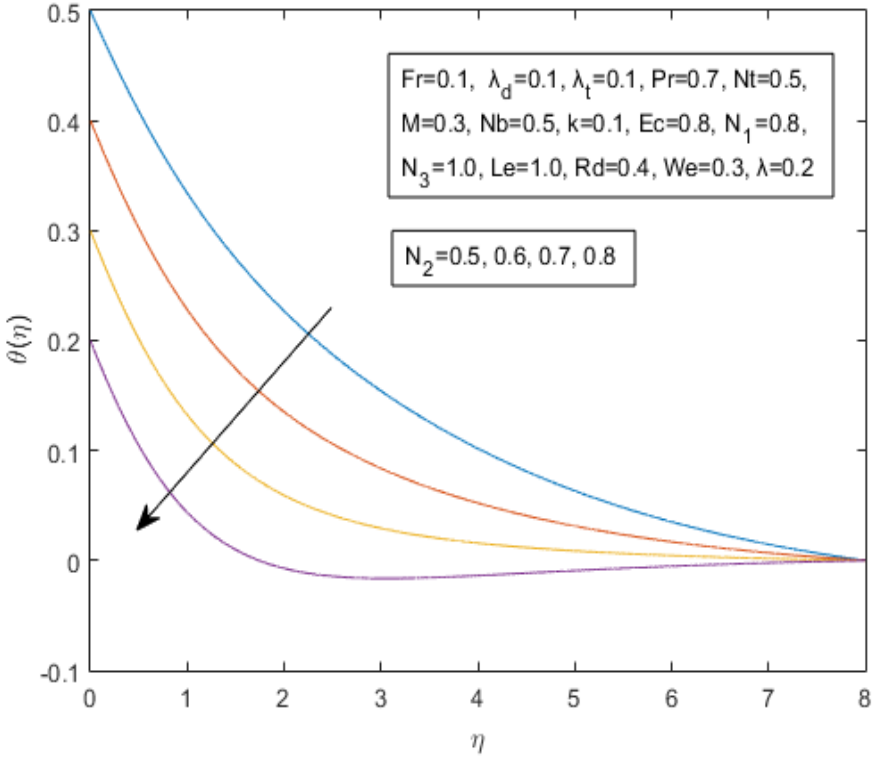

FIGURE 4.10: Influence of N_2 on $\theta(\eta)$

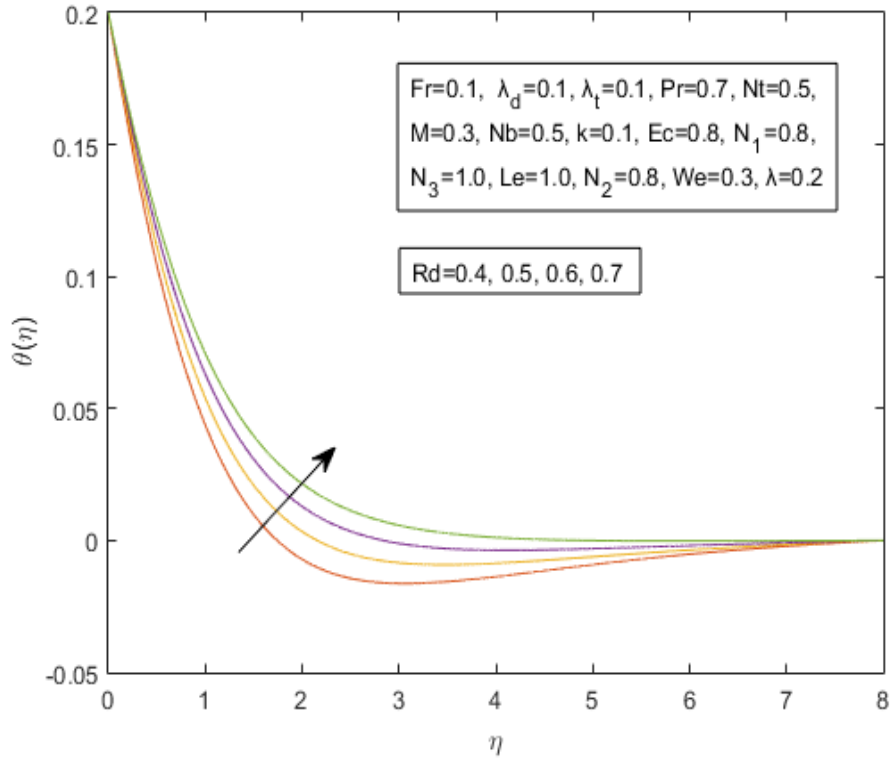

FIGURE 4.11: Influence of Rd on $\theta(\eta)$

4.5.3 Concentration Profile

The influence of various dimensionless parameters on the concentration profile on a stratified sheet is briefly discussed in this segment. From the graphs, plotted against the variations in distinct dimentionless parameters, the results corresponding to the concentration profile are lined up as follow:

- As the value of the solutal stratification parameter rises, the concentration profile declines (See Figure 4.12).
- As the value of the Lewis number rises, so does the concentration profile (See Figure 4.13).
- Rising Prandtl numbers cause a drop in the concentration profile (See Figure 4.14).

- As the thermophoresis parameter values rise, the concentration profile behaves in decreasing order (See Figure 4.15).

- As the values of the Brownian motion parameters increase, the concentration profile decreases (See Figure 4.16).

- The concentration profile acts in a decreasing fashion near the surfase, when the chemical reaction parameter increases, but in a rising manner for away from the surface (See Figure 4.17).

- A reduction in the concentration distribution is observed as λ_d, the Cattaneo-Christov concentration parameter, increases in value (See Figure 4.18).

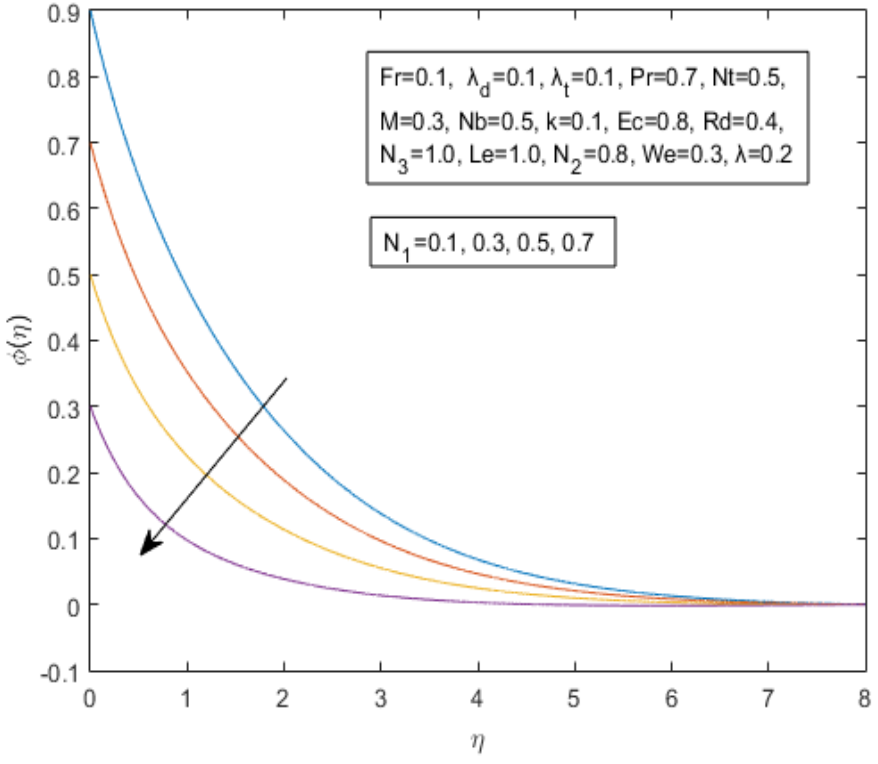

FIGURE 4.12: Influence of N_1 on $\phi(\eta)$

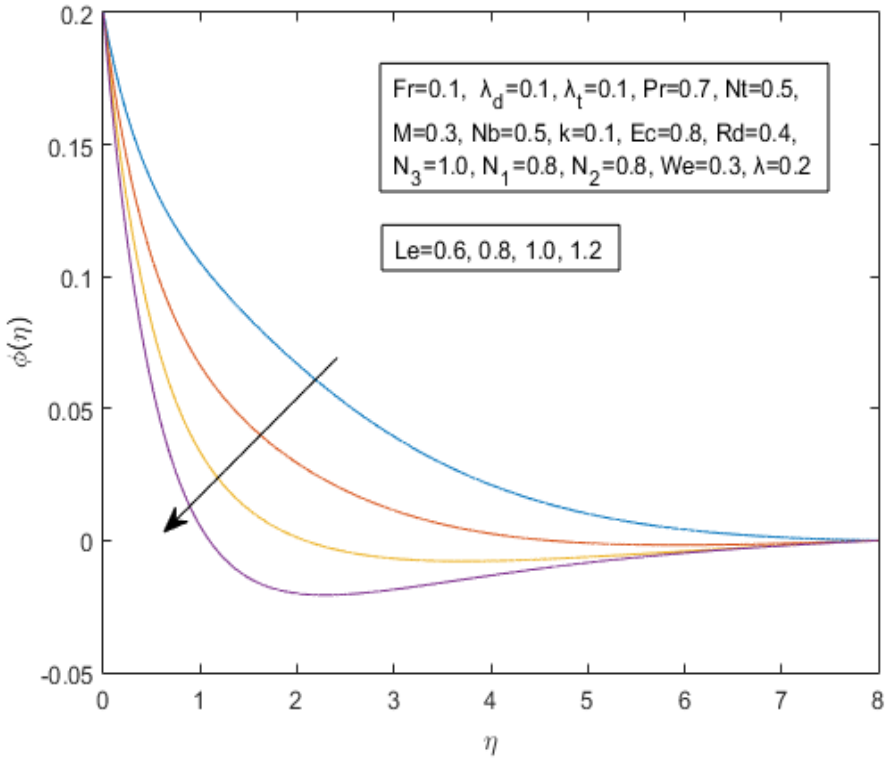

FIGURE 4.13: Influence of Le on $\phi(\eta)$

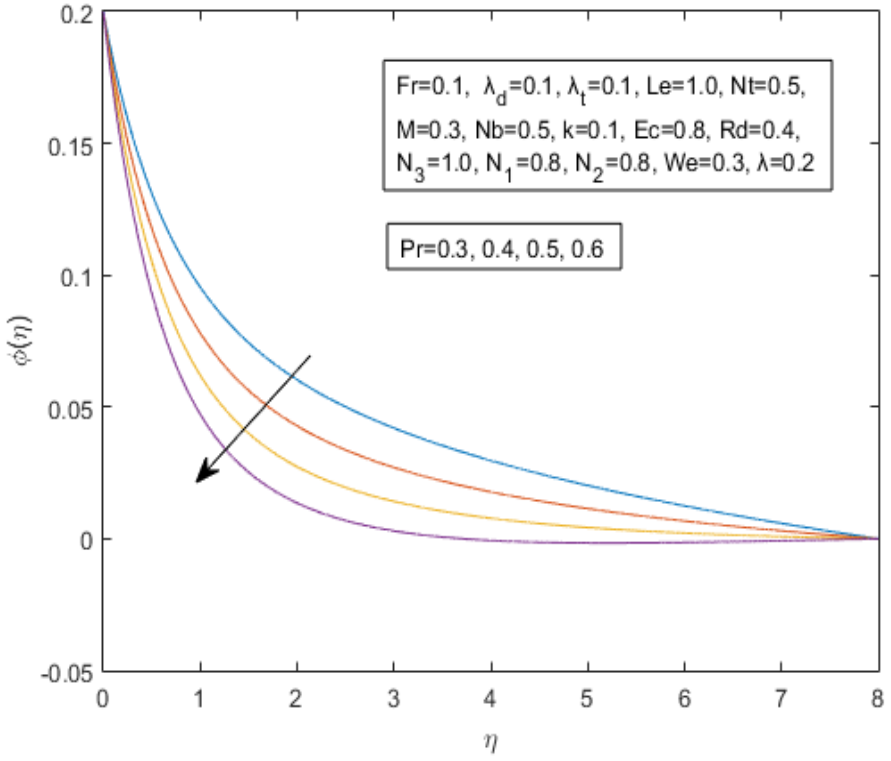

FIGURE 4.14: Influence of Pr on $\phi(\eta)$

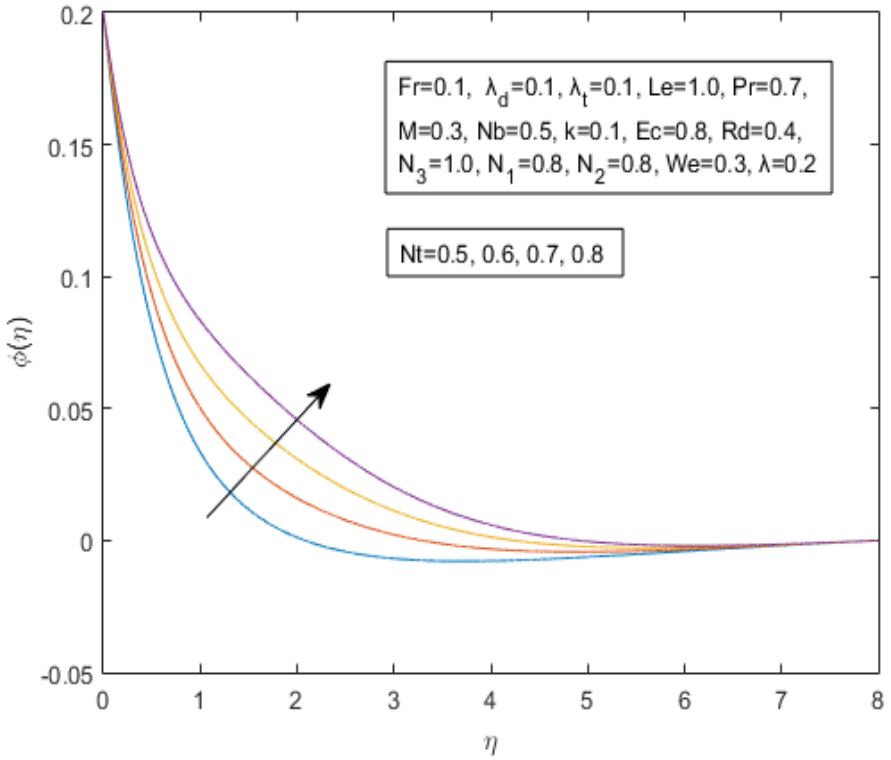

FIGURE 4.15: Influence of Nt on $\phi(\eta)$

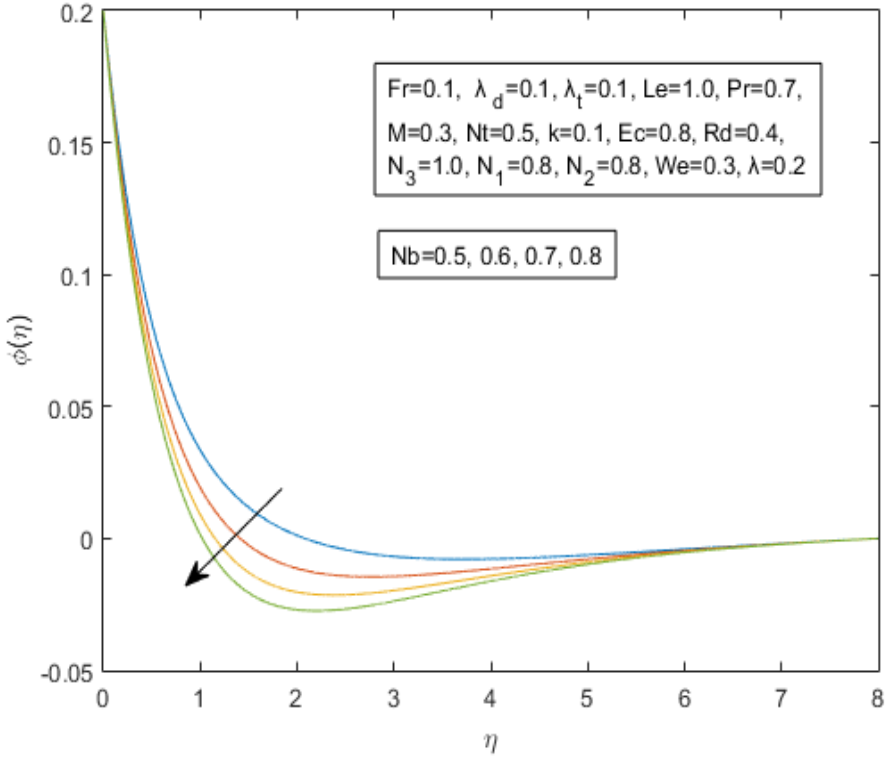

FIGURE 4.16: Influence of Nb on $\phi(\eta)$

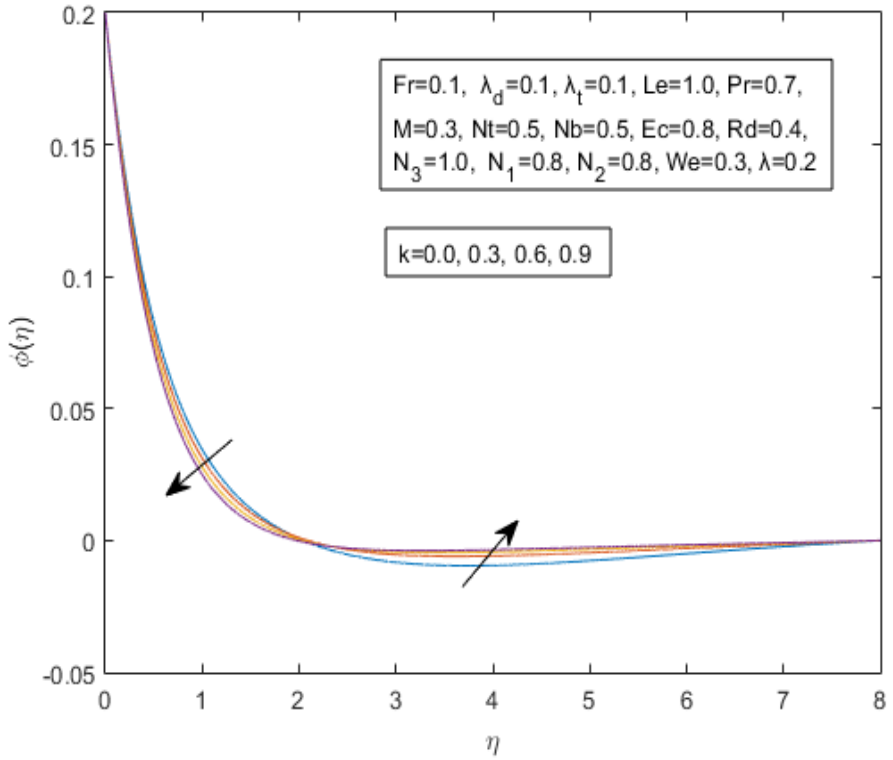

FIGURE 4.17: Influence of k on $\phi(\eta)$

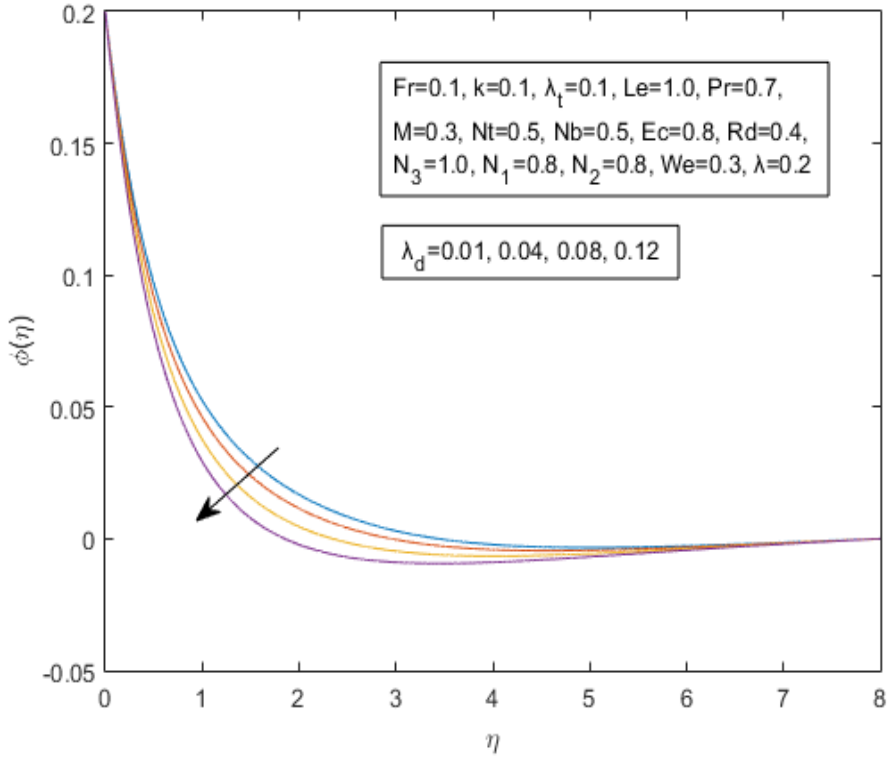

FIGURE 4.18: Influence of λ_d on $\phi(\eta)$

4.5.4 Entropy Generation

This segment discusses the impact of variation of various non-dimentional parameters on the entropy generation. The following points illsutrate the implications that have been shown through graphs.

- In Figure 4.19, the effect of the Brinkman number on the entropy generation is depicted. According to the definition of Brinkman number, molecular absorption leads to viscous heating, which slows down the rate of heat transfer. The realization of a sizable quantity of heat between the layers of the non-Newtonian fluid is the real cause of an increase in the entropy generation.

- Figure 4.20 illustrates the gradual effect of the magnetic parameter on the entropy generation. Entropy produced in the system is directly proportional to the strength of the magnetic field away from the surface, whereas slightly decreasing pattern near the surface.

- The rate of entropy generation with respect to the Weissenberg number is discussed in Figure 4.21. As the Wesseinburg number rises, the entropy generation rate increases away from surface and then shows a decreasing behaviour near the surface.

- The entropy generation displays an increasing pattern when the value of the temperature difference parameters increases. This phenomenon can bee seen through Figures 4.22 and 4.23.

- The entropy production displays an increasing pattern as the diffusion parameter's value increases, as can be seen from Figure 4.24.

- Entropy generation is observed to have increased in accordance with the Cattaneo-Christov double diffusion entropy parameters. This can be seen through Figures 4.25 and 4.26.

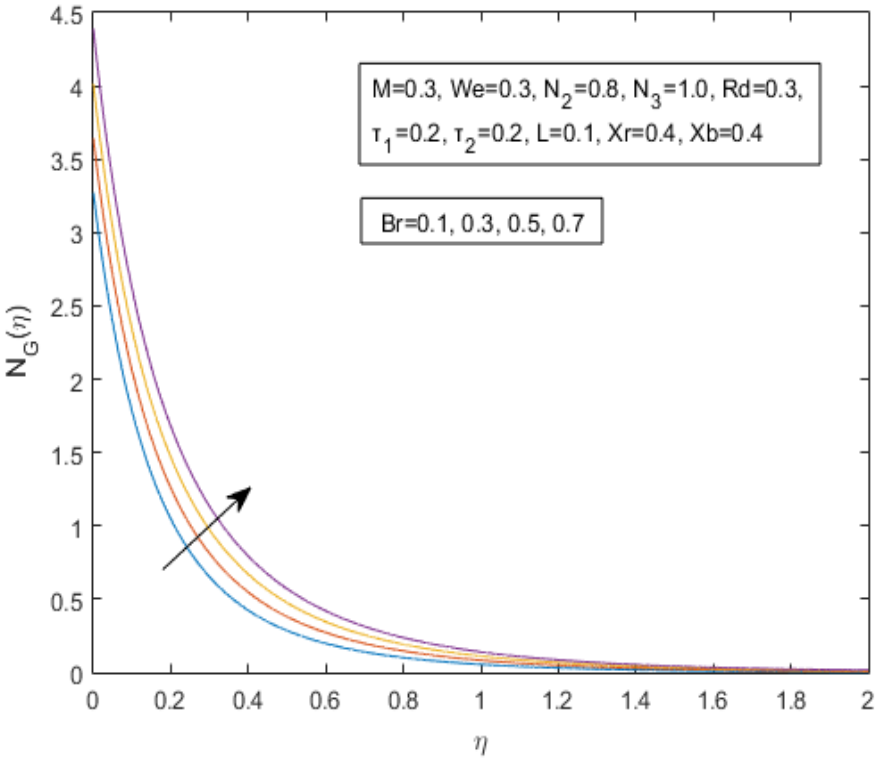

FIGURE 4.19: Influence of Br on $N_G(\eta)$

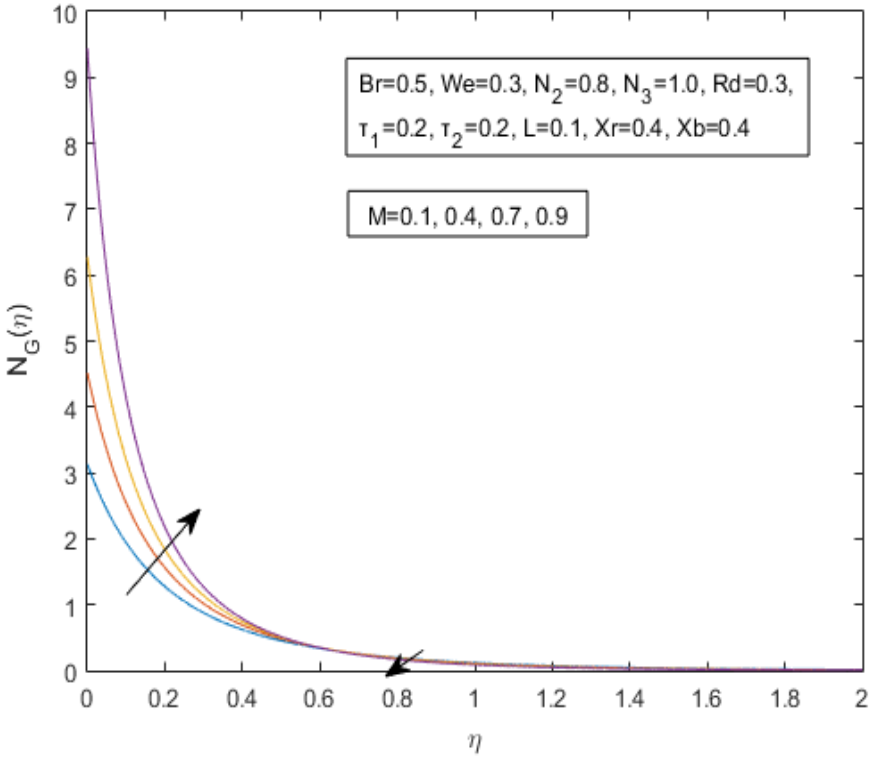

FIGURE 4.20: Influence of M on $N_G(\eta)$

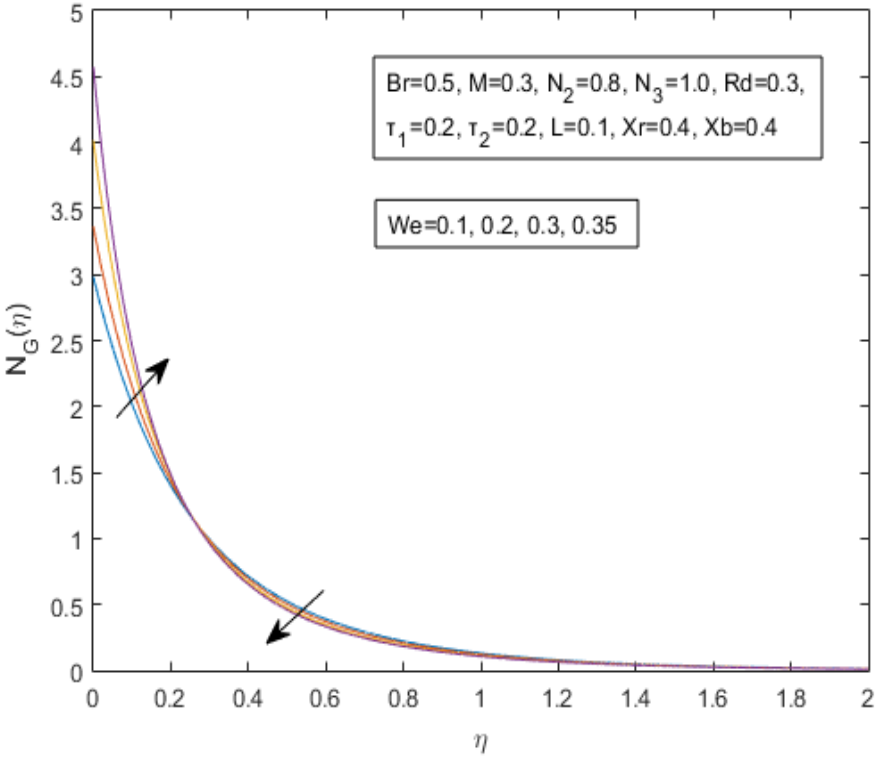

FIGURE 4.21: Influence of We on $N_G(\eta)$

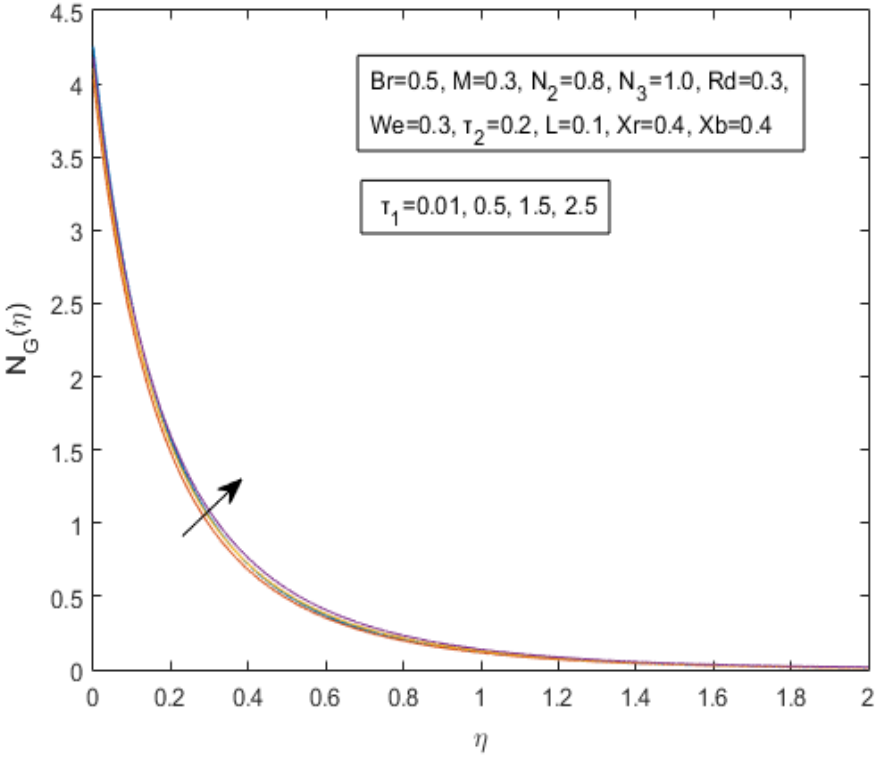

FIGURE 4.22: Influence of τ_1 on $N_G(\eta)$

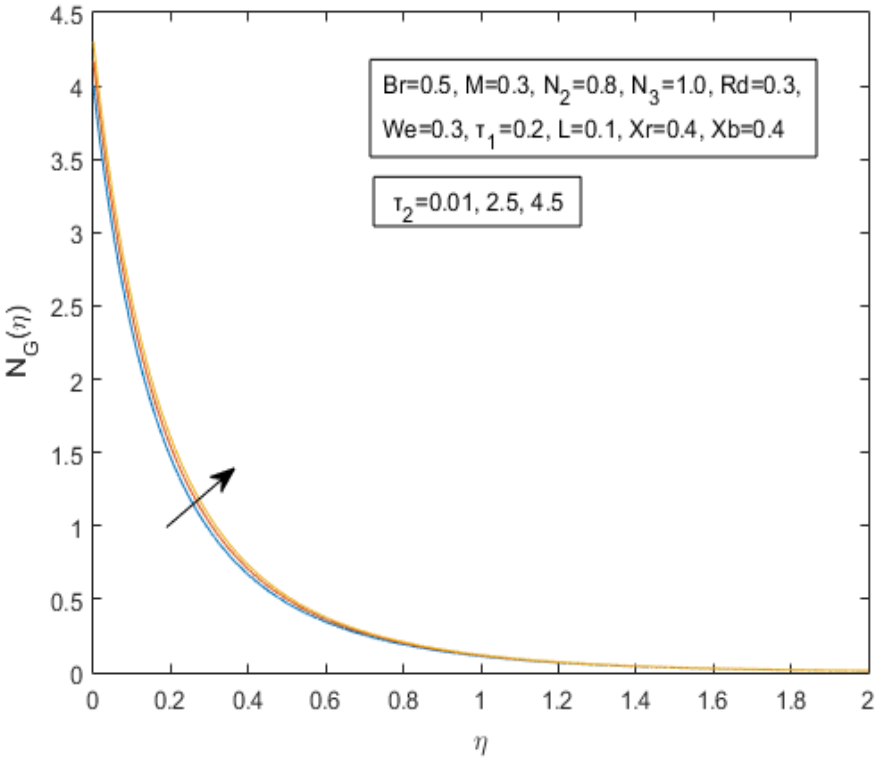

FIGURE 4.23: Influence of τ_2 on $N_G(\eta)$

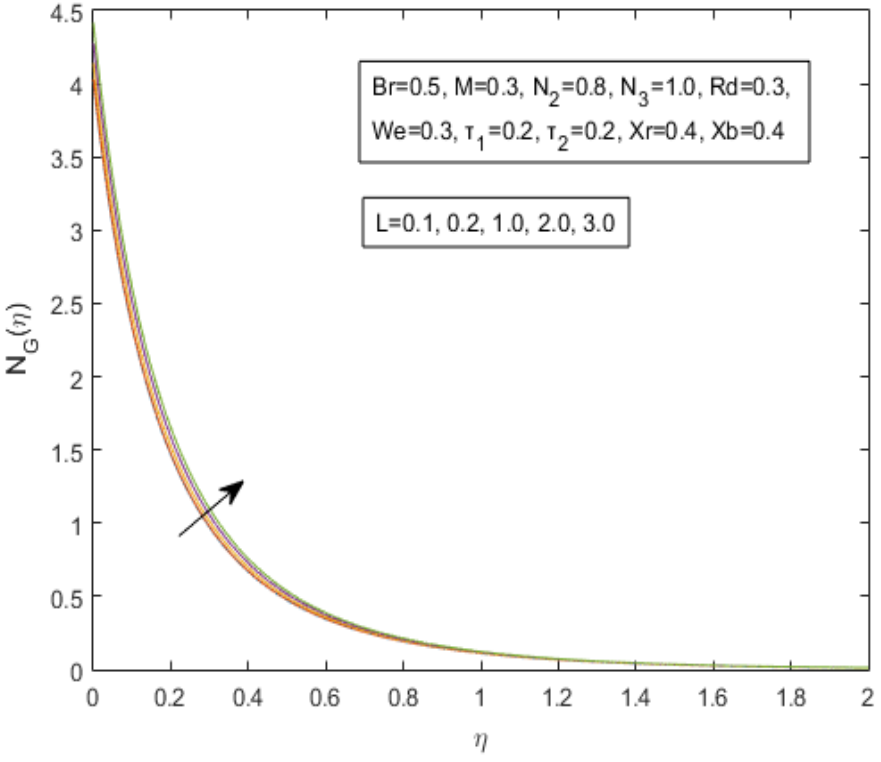

FIGURE 4.24: Influence of L on $N_G(\eta)$

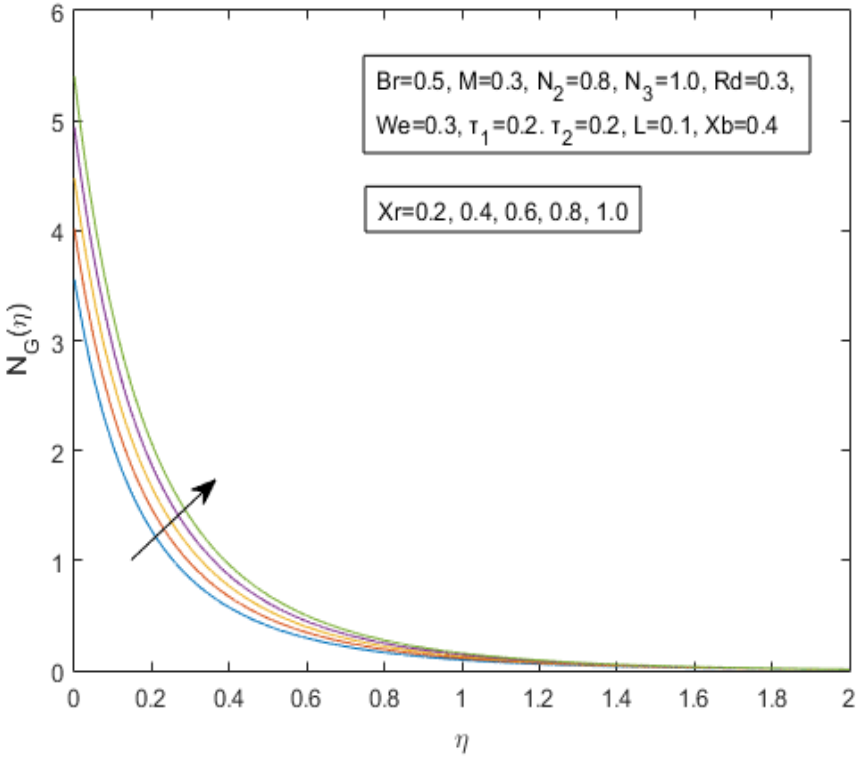

FIGURE 4.25: Influence of Xr on $N_G(\eta)$

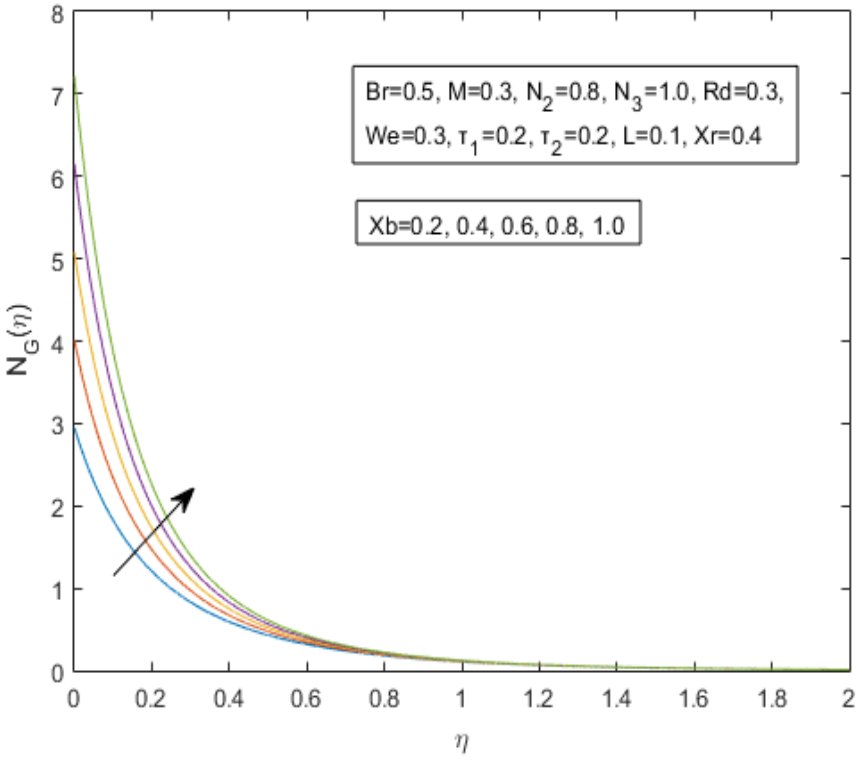

FIGURE 4.26: Influence of Xb on $N_G(\eta)$

Chapter 5

Conclusion

This thesis reviews and extends the work of [37], taking into account the effect of Cattaneo-Christov double diffusion model. To begin, momentum, energy, and concentration equations are transformed into ODEs using similarity transformations. The shooting technique was used to get the numerical solution for the modified ODEs. The results have been provided for velocity, temperature, concentration profiles and for physical parameters in the form of tables and graphs using various values of the regulating physical factors. The following are the accomplishments of the current study:

- The velocity profile drops as the value of We rises whereas the temperature profile rises.
- As the magnetic parameter M increases, the velocity profile decreases while the temperature profile rises.
- The velocity profile is reduced as the porosity parameter λ rises, whereas the temperature profile is enhanced.
- As the inertial coefficient Fr increases, the velocity profile decreases but the temperature profile behaves the other way.
- The temperature profile falls as the temperature ratio N_2 rises.

- The concentration profile falls as λ_d, the Cattaneo-Christov diffusion parameter increases.
- The temperature profile drops as the Cattaneo-Christov temperature parameter λ_t rises.
- The Nusselt number decreases as the value of the thermal radiation parameter Rd climbs whereas the Sherwood number rises.
- Because of the climbing values of the thermophoresis parameter Nt, the Nusselt and Sherwood numbers also decrease.
- The growing values of the Prandtl number Pr cause a decrement in the temperature and concentration distributions.
- The temperature profile rises while the concentration profile falls due to the rising values of the Brownian motion parameter Nb.
- The concentration distribution drops as the Lewis number Le increases in value.
- When the Cattaneo-Christov temperature parameter λ_t is decreased, the Nusselt number decreases and the Sherwood number rises.
- The Nusselt number increases as the Cattaneo-Christov concentration parameter λ_d is decreased whereas the Sherwood number is droped.
- The temperature profile increases as the Eckert number Ec increases in value.
- The values of the Nusselt number $Nu(Re_x)^{-\frac{1}{2}}$ are increased when the solutal stratification parameter N_1 ascends whereas the values of the Sherwood number $Sh(Re_x)^{-\frac{1}{2}}$ are dropped.
- The entropy generation rate increases due to the increasing values of the Brinkman number Br.
- The increasing values of the magnetic parameter M lead to a rise in the entropy generation rate.

- The rate of entropy generation increases as the values of the Weissenburg number We rise.
- The increasing values of the temperature difference parameter τ_1 lead to an increase in the entropy generation rate.
- As the value of the concentration difference τ_2 increases, the rate of entropy creation increases.
- The increasing values of the diffusion parameter L lead to a rise in the entropy generation rate.
- The entropy generation rate increases when the Cattaneo-Christov double diffusion parameters rise in value.

Bibliography

[1] Y. Cengel, J. Cimbala, and R. Turner, *EBOOK: Fundamentals of Thermal-Fluid Sciences (SI units)*. McGraw Hill, 2012.

[2] B. Xia and D.-W. Sun, "Applications of computational fluid dynamics (cfd) in the food industry: a review," *Computers and Electronics in Agriculture*, vol. 34, no. 1-3, pp. 5–24, 2002.

[3] E. P. Shipley, *Study of Natural Gas Vehicles (NGV) during the fast fill process*. West Virginia University, 2002.

[4] R. Dash, K. Mehta, and G. Jayaraman, "Casson fluid flow in a pipe filled with a homogeneous porous medium," *International Journal of Engineering Science*, vol. 34, no. 10, pp. 1145–1156, 1996.

[5] R. V. Williamson, "The flow of pseudoplastic materials," *Industrial & Engineering Chemistry*, vol. 21, no. 11, pp. 1108–1111, 1929.

[6] S. Nadeem, S. Hussain, and C. Lee, "Flow of a Williamson fluid over a stretching sheet," *Brazilian journal of chemical engineering*, vol. 30, pp. 619–625, 2013.

[7] S. U. Choi, "Nanofluid technology: current status and future research," tech. rep., Argonne National Lab.(ANL), Argonne, IL (United States), 1998.

[8] J. A. Eastman, S. Phillpot, S. Choi, and P. Keblinski, "Thermal transport in nanofluids," *Annual review of materials research*, vol. 34, p. 219, 2004.

[9] W. Ibrahim and B. Shankar, "MHD boundary layer flow and heat transfer of a nanofluid past a permeable stretching sheet with velocity, thermal and

solutal slip boundary conditions," *Computers & Fluids*, vol. 75, pp. 1–10, 2013.

[10] M. H. Abolbashari, N. Freidoonimehr, F. Nazari, and M. M. Rashidi, "Analytical modeling of entropy generation for Casson nanofluid flow induced by a stretching surface," *Advanced Powder Technology*, vol. 26, no. 2, pp. 542–552, 2015.

[11] S. Naramgari and C. Sulochana, "MHD flow over a permeable stretching/shrinking sheet of a nanofluid with suction/injection," *Alexandria Engineering Journal*, vol. 55, no. 2, pp. 819–827, 2016.

[12] M. Krishnamurthy, B. Prasannakumara, B. Gireesha, and R. S. R. Gorla, "Effect of chemical reaction on mhd boundary layer flow and melting heat transfer of Williamson nanofluid in porous medium," *Engineering Science and Technology, an International Journal*, vol. 19, no. 1, pp. 53–61, 2016.

[13] S. Ghadikolaei, K. Hosseinzadeh, D. Ganji, and B. Jafari, "Nonlinear thermal radiation effect on magneto Casson nanofluid flow with Joule heating effect over an inclined porous stretching sheet," *Case Studies in Thermal Engineering*, vol. 12, pp. 176–187, 2018.

[14] F. Shahzad, M. Sagheer, and S. Hussain, "MHD tangent hyperbolic nanofluid with chemical reaction, viscous dissipation and Joule heating effects," *AIP Advances*, vol. 9, no. 2, p. 025007, 2019.

[15] H. Alfvén, "Existence of electromagnetic-hydrodynamic waves," *Nature*, vol. 150, no. 3805, pp. 405–406, 1942.

[16] H. A. Attia, "Unsteady MHD Couette flow and heat transfer of dusty fluid with variable physical properties," *Applied Mathematics and Computation*, vol. 177, no. 1, pp. 308–318, 2006.

[17] I. Mbeledogu and A. Ogulu, "Heat and mass transfer of an unsteady MHD natural convection flow of a rotating fluid past a vertical porous flat plate in

the presence of radiative heat transfer," *International Journal of Heat and Mass Transfer*, vol. 50, no. 9-10, pp. 1902–1908, 2007.

[18] D. Chauhan and R. Agrawal, "MHD flow and heat transfer in a channel bounded by a shrinking sheet and a plate with a porous substrate," *Journal of Engineering Physics and Thermophysics*, vol. 84, no. 5, pp. 1034–1046, 2011.

[19] L. Zheng, J. Niu, X. Zhang, and Y. Gao, "MHD flow and heat transfer over a porous shrinking surface with velocity slip and temperature jump," *Mathematical and Computer Modelling*, vol. 56, no. 5-6, pp. 133–144, 2012.

[20] M. E. Yazdi, A. Moradi, and S. Dinarvand, "MHD mixed convection stagnation-point flow over a stretching vertical plate in porous medium filled with a nanofluid in the presence of thermal radiation," *Arabian Journal for Science and Engineering*, vol. 39, no. 3, pp. 2251–2261, 2014.

[21] H. M. Shawky, N. Eldabe, K. A. Kamel, and E. A. Abd-Aziz, "MHD flow with heat and mass transfer of Williamson nanofluid over a stretching sheet through porous medium," *Microsystem Technologies*, vol. 25, no. 4, pp. 1155–1169, 2019.

[22] M. Abu-Qudais and E. A. Nada, "Numerical prediction of entropy generation due to natural convection from a horizontal cylinder," *Energy*, vol. 24, no. 4, pp. 327–333, 1999.

[23] E. Abu-Nada, "Numerical prediction of entropy generation in separated flows," *Entropy*, vol. 7, no. 4, pp. 234–252, 2005.

[24] E. Abu-Nada, "Entropy generation due to heat and fluid flow in backward facing step flow with various expansion ratios," *International Journal of Energy*, vol. 3, no. 4, pp. 419–435, 2006.

[25] S. Chen, H. Han, Z. Liu, J. Li, and C. Zheng, "Analysis of entropy generation in non-premixed hydrogen versus heated air counter-flow combustion,"

International Journal of Hydrogen Energy, vol. 35, no. 10, pp. 4736–4746, 2010.

[26] R. Ellahi, M. Hassan, and A. Zeeshan, "A study of heat transfer in power law nanofluid," *Thermal Science*, vol. 20, no. 6, pp. 2015–2026, 2016.

[27] R. Ellahi, M. Raza, and N. S. Akbar, "Study of peristaltic flow of nanofluid with entropy generation in a porous medium," *Journal of Porous Media*, vol. 20, no. 5, 2017.

[28] L. Govone, M. Torabi, G. Hunt, and N. Karimi, "Non-equilibrium thermodynamic analysis of double diffusive, nanofluid forced convection in microreactors with radiation effects," *Entropy*, vol. 19, no. 12, 2017.

[29] M. I. Afridi and M. Qasim, "Entropy generation and heat transfer in boundary layer flow over a thin needle moving in a parallel stream in the presence of nonlinear Rosseland radiation," *International Journal of Thermal Sciences*, vol. 123, pp. 117–128, 2018.

[30] M. K. Nayak, S. Shaw, H. Waqas, and T. Muhammad, "Numerical computation for entropy generation in Darcy-Forchheimer transport of hybrid nanofluids with Cattaneo-Christov double-diffusion," *International Journal of Numerical Methods for Heat & Fluid Flow*, 2021.

[31] N. S. Akbar, M. Raza, and R. Ellahi, "Peristaltic flow with thermal conductivity of water and ferric nanofluids and entropy generation," *Results in Physics*, vol. 5, pp. 115–124, 2015.

[32] N. S. Akbar and A. W. Butt, "Entropy generation analysis for the peristaltic flow of Cu-water nanofluid in a tube with viscous dissipation," *Journal of Hydrodynamics*, vol. 29, no. 1, pp. 135–143, 2017.

[33] M. Rashidi, S. Bagheri, E. Momoniat, and N. Freidoonimehr, "Entropy analysis of convective MHD flow of third grade non-Newtonian fluid over a stretching sheet," *Ain Shams Engineering Journal*, vol. 8, no. 1, pp. 77–85, 2017.

[34] J. Qing, M. M. Bhatti, M. A. Abbas, M. M. Rashidi, and Ali, "Entropy generation on MHD Casson nanofluid flow over a porous stretching/shrinking surface," *Entropy*, vol. 18, no. 4, p. 123, 2016.

[35] T. Hayat, M. Kiyani, A. Alsaedi, M. I. Khan, and I. Ahmad, "Mixed convective three-dimensional flow of Williamson nanofluid subject to chemical reaction," *International Journal of Heat and Mass Transfer*, vol. 127, pp. 422–429, 2018.

[36] M. I. Khan, S. Qayyum, T. Hayat, M. I. Khan, A. Alsaedi, and T. A. Khan, "Entropy generation in radiative motion of tangent hyperbolic nanofluid in presence of activation energy and nonlinear mixed convection," *Physics Letters A*, vol. 382, no. 31, pp. 2017–2026, 2018.

[37] M. Bilal, M. Ramzan, Y. Mehmood, M. Kbiri Alaoui, and R. Chinram, "An entropy optimization study of non-Darcian magnetohydrodynamic Williamson nanofluid with nonlinear thermal radiation over a stratified sheet," *Proceedings of the Institution of Mechanical Engineers, Part E: Journal of Process Mechanical Engineering*, vol. 235, no. 6, pp. 1883–1894, 2021.

[38] M. I. Khan, S. Qayyum, T. Hayat, M. I. Khan, and A. Alsaedi, "Entropy optimization in flow of Williamson nanofluid in the presence of chemical reaction and Joule heating," *International Journal of Heat and Mass Transfer*, vol. 133, pp. 959–967, 2019.

[39] R. W. Fox, A. T. McDonald, and J. W. Mitchell, *Fox and McDonald's Introduction to Fluid Mechanics*. John Wiley & Sons, 2020.

[40] R. Bansal, *A Textbook of Fluid Mechanics*. Firewall Media, 2005.

[41] J. A. Schetz and A. E. Fuhs, *Fundamentals of Fluid Mechanics*. John Wiley & Sons, 1999.

[42] Y. Cengel and J. Cimbala, *EBOOK: Fluid Mechanics: Fundamentals and Applications (SI units)*. McGraw Hill, 2013.

[43] D. L. Logan, *A First Course in the Finite Element Method*. Cengage Learning, 2016.

[44] J. G. Brennan and A. S. Grandison, "Food Processing Handbook," 2012.

[45] P. A. Davidson, "An introduction to magnetohydrodynamics," 2002.

[46] I. Dincer and Y. A. Cengel, "Energy, entropy and exergy concepts and their roles in thermal engineering," *Entropy*, vol. 3, no. 3, pp. 116–149, 2001.

[47] B. R. Munson, T. H. Okiishi, W. W. Huebsch, and A. P. Rothmayer, *Fluid Mechanics*. Wiley Singapore, 2013.

[48] R. J. Hosking and R. L. Dewar, *Fundamental Fluid Mechanics and Magnetohydrodynamics*. Springer, 2016.

[49] J. N. Reddy and D. K. Gartling, *The Finite Element Method in Heat Transfer and Fluid Dynamics*. CRC press, 2010.

[50] R. W. Lewis, P. Nithiarasu, and K. N. Seetharamu, *Fundamentals of the Finite Element Method for Heat and Fluid Flow*. John Wiley & Sons, 2004.

[51] E. Rathakrishnan, *Instrumentation, Measurements, and Experiments in Fluids*. CRC press, 2007.

[52] D. W. Pepper and J. C. Heinrich, *The Finite Element Method: Basic Concepts and Applications*. Taylor & Francis, 2005.

[53] A. D. Polyanin and A. Chernoutsan, *A Concise Handbook of Mathematics, Physics, and Engineering Sciences*. CRC Press, 2010.

[54] J. Reddy and D. Gartling, "The Finite Element Method in Heat Transfer and Fluid Dynamics,"

[55] Y.-M. Chu, F. Shah, M. I. Khan, S. Farooq, S. Kadry, and Z. Abdelmalek, "Investigation of viscous dissipation and entropy generation in third grade nanofluid flow over a stretched riga plate with Cattaneo-Christov Double Diffusion (CCDD) model," *Physica Scripta*, vol. 95, no. 11, p. 115004, 2020.